UNCLASSIFIED

AD NUMBER

AD323899

CLASSIFICATION CHANGES

TO: unclassified

FROM: confidential

LIMITATION CHANGES

TO:

Approved for public release, distribution unlimited

FROM:

Distribution authorized to U.S. Gov't. agencies only; Administrative/Operational Use; Apr 1961. Other requests shall be referred to Bureau of Naval Weapons, Washington, DC.

AUTHORITY

15 Apr 1973 per DoDD 5200.10 document marking; Naval Air Systems Command ltr dtd 6 Apr 1977

THIS PAGE IS UNCLASSIFIED

CONFIDENTIAL

AD 323 899

Reproduced
by the

ARMED SERVICES TECHNICAL INFORMATION AGENCY
ARLINGTON HALL STATION
ARLINGTON 12, VIRGINIA

NOTICE: When government or other drawings, specifications or other data are used for any purpose other than in connection with a definitely related government procurement operation, the U. S. Government thereby incurs no responsibility, nor any obligation whatsoever; and the fact that the Government may have formulated, furnished, or in any way supplied the said drawings, specifications, or other data is not to be regarded by implication or otherwise as in any manner licensing the holder or any other person or corporation, or conveying any rights or permission to manufacture, use or sell any patented invention that may in any way be related thereto.

CAT LOGED BY
AS D NO.

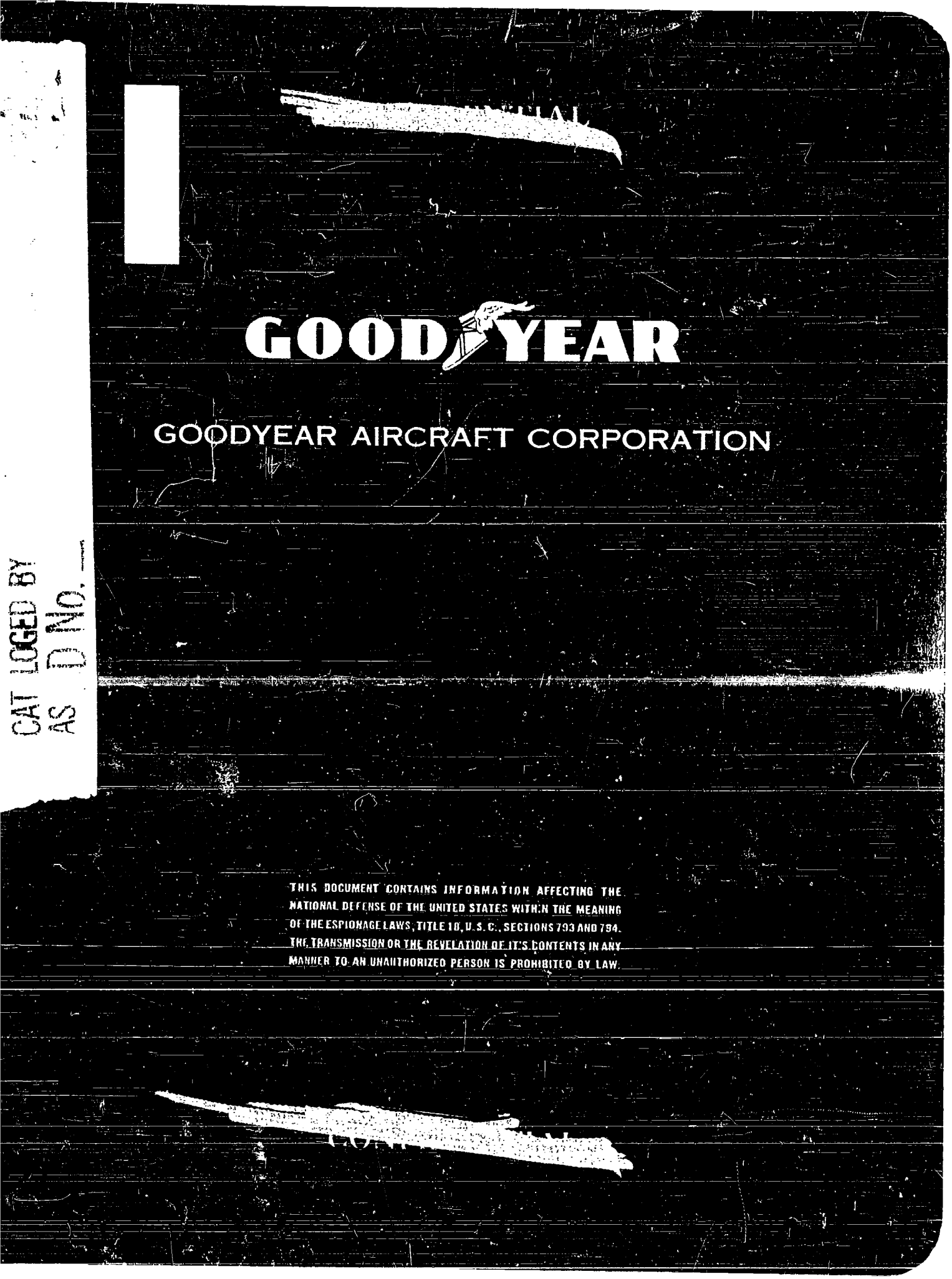

GOODYEAR

GOODYEAR AIRCRAFT CORPORATION

THIS DOCUMENT CONTAINS INFORMATION AFFECTING THE NATIONAL DEFENSE OF THE UNITED STATES WITHIN THE MEANING OF THE ESPIONAGE LAWS, TITLE 18, U.S.C., SECTIONS 793 AND 794. THE TRANSMISSION OR THE REVELATION OF ITS CONTENTS IN ANY MANNER TO AN UNAUTHORIZED PERSON IS PROHIBITED BY LAW.

CONFIDENTIAL

GER- 10176
CODE 25500
DATE April 15, 1961

Releasable to Military and government Executive agencies upon request; to contractors only upon specific approval of the Bureau of NAVAL WEAPONS

GOODYEAR

GOODYEAR AIRCRAFT CORPORATION

AKRON, OHIO

THIS DOCUMENT CONTAINS INFORMATION AFFECTING THE NATIONAL DEFENSE OF THE UNITED STATES WITHIN THE MEANING OF THE ESPIONAGE LAWS, TITLE 18, U.S.C., SECTIONS 793 AND 794. THE TRANSMISSION OR THE REVELATION OF ITS CONTENTS IN ANY MANNER TO AN UNAUTHORIZED PERSON IS PROHIBITED BY LAW.

DOWNGRADED AT 3 YEAR INTERVALS
DECLASSIFIED AFTER 12 YEARS
GOOD DIR 5200.10

AERODYNAMIC ANALYSIS OF A 1/20-SCALE POWERED WIND TUNNEL MODEL OF AN AIRSHIP WITH TWO-WAKE PROPELLER CONFIGURATIONS AND COMPARISON WITH CONVENTIONAL AND FIN-MOUNTED POWERPLANT CONFIGURATIONS.

Bureau's Contract No(s) 54-900
Amendments 5, 10, and 14

GER 10176 April 15, 1961

COPY 3 OF 30 COPIES

REVISIONS

REV	DATE	MADE BY	APPD BY	PAGES AFFECTED	REMARKS

218-51A (1-60)M

CONFIDENTIAL

TABLE OF CONTENTS

		Page
	LIST OF FIGURES	iv
	LIST OF SYMBOLS	viii
I	SUMMARY	1
II	INTRODUCTION	2
III	ANALYSIS OF WAKE PROPELLER CONFIGURATIONS	4
	A. Description of Test and Instrumentation	4
	B. Propulsive Efficiency	5
	1. Apparent Efficiency	5
	2. Effective Efficiency	6
	a. Change in Drag Due to Wake Propeller Operation	7
	(1) Drag Evaluation from Wind Tunnel Force Balance System	8
	(2) Pressure Drag Evaluation from Hull Static Pressure Distributions	10
	b. Discussion of Effective Efficiencies	14
	C. Effect of Angle of Attack and Elevator Deflection on Wake Propeller Efficiency	15
	D. Effect of Wake Propeller on Aerodynamic Characteristics	17
	1. Drag Coefficient	17
	2. Lift Coefficient	18
	3. Pitching Moment Coefficient	18
	4. Sideforce, Yawing Moment, and Rolling Moment	20
	E. Boundary Layer and Wake Velocity Measurements	21
	1. Non-Dimensional Boundary Layer Velocities	21
	2. Velocity Distributions in the Wake	22
	a. Static Pressure in the Wake	22
	b. Comparison of Wake Velocity Ratios for Various Airships	23
	c. Effect of Propeller Operation on Wake Velocity Ratios	24
	d. Drag Evaluation from Wake Measurements	25

CONFIDENTIAL

JR 2169 (3-52)M

CONFIDENTIAL

TABLE OF CONTENTS - continued

	Page
F. CONCLUSIONS - Wake Propeller Analysis	29
IV. COMPARATIVE ANALYSIS OF VARIOUS PROPULSIVE ARRANGEMENTS	30
A. Performance Comparison	30
B. Stability and Control Comparison	33
C. Conclusions and Recommendations	36
References	37
Figures 1 through 61	38-100

JR 2185 (3-52)M

CONFIDENTIAL

LIST OF FIGURES

Figure No.		Page
1.	Descriptive Arrangement - Wake Propeller Configurations	38
2.	GAC Wake Propeller Configuration in the NASA-Langley Full-Scale Tunnel	39
3.	Transcendental Wake Propeller Configuration in the NASA-Langley Full-Scale Tunnel	40
4.	GAC Wake Propeller	41
5.	Transcendental Wake Propeller	42
6.	Pressure Ratios Measured at Plane of Propeller	43
7.	Wake Velocity	44
8.	Axial Velocity Increase in Slipstream	45
9.	Tangential Velocity Distribution in Slipstream	46
10.	GAC Propeller Characteristics	47
11.	Aerodynamic Pitch Angle, Blade Angle and Blade Thickness Ratio	48
12.	Aerodynamic Pitch Angle	49
13.	Propeller Blade Width Factor	50
14.	Propeller Power Loading	51
15.	Propeller Thrust Loading	52
16.	Variation of Propeller Thrust Coefficient with Advance Ratio-GAC Wake Propeller	53
17.	Variation of Propeller Power Coefficient with Advance Ratio-GAC Wake Propeller	54
18.	Variation of Propeller Thrust Coefficient with Advance Ratio-Trans. Propeller	55
19.	Variation of Propeller Power Coefficient with Advance Ratio - Trans. Propeller	56

JR 2188 (3-52)M

CONFIDENTIAL

LIST OF FIGURES - continued

Figure No.		Pages
20.	Variation of Apparent Propeller Efficiency with Advance Ratio and Blade Angle - GAC Wake Propeller	57
21.	Variaton of Apparent Propeller Efficiency with Advance Ratio and Blade Angle - Trans. Propeller	58
22.	Comparison of Measured Hull Pressure Distributions for Various Airship Models - R $\approx$ 12 x 10^6	59
23.	Comparison of Measured Hull Pressure Distributions for Various Airship Models - R $\approx$ 18 x 10^6	60
24.	Non-Dimensional Hull Static Pressures VS (Local Hull Radius)^2 Propeller Off $\sim V_{avg}$ = 93.75 ft/sec (12 TP) . .	61
25.	Non-Dimensional Hull Static Pressures VS (Local Hull Radius)^2 Propeller Off $\sim V_{avg}$ = 137.5 ft/sec (20TP). .	62
26.	Variation of Pressure Drag Coefficient with Reynolds Number for Three Airship Models.	63
27.	Non-Dimensional Hull Static Pressures VS (Local Hull Radius)^2 GAC Propeller $\sim\beta$ = 20°, V=94.6 ft/sec T= 2.75 lbs.	64
28.	Non-Dimensional Hull Static Pressure-GAC Propeller β =20° V=94.6 ft/sec T =10.05 lbs	65
29.	Non-Dimensional Hull Static Pressures-GAC Propeller β =20° V=94.9 Ft/Sec T = 18.80 Lbs.	66
30.	Non-Dimensional Hull Static Pressures-GAC Propeller β =20° V=94.7 ft/sec T=23.95 lbs.	67
31.	Non-Dimensional Hull Static Pressures-GAC Propeller β =20° V=140.3 ft/sec T=3.90 lbs.	68
32.	Non-Dimensional Hull Static Pressures-GAC Propeller β =20° V=140.0 ft/sec T=13.61 lbs	69
33.	Non-Dimensional Hull Static Pressures-GAC Propeller β=20° V=139.7 ft/sec T=24.91 lbs	70
34.	Non-Dimensional Hull Static Pressures Trans. Propeller $\sim\beta$ = 20° V=92.8 ft/sec T=13.65 lbs..	71

JR 2188 (3-32)M

CONFIDENTIAL

LIST OF FIGURES - continued

Figure No.		Pages
35.	Non-Dimensional Hull Static Pressures-Trans. Propeller β = 20° ~ V = 138.3 ft/sec T = 11.35 lbs	72
36.	Variation of the Change in Pressure Drag, Due to Wake Propeller Operation, with Thrust Coefficient.	73
37.	Variation of Effective Drag Coefficient with Propeller Advance Ratio and Blade Angle for the GAC Wake Propeller	74
38.	Comparison of Apparent Efficiency and Effective Efficiency as Determined by Several Methods.	75
39.	Comparison of Apparent Efficiency Determined during Propeller Evaluation and during Aerodynamic Characteristics Evaluations	76
40.	Effect of Angle of Attack on Apparent Effiency.	77
41.	Effect of Elevator Deflection on Apparent Efficiency. .	78
42.	Effect of Combined Elevator Deflection and Attack Angle on Apparent Efficiency.	79
43.	Effect of Combined Attack Angle and Elevator Deflection on Apparent Efficiency.	80
44.	Effect of Wake Propeller on the Longitudinal Aerodynamic Characteristics in Pitch - GAC Propeller ~β = 20°	
	a. Lift Coefficient.	81
	b. Pitching Moment Coefficient	82
	c. Drag Coefficient.	83
45.	Typical Effect of Wake Propeller on the Lateral Aerodynamic Characteristics in Pitch (cross-derivatives)-GAC Propeller ~β = 20°	84
46.	Typical Effect of Wake Propeller on Boundary Layer Velocity Profiles at Two Hull Stations-$V_o \cong$ 94 ft/sec (12 TP)	85
47.	Typical Effect of Wake Propeller on Boundary Layer Velocity Profiles at Two Hull Stations-$V_o \cong$ 140 ft/sec (21TP)	86

JR 2109 (3-52)M

CONFIDENTIAL

LIST OF FIGURES - continued

Figure No.		Pages
48.	Variation of Local Static Pressure in the Wake Behind the Airship Model for Two Tunnel Velocities - Propeller Off	87
49.	Comparison of Local Static Pressure Ratios in the Wake with and without Wake Propeller Operation	88
50.	Comparison of Wake Velocity Distributions for Various Airships	89
51.	Effect of Wake Propeller Operation on Wake Velocity Distributions-GAC Propeller $\sim\beta = 15^{\circ}$	90
52.	Effect of Wake Propeller Operation on Wake Velocity Distributions-GAC Propeller $\sim\beta = 20^{\circ}$	91
53.	Effect of Wake Propeller Operation on Wake Velocity Distributions-GAC Propeller $\sim\beta = 25^{\circ}$	92
54.	Effect of Wake Propeller Operation on Wake Velocity Distributions-Trans. Propeller $\sim\beta = 20^{\circ}$	93
55.	Ratio of Effective Drag Coefficient to Basic Drag Coefficient for Various Advance Ratios and Blade Angles-GAC Wake Propeller	94
56.	Ratio of Effective Drag Coefficient to Basic Drag Coefficient for Various Advance Ratios and Blade Angles - Conventional and Fin-Mounted Propellers	95
57.	Horsepower Required for Varied Flight Conditions GAC Wake Propeller	96
58.	Horsepower Required for Varied Flight Conditions Conventional and Fin-Mounted Propellers	97
59.	Variation of Propeller Efficiency with Advance Ratio and Blade Angle~Conventional and Fin-Mounted Propellers	98
60.	Comparison of Apparent Propeller Efficiencies for Varied Flight Conditions	99
61.	Comparison of Horsepower Required for Varied Flight Conditions	100

CONFIDENTIAL

LIST OF SYMBOLS

C_D	=	drag coefficient, $D/q\forall^{2/3}$
C_{D_o}	=	basic drag coefficient (drag coefficient with propeller off)
C_{D_e}	=	effective drag coefficient
$C_{D_{run}}$	=	drag coefficient measured during test with propeller operating (includes thrust and drag)
C_{D_p}	=	pressure drag coefficient
C_{D_T}	=	non-dimensional thrust, $T/q\forall^{2/3}$
C_L	=	lift coefficient, $L/q\forall^{2/3}$
C_Y	=	sideforce coefficient, $Y/q\forall^{2/3}$
C_m	=	pitching moment coefficient $M/q\forall$
C_n	=	yawing moment coefficient $N/q\forall$
C_ℓ	=	rolling moment coefficient $\ell/q\forall$
C_{m_q}	=	rotary moment coefficient
C_{L_q}	=	rotary lift coefficient
C_T	=	thrust coefficient, $\frac{T}{\rho n^2 D^4}$
C_p	=	power coefficient, $\frac{BHP\ (550)}{\rho n^3 D^5}$
α	=	angle of attack, degrees (positive = nose-up)
δ_e	=	elevator deflection, degrees (positive = T.E. down)
β	=	propeller blade angle setting, degrees
η	=	propeller efficiency (apparent usually implied), $\frac{C_T}{C_p}$ (V/nD)
η_A	=	apparent propulsive or propeller efficiency
η_e	=	effective propulsive or propeller efficiency
D	=	propeller diameter (or drag)
D_p	=	hull pressure drag

JR 2168 (3-32)M

CONFIDENTIAL

CONFIDENTIAL

LIST OF SYMBOLS - continued

D_e	=	effective drag ($D_o - \Delta D$)
I	=	dynamic stability index
L	=	envelope or hull length
R	=	Reynold's Number based on hull length, VL/ν
T	=	propeller Thrust
T_e	=	effective propeller thrust ($T - \Delta D$)
V or V_o	=	freestream or wind tunnel velocity
V_L	=	local velocity in boundary layer or wake
V_1	=	local velocity in boundary layer or wake
V_2	=	theoretical velocity far downstream in wake
$\forall$	=	Hull volume
H_L	=	local total head pressure
p_L	=	local static pressure
p_o	=	freestream static pressure
HP	=	horsepower (also brake horsepower)
k_x	=	theoretical longitudinal inertia coefficient
r	=	local hull radius, or distance from hull, or distance from hull center line
p/q	=	non-dimensional hull static pressure
n	=	propeller revolutions per second
V/nD	=	propeller advance ratio
q or q_o	=	freestream or wind tunnel dynamic pressure, $\rho V^2/2$
$\mathcal{X}$	=	distance from hull nose
TP	=	wind tunnel velocity setting
GAC	=	Goodyear Aircraft Corporation
Trans.	=	Transcendental Aircraft Corporation
NASA	=	National Aeronautics and Space Administration

NOTE: Δ preceding any symbol denotes the change in the parameter due to propeller operation

CONFIDENTIAL

JR 2188 (3-52)W

CONFIDENTIAL

I SUMMARY

This report presents an analysis of the results of a wind tunnel investigation of the aerodynamic and propeller characteristics of two wake propeller configurations tested on a 1/20-scale powered model of a modified ZPG-3W airship. In addition, the report compares the characteristics of these configurations with the characteristics of a fin-mounted powerplant arrangement and a conventional car-mounted powerplant configuration previously tested on the same basic model hull. All tests were conducted in the NASA Full-Scale Tunnel at Langley Field, Virginia.

The evaluation of the two wake propellers, one designed by Goodyear Aircraft Corporation and the other proposed and designed by another company, indicated that the Goodyear wake propeller was superior in that the alternate wake propeller did not produce sufficient thrust for the higher velocities contemplated. It is shown that a wake propeller designed for a specific wake velocity distribution will produce propulsive efficiencies approaching 100 percent and will agree with the theoretically predicted values for such a propeller. The wake propeller propulsive efficiencies for the design condition are approximately 30 percent higher than the maximum efficiencies obtained for conventional airship propellers operating in freestream conditions.

The GAC wake propeller configuration, the fin-mounted powerplant configuration, and the conventional car mounted powerplant configuration are compared on the basis of the effects of the various propulsive systems on the performance, stability and control of an airship. The wake propeller configuration (with propeller operating) produces an increase in endurance (or range) of approximately 30 percent over the other configurations with no appreciable change in stability and control characteristics due to the propeller. The fin-mounted powerplant configuration results in a significant improvement in stability and control characteristics (with propellers operating) over either of the other two configurations, with propeller efficiencies comparable to normal airship propellers.

JR 2168 (3-32)M

CONFIDENTIAL

II INTRODUCTION

This report summarizes and compares the results of a wind tunnel investigation conducted in the NASA Full-Scale tunnel at Langley Field, Virginia on a 1/20-scale model of a modified ZPG-3W airship with four propulsive system arrangements. This is the final report required to be submitted under Bureps Contract NOa(s) 54-900c, Lot VI, Amendments 5, 10 and 14. It was the original intent to make this report a final summary report of all four configurations tested but since the requirement for a separate analysis report for the two wake propeller configurations were deleted by Amendment 14 of the subject contract, it is necessary to include much of the analyses of these configurations in this report so that all data from which summary comparisons and conclusions are obtained will be readily available for referal and to provide continuity and completeness of the data obtained for all propulsive arrangements. The results of the investigations of the car-mounted and fin-mounted powerplant configurations are presented in Reference a.

A major advantage of the investigations now completed is that all configurations utilized the same basic airship model (hull and empennage) and were all tested in the same wind tunnel facility at practically identical conditions, thus resulting in data that can be compared with very little regard to corrections due to variable test conditions and instrumentation. The models were tested at Reynold's Numbers from 12×10^6 to 18×10^6 compared to the full scale flight regime of approximately 100×10^6 to 350×10^6 which though not exactly adequate for accurate simulation of full-scale drag values it is better than most airship model tests and the comparative drag effects of the various models should have been acceptable and are all that were to be expected from the tests.

One of the major purposes of these investigations is to evaluate the various propulsive arrangements and to determine the best configuration for any future application to airships or to possible application to similar bodies such as submarines. This involves both the evaluation of the propulsive efficiency of the whole system and the effect of the system on the vehicle stability and control. The tests of the conventional car (or outrigger) mounted powerplants configuration are used as a basis for comparison and also to evaluate the effects of its propulsive system on the well-known stability and control characteristics of unpowered models. The fin-mounted powerplant arrangement has been investigated as a system that would both decrease the noise and vibration level in crew quarters of an airship, resulting in greater crew comfort and efficiency, and give significant increases in stability and control of the airship. Two stern propelled or wake propeller configurations have been tested. The primary advantage of such configurations is that the propeller operates in the wake of the airship hull, which is an area of reduced local velocities compared to freestream conditions, and thus propulsive efficiencies approaching or greater than 100% can be attained with less expenditure

JR 2189 (3-52)M

CONFIDENTIAL

II INTRODUCTION - continued

of power than with airship propellers operating in freestream conditions which normally attain efficiencies of only 70% to 85%. The theory and study of wake propellers is not new but very few systematic attempts have been made to properly design such a propeller and to prove that such a design will actually produce the predicted efficiencies and performance. In addition very little experimental data is available of the effect of pitch, yaw, or control surface deflection on the propulsive efficiency or of the effect of the wake propeller operation on the aerodynamic characteristics, stability and control of the airship.

An analytical study embodying the latest information on the design of a propeller operating in the wake of a body was conducted and presented in Reference b. From this study Goodyear Aircraft Corporation designed a wake propeller for the 1/20-scale airship model on the basis of wake or boundary layer measurements made on the model during previous tests on a dummy tail cone (reference i) at the proposed location of the wake propeller. This wake propeller, hereafter referred to as the GAC propeller was installed and tested on the 1/20-scale model of a modified ZPG-3W airship.

In addition to the GAC propeller, the subject contract required the contractor to fabricate and test a model wake propeller, similar to a helicopter rotor, designed and proposed by General Development Corporation and subsequently Transcendental Aircraft Corporation. Design information for this configuration, referred to as the Transcendental Propeller or Rotor, was obtained from References c and d and the contractors interpretation and model concept of their design was approved by personnel associated with the project.

Figures 1 thru 5 present a descriptive arrangement and photographs of the GAC and Transcendental Wake Propeller configurations. Figures 6 thru 15 present the wake characteristics for which the GAC propeller was designed and pertinent propeller design data and curves.

The first portions of this report presents the analysis of the wake propeller configurations and the second portion compares all configurations tested on the basis of performance, stability and control.

CONFIDENTIAL

III ANALYSIS OF THE WAKE PROPELLER CONFIGURATIONS

A. Description of Test and Instrumentation

Detailed descriptions of the test, test program, instrumentation and models are given in References (e) and (f) and only a brief description will be given in this report. The 1/20-scale model consisted of a scaled version of the ZPG-3W envelope or hull with the inverted "Y" empennage utilized during the car-mounted powerplant tests. The complete model was mounted on a single strut from the wind tunnel balance system which also provided pitch actuation. In order to accommodate a strain-gage drag beam device for more accurate drag measurement during these tests a much larger (in height or depth) car than the normal ZPG-3W car tested on the other configurations was fabricated and installed for all the wake propeller tests. The motor which provided power to the propeller was mounted in the aft end of the hull on a strain-gage mount which measured propeller thrust and torque.

Boundary layer total and static pressure surveys were made during the propulsive efficiency evaluations at two stations, one and two propeller radii forward of the GAC propeller plane. The rakes were mounted on the hull 60° from the top center-line so that the fin and ruddervator influence was negligible or minimum. Wake surveys also were conducted one foot aft of the propeller plane for all major propeller efficiency tests. In addition, the hull was provided with 25 flush mounted static pressure orifices located along the side center lines of the hull to provide information about hull pressure distributions with and without propeller operation. All these additional data were acquired to provide information about the effect of wake propeller operation on the parameters measured and to provide a possible basis for propeller design improvements or in the case of hull pressure to evaluate the change in pressure drag of the airship hull due to the propeller.

Basically the test program consisted of a propeller or propulsive efficiency portion wherein data was obtained for a range of operating conditions for each propeller and a second portion which evaluated the effects of propeller operation on the aerodynamic characteristics due to pitch and elevator deflection and conversely the effects of pitch (angle of attack) and elevator deflection on the propeller efficiency. Since the model was mounted on the tunnel balance system, six component force data were measured for most portions of the test program.

JR 2488 (3-52)M

It should be noted that all calculations and data for these tests are based on data obtained from NASA as preliminary data on 13 May 1960. Since this time, some of these data have been corrected by NASA personnel and it is felt that, with all corrections which were forwarded to the contractor by NASA, the data now employed represents the final data which is or will be presented in Reference (f). During the present analysis some apparent discrepancies have been discovered or noted and whenever possible were relayed to NASA personnel for their consideration and utilization.

The propeller efficiency evaluations were conducted at two free-stream tunnel velocities in order to cover the operating range for the propeller blade angles (β) investigated. The two tunnel velocity settings utilized are often referred to as the twelfth and twenty-first tunnel points or in abbreviated form, 12TP and 21TP, and correspond to freestream velocities of approximately 94 ft/sec and 140 ft/sec respectively with the slight variances in velocity at a setting being mainly a function of temperature, humidity and air density.

The GAC and Transcendental Wake Propellers were each tested at three blade angles for the following range of advance ratios (V/nD), power coefficients (Cp), and thrust coefficients (C_T)

Propeller	Blade Angle	V/nD Range	C_p Range	C_T Range
GAC	15°	0.5 to 1.0	0 to .05	0 to .09
GAC	20°	0.6 to 1.35	0 to .075	0 to .11
GAC	25°	0.7 to 1.6	.02 to .12	0 to .13
Trans.	20°	0.5 to 1.2	.03 to .065	.02 to .09
Trans.	25°	0.6 to 1.4	.045 to .10	.04 to .10
Trans.	30°	0.5 to 1.5	.085 to .145	.08 to .11

B. Propulsive Efficiency Evaluation

1. Apparent Efficiency (η_A)

Figures 16 thru 19 present the measured variations of propeller thrust and power coefficients with advance ratio for both the GAC and Transcendental configurations and were obtained from the strain-gage instrumented motor mount. The

JR 208 (3-52)M

apparent propeller efficiency (η_A) is obtained from these data from the conventional formula;

$$\eta_A = \frac{C_T}{C_p} (V/nD)$$

and the results are plotted in Figures 20 and 21 for the two propellers. These efficiencies are denoted as apparent efficiencies since they do not truly represent the propulsive efficiency of the whole system of the vehicle and propeller.

During the tests of the Transcendetal propeller it was noted that for the recommended blade angle of 17° (Ref. c) and also at 15° and 20° insufficient thrust was developed by this propeller to match the drag at $V \cong 140$ ft/sec (21TP). In an attempt to increase the propeller thrust the Transcendental test program was changed and all tests were conducted for blade angle settings of 20°, 25°, and 30°. Although this increased the thrust to some extent it was still deficient and less than the model drag at the 21TP velocity. Consequently, tests were conducted at RPM's up to 8000, or 3000 RPM above those programmed, with the propeller thrust still being less than the drag at $V \cong 140$ ft/sec. Due to stress limitations for sustained operation it was not advisable to run these propellers over 8000 RPM and no further attempts were made to obtain more thrust. The apparent efficiencies for the Transcendental propeller at T= D for $V \cong 94$ ft/sec are less than the comparable apparent efficiencies for the GAC propeller at T = D at thisvelocity and at $V \cong 140$ ft/sec. Therefore, since the Transcendental rotor configuration produced lower apparent efficiencies and did not produce sufficient thrust at $V \cong 140$ ft/sec it is not considered desirable to continue with any further analysis effort on this configuration. Reference (f) presents data showing the thrust deficiency for the Transcendental propeller with $V \cong 140$ ft/sec.

2. Effective Efficiency (η_e)

The effective efficiency in moving the airship through the air must take into account all drag increments which are a direct result of the wake propeller operation or its propulsion system. These include such drag losses (or increases) as propeller blade profile drag and any increase in the airship frictional drag and profile or pressure drag due to propeller operation. Generally the predominant increase in drag is produced by the reduction in positive pressures over the extreme aft end of the airship hull due to propeller operation.

JR 2-68 (3-52)M

The increase in frictional drag due to the increased velocity in the boundary layer with the propeller running is relatively small since only a small portion of the hull is affected (approximately 5% Lto 8%L at the aft end). The effect of propeller profile drag on the wake propeller efficiency was investigated in Reference (b) and generally it can be conservatively concluded that this might reduce the apparent efficiency by 10 to 20 percent depending upon the propeller RPM. This reduction is extremely difficult to estimate exactly since the profile drag of a wake propeller is also dependent upon the amount of turbulence in the wake. It should also be recognized that the measured thrust of the model propeller includes the propeller drag and therefore is accounted for in our data analysis.

Regardless of the origin of the increases in drag due to the wake propeller the total change in drag could be evaluated from the measured drag with the propeller off and that measured with the propeller operating and utilized to determine the effective efficiency of the configuration. The change in total drag due to propeller operation would be subtracted from the measured thrust to obtain the effective thrust utilized to propel the airship with a wake propeller.

a. Change in Drag Due to Wake Propeller Operation

It was recognized early in the planning stages of these tests that the highest possible accuracy in the measurement of drag would be required to yield acceptable values since the changes in drag would usually be the difference between two relatively small numbers. Therefore, NASA personnel designed and fabricated a drag balance instrumented with strain-gages that was to be mounted in the airship car and attached to the main tunnel support strut. This drag balance would be free of strut tare drags and would only require correction for the effect of strut-car interference drag. It was predicted that the accuracy of this balance would be at least ±0.1 pound of drag. The size of the drag balance necessitated the fabrication by NASA of a larger (deeper) car as noted previously to accommodate it, but unfortunately either the balance deflections exceeded expectations, or excessive vibration was present, or the car was just not large enough and much of the data was not usable due to apparent fouling between the car and drag balance device. Therefore, rather than try to guess or find which data was good and which bad all data obtained from this source has been discarded as inaccurate and thus drag data of probable high accuracy is not available.

GR 208 (3-52)M

There are two alternate means of drag change evaluation available; the first is evaluation of the drag measured by the wind tunnel balance system and the second is the determination of the pressure drag from the integration of the hull pressure distributions measured during the propeller efficiency evaluation. Both methods are considered to be less accurate than the desired accuracy as the stated accuracy of the tunnel balance system is in the order ±.2 lb for drag and it has always been recognized that the integration of a single row of hull static pressures (with their possible fluctuations and inaccuracies) is not a highly accurate procedure to determine pressure drag. However, since the determination of the drag change due to the propeller operation is absolutely necessary for the evaluation of the propulsive efficiency, which is needed to prove the wake propeller theory and concepts, an attempt has been made to evaluate the drag by the two alternate methods.

(1) Drag Evaluation from Wind Tunnel Force Balance System

The first attempt to determine the drag change due to propeller operation was made directly from the measured drag coefficients for the various operating conditions along with the measured propeller torque or power. The drag changes which are sought are mainly those due to the axial velocity increase in the propeller area and their effect on hull pressures and from classical and experimental propeller theory the axial velocity increase due to a propeller is primarily a function of the thrust coefficient (C_T). Therefore, the measured differences in drag coefficient from the propeller running and the propeller off were plotted against C_T. These data are very erratic and could not be faired into any logical variation and were abandoned as being too inaccurate.

A second evaluation of the tunnel force system data was conducted on the basis of the following derived method. If we define the effective drag coefficient (C_{D_e}) as the difference in the drag measured with the propeller off and the drag measured with the propeller running the following relationship of the items measured can be determined when it is understood that the tunnel balance system also "feels" the thrust of the propeller or the net drag (or thrust) of the whole airship system.

JR 2188 (5-52)M

CONFIDENTIAL

Let C_{D_o} = Drag coefficient without propeller or basic model drag coefficient

$C_{D_{run}}$ = Drag coefficient with propeller running

Then: $C_{D_e} = C_{D_o} - C_{D_{Run}} = C_{D_o} - (C_{D_o} + \Delta C_D - C_{D_T})$

where: ΔC_D = increase in drag due to propeller operation

C_{D_T} = measured propeller thrust converted to drag terminology

$$C_{D_T} = \frac{T_{meas.}}{q \, V^{2/3}}$$

This equation reduces to the form:

$$C_{D_e} = C_{D_T} - \Delta C_D$$

It can also be shown that C_{D_e} is proportional to or can be converted into the effective thrust $(T - \Delta D)$ and then into the effective thrust coefficient (C_{T_e}) from which the effective efficiency can be determined.

By definition and since the previous derivation shows that the effective thrust (T_e) is equal to the effective drag (D_e) then:

$$T_e = D_e$$

$$C_{T_e} \rho \, n^2 D^4_{PROP} = C_{D_e} \quad q \, V^{2/3}$$

$$\text{or } C_{T_e} = \frac{C_{D_e} \, 1/2 \rho \, V^2 V^{2/3}}{\rho \, n^2 D^4_{PROP}} = C_{D_e} \frac{V^2 V^{2/3}}{2 \, n^2 D^4_{PROP}} =$$

$$C_{D_e} \left(\frac{V}{nD}\right)^2 \left(\frac{V^{2/3}}{2D^2_{PROP}}\right)$$

Substituting the given values of the $(\text{volume})^{2/3}$ and the propeller diameter the following relationship is established for the GAC propeller data.

$$C_{T_e} = 4.025 \, (C_{D_e}) \left(\frac{V}{nD}\right)^2$$

CONFIDENTIAL

JR 2168 (5-52)M

CONFIDENTIAL

$$C_{T_e} = 4.025 \overset{\text{or}}{(C_{D_o} - C_{D_{run}})} \left(\frac{V}{nD}\right)^2$$

since $\eta = \frac{C_T}{C_p} (V/nD)$

then $\eta_e = \frac{C_{T_e}}{C_p} \left(\frac{V}{nD}\right) = \frac{4.025(C_{D_o} - C_{D_{run}}) \left(\frac{V}{nD}\right)^3}{C_p}$

With this equation, utilizing the actual measured values of C_{D_o}, $C_{D_{run}}$, V/nD and faired values of C_p obtained from Figure 17, the effective efficiency is derived in a slightly different manner although the same data as before is utilized. These effective efficiencies are plotted against the propeller advance ratio in Figure 38.

Another slightly different variation utilizing these same basic data can be obtained by plotting C_{D_e} vs V/nD as presented in Figure 37 and using the faired variations of both C_{D_e} and C_p in the above equation. These data for η_e are also plotted in Figure 38.

(2) Pressure Drag Evaluation from Hull Static Pressure Distributions

It is usually considered that the major change in drag of the airship due to the wake propeller is due to the change in hull pressure drag as noted previously.

Therefore since the propeller profile drag is included in the measured thrust and if it is assumed that the change in hull frictional drag is small or negligible, the evaluation of the pressure drag for the various propeller conditions should result in a close approximation of the total drag change.

Naturally since it will be used for every data point of the propeller's operating range the magnitude of the pressure drag of the hull without the propeller is very important. The hull static pressures were obtained for the propeller-off condition but due to faulty camera operation (improper lens opening) during this particular set of tests the pictures of the manometer tubes were extremely faint and the fluid levels could not be accurately read although many attempts were made to increase their legibility by use of photographic techniques, magnifying glasses and other means.

JR 2168 (3-32)M

The best values obtained were erratic and did not compare at all with theoretical values or measurements made on other models as given in References (g) and (h). Therefore it was necessary and judged to be valid to utilize hull pressure data obtained with the propellers running at very low RPM and practically zero thrust. Tests of this nature (approx. zero thrust) for both propellers (GAC and Transcendental) at each blade angle were utilized in determining the average pressure distribution over the hull length for both tunnel test velocities. The average values of the hull static pressures for these approximately zero thrust conditions are plotted in Figures 22 and 23 and compared with measured hull pressures from other model tests of References (g) and (h). These comparisons indicate that the utilization of the low thrust average static pressures as zero thrust or power values is a reasonable or very good substitution as the various distributions, especially compared to the Reference (g) data, show excellent agreement.

It can be shown that the pressure drag of an airship can be obtained by integrating the area of the curve formed by plotting the non-dimensional hull static pressures against the square of the local hull radius at the longitudinal location of the pressure orifice.

The resultant mathematical expression is:

$$C_{D_p} = \frac{\pi}{\forall^{2/3}} \int_{r@\psi=0}^{r@\psi=L} P/q \, r \, dr$$

or

$$C_{D_p} = \frac{\pi}{\forall^{2/3}} \int_{r^2@\psi=0}^{r^2@\psi=L} P/q \, (dr^2)$$

Figures 24 and 25 present the variation of the quasi-propeller off non-dimensional hull static pressures plotted against the square of the local radius corresponding to the longitudinal location of each orifice for the two freestream tunnel velocities utilized during these tests.

JR 2468 (9-52)M

Integration of these curves yield pressure drag coefficients of 0.0059 and 0.0054 for the 12TP ($V_o \cong 94$ ft/sec) and 21TP ($V_o \cong 140$ ft/sec), respectively. These two values represent and are used as the airship pressure drag coefficients for the propeller off or zero thrust condition. As an indication of their relative accuracy Figure 26 plots these values as a function of Reynold's Number along with pressure drag coefficients obtained from Reference (g) and (h) data.

The hull static pressure distributions for all the GAC propeller operating conditions of the efficiency evaluation were plotted in the same manner as Figures 24 and 25 and were integrated to obtain the pressure drag for each condition and the corresponding increase in drag due to propeller operation. Typical variations of these power-on data are given in Figures 27 through 35 for both the GAC propeller and the Transcendental propeller. The GAC propeller data is for the design blade angle of $\beta = 20^{\circ}$ and the various curves show the decrease in positive pressure over the aft portion of the hull as the propeller thrust (or C_T)increases, resulting in an increase in pressure drag and thus a larger change in pressure drag with respect to the propeller off condition. Since the hull contour and the local axial velocity determine the hull pressures and because the increase in the axial velocity due to a propeller is primarily a function of the thrust coefficient, the increases in pressure drag for the GAC propeller are plotted in Figure 36 as a function of C_T for the three blade angles investigated at each tunnel velocity.

The variations of ΔC_{D_P} with C_T in Figure 36 indicate that in these tests the change in pressure drag is highly dependent on the propeller blade angle and freestream velocity. The value of ΔC_{D_P} increases with decreasing blade angle. It was at first believed that there should be very little effect due to the relatively small difference in the two velocities utilized. As will be shown in a later section of the report, there are differences in the non-dimensional boundary layer and wake velocities for the two tunnel velocities employed which might be a reason for the dependence on freestream conditions. An additional factor which might contribute to the variation of drag change with freestream velocity is one of the possible reasons for the drag coefficient differences at the two tunnel velocities as measured on the tunnel balance system for the propeller off condition. These values corrected for strut tare effects and other standard corrections resulted

JR 2188 (3-32)M

in C_{D_o} values of .0208 and .0215 for the 12 TP and 21 TP, respectively. Since the lower velocity (12TP) has a lower drag coefficient, which is contrary to normal test values obtained at Reynolds Numbers within the turbulent flow regime, it might be concluded that the lower TP tests, which have a Reynolds Number of approximately 12×10^6, are either experiencing laminar flow conditions or possibly are in the transition region. The majority of airship test data indicates that this test should have had turbulent flow at this Reynolds Number although it is close to the transition region and therefore it is possible that a lower total drag coefficient could have been measured. It is also possible that the car drag might have an appreciable effect on these values. During tare evaluations car drag coefficients were ascertained with the $C_{D_{car}}$ at the 21 TP being almost twice as large as that at the 12 TP. If these measured car drag coefficients are subtracted from the measured total drag coefficients, the resulting values of C_D = .0189 for the 12TP and C_D = .0183 for the 21TP show a more normal relationship with the airship Reynolds Number. Although the exact reasons as to the behavior of the ΔC_{D_p} values can only be theorized at this time, the values plotted are accepted along with the knowledge that the integrations of these curves based on hull pressures along one plane are subject to possible inaccuracies.

Values from the faired curves of Figure 36 were converted into drag values in pounds and utilized with the measured thrust, velocity and horsepower to obtain the effective efficiency from the following equation.

$$\eta_e = \frac{(T - \Delta D_p)\, V}{550\ BHP} = \frac{T_e\, V}{550\ BHP}$$

Where $\Delta D_p = \Delta C_{D_p}\ q\ V^{2/3}$, lbs ($\Delta C_{D_p}$ from Fig. 36)

T = Measured thrust, lbs.
T_e = Effective Thrust, lbs.
V = Freestream tunnel Velocity, ft/sec
BHP = Horsepower obtained from measured torque

The results of these calculations for the GAC wake propeller configuration are plotted in Figure 38 along with the efficiencies obtained from the drag measurements of the tunnel balance system.

JR 2168 (3-52)M

b. Discussion of Effective Efficiencies

The effective propulsive efficiencies for the GAC wake propeller at three blade angles as determined by the three methods discussed previously are shown in Figure 38 along with the apparent efficiencies (η_A) obtained from Figure 20. The most evident item is the separate variations of η_e, calculated from the hull pressure drag, for the two velocities involved along with the decreasing variance (less separation between the two velocity curves)as the blade angle is increased. In general, the three methods for obtaining η_e agree fairly well at low V/nD (high thrust values) but show marked disagreement at high V/nD (low thrust values) and in fact the effective efficiencies derived from force data show unrealistic values at high advance ratios (above V/nD = 1.0). It is believed that this is due to the inaccuracy of all the measurements including drag, thrust, and torque which are relatively small in this range. The shape and magnitude of the effective efficiency curves were expected to correspond to those indicated by the evaluations of the pressure drag except for the variation with the two velocities. Since thrust measurements were corrected for a "base pressure" existing on the motor mount without the propeller, it is possible that this "base pressure" correction varied with the RPM or thrust of the propeller although no data is available from which this effect could be evaluated. The variation with velocity cannot be satisfactorily explained aside from theorizing about the relative effect of the propeller thrust on the non-dimensional pressures on the aft hull (for the two velocities) which were measured and found to differ even with zero power. The decreasing effect of velocity with increasing blade angle indicates that the velocity effect might be due to propeller characteristics not envisaged in the design.

The boundary layer and wake velocity measurements discussed later in this report show some differences for the two velocities and might have some effect on the efficiencies. However, reference (b) investigated theoretically the influence of a different wake velocity distribution on a particular wake propeller's characteristics which indicated minor differences in the efficiencies obtained and definitely not as large as the 12% approximate difference shown for the two velocity conditions obtained from the pressure drag evaluations at the design V/nD of .91 and blade angle of 20°.

At the design conditions for the propeller (β = 20°, V/nD = .91, T=D=20 lbs, BHP ≅ 5, V = 140 ft/sec) an effective efficiency of approximately 98% had been predicted

JR 2188 (3-52)M

in Reference (e). The plotted test data of the various methods at V/nD = .91 ranges from η_e = 86% to η_e = 104% with almost exactly 98% being observed from the pressure drag data at $V_o \cong 94$ ft/sec. Though it could be claimed that the predicted efficiency was obtained or exceeded by most of the data, and that a wake propeller can thus be designed that will produce predicted efficiencies and thrust, and will absorb a certain amount of power; it is probably more appropriate to state that the theories and design of wake propellers have been essentially substantiated but that some items need further analysis and investigation or must be ignored on the basis of the accuracy of the determination of η_e.

When it is considered that the preferred method of drag evaluation could not be utilized, the effective efficiency variations of Figure 38 are almost better than could be expected but do not yield quantitative values which could be used in any exact performance comparison that would show the distinct advantages of this type of propulsive system over the conventional or fin mounted powerplant arrangements. General comments and information pertaining to the performance characteristics are made in Section IV of this report.

C. Effect of Angle of Attack and Elevator Deflection on Wake Propeller Efficiency (η_A)

The effect of angle of attack and elevator deflection was measured on the model subsequent to the basic efficiency evaluation. Figure 39 shows a comparison of the efficiency data obtained during the basic propeller evaluation and the efficiencies obtained for three power settings (RPM's) at or near thrust equals drag for a range of angles of attack from -10° to +10° and an elevator deflection range from +20° to -20°. The apparent efficiencies obtained during these tests at α = 0° and δ_e = 0° are identified and a curve drawn through them while most of the other data is not identified explicitly but just shown as a value to establish an envelope curve for comparative uses. Figure 40 shows the effect of angle of attack on η_A for the three power settings, while Figure 41 plots the variation of η_A with elevator deflection, and Figures 42 and 43 show the effect of combined elevator and angle of attack on the apparent efficiency for one or two power settings only. The following conclusions are derived from these data:

(a) At α = 0° the effect of elevator deflection on η_A is negligible up to 10° or 20° (T.E. up or down) with a maximum increase due to 20° down elevator of three percentage points being measured at the lowest power setting (highest V/nD). (See Figure 41)

JR 2188 (3-32)W

(b) There is a steady decrease in η_A with $+\alpha$ with an average maximum decrease for the three power settings of approximately 8 percentage points at $\alpha = +10^\circ$ (See Figure 40).

(c) Disregarding the point at negative α's obtained for the low power setting since they appear to be in error, it can be seen that the efficiency increases slightly to $\alpha = -5^\circ$ and then decreases to an efficiency at $\alpha = -10^\circ$ which is only slightly less than the efficiency measured at $\alpha = 0^\circ$. (See Figure 40)

(d) The effects of combined elevator and angle of attack are generally the same as for plain elevator and plain angle of attack with the effect of α predominating and relatively small effects due to elevator at any particular attack angle. (See Figures 42 and 43)

A few comments are in order with regards to the comparisons presented in Figure 40 and the values obtained from the lowest power setting of 4220 RPM ($V/nD \cong 1.018$). Figure 40 shows data points at $\alpha = -3^\circ$ and $\alpha = -5.5^\circ$ that definitely appear to be in error and not at all consistent with other values. This discrepancy also is shown in Figure 39 where these values form a group of points for various δ_e's and α's that are inconsistent. Therefore it appears that these data points should probably be discarded. Also shown on Figure 40 is a curve representing a probable variation of η_A with α for the lowest power setting which would indicate a fairly large difference in the value of η_A at $\alpha = 0$ over the actual measured value. It was first felt that this curve would be more correct but the comparisons shown in Figure 39 show the great majority of data points for other δ_e's and α's at this V/nD occurring in a general envelope of all data points measured in a manner tending to support the actual measured value at $\alpha = 0^\circ$. Therefore, there is an indication that the apparent efficiencies determined at the time of these later tests were different than those determined during the basic propeller efficiency evaluation tests. The magnitude of the difference is shown in Figure 39 and if it is correct either indicates the lack of repeatibility for similar conditions due to inaccuracies in the measured data or varying flow or wake conditions existing during the tests.

In conclusion it can be stated that normal elevator only deflection has little effect on the wake propeller efficiency while the effect of angle of attack is variable but should not exceed a 10% reduction for normal airship angles of attack in excess of +5%.

JR 2188 (3-32)NJ

CONFIDENTIAL

D. Effect of Wake Propeller on Aerodynamic Characteristics

The effect of the wake propeller on the non-dimensional lift, pitching moment, and drag were obtained for three power conditions at or around thrust equals drag in addition to these values with the propeller off. Figures 44a, 44b and 44c present these data as well as comparative data obtained from the car-mounted and fin-mounted powerplant configuration tests. All drag data has been corrected for wind tunnel support tares and their variation with angle of attack. The effect of the wind tunnel support strut on lift and pitching moment is generally small and since it is not included in the car or fin mounted powerplant data it is not utilized in these plots for the wake propeller configuration. All lift data has been corrected for direct propeller thrust components in a manner similar to that utilized in Reference (a).

1. Drag Coefficient

Since the elevator effect on drag coefficient was not obtained for the zero power condition and since the actual drag coefficient magnitudes from such tests are not utilized for full-scale work, only the changes due to the wake propeller are important and these are only available for the zero elevator condition. In most respects the drag coefficient increase due to effects of the three power settings utilized is fairly uniform throughout the angle of attack range at $\delta_e = 0$ with increasing drag occurring with increasing RPM or thrust. The maximum increase in drag coefficient due to the highest power condition utilized in these particular tests is in the order of $\Delta C_D \cong .0055$, occurs near $\alpha = 0$, and represents an increase of approximately 25 percent over the power off condition. The increase in drag coefficient appears to be slightly smaller at high negative and positive angles of attack but it would be conservative to assume equal ΔC_D for all attack angles. Of course this ΔC_D at a high attack angle represents less percentage increase in drag over that at the same attack angle for power-off. In order to illustrate the effects of varying power with the elevator deflected, the data for $\delta_e = \pm 20^o$ is plotted in Figure 44a although data for propeller off is not available. The majority of this data also shows uniform effects of power similar to that observed at $\delta_e = 0$ with probably no significant increase in ΔC_D (change in drag due to propeller operation) over that observed at $\delta_e = 0$, if a value of drag coefficient without power is estimated.

It therefore appears reasonable to conclude that the angle of attack and elevator deflection has little effect on the drag coefficient increase due to the wake propeller operation for the conditions tested. The drag coefficients plotted in Figure 44c are pure drag in that the measured thrust has been

JR 2108 (3-32)M

added to the measured T - D, but it should also be noted that thrust was only approximately equal to drag around zero angle of attack, zero elevator and the highest power condition and no attempt was made to simulate T = D for other conditions although essentially they would represent such a condition at a lower velocity which would also occur on an actual airship flying with constant power at various angles of attack and elevator deflections.

2. Lift Coefficient

The lift coefficients with the wake propeller off for various α's and δ_e's are compared in Figure 44a with similar data from the Reference (a) tests and show fairly good agreement in most respects. The slight differences which do exist are probably due to the larger car on the wake propeller configuration, slightly different tares due to different support arrangements, and general data repeatibility and accuracy. Curves are drawn through the power-off data at $\delta_e = 0^\circ$ and data points (corrected for direct thrust effects) are shown for the three power conditions investigated. The other wake propeller curves for various δ_e's are just faired curves through the power-on data. The data at $\delta_e = 0^\circ$ for which power-off data is available show no particularly consistent behavior due to the wake propeller operation with data at one angle of attack showing no change in lift coefficient and data at other angles of attack indicating reductions or increases in lift. The maximum change in lift coefficient measured is in the order of $C_L = \pm.004$ which for a full-scale ZPG-3W airship flying at 5000 ft altitude with an airspeed of 50 knots is equal to less than 500 lbs of lift. Since all the power-on data points exhibit changes which are small and vacillating, it can be concluded that the wake propeller has no effect upon the lift characteristics.

3. Pitching Moment Coefficient

The variation of the pitching moment coefficient with angle of attack and elevator deflection for the GAC wake propeller configuration at various power conditions is given in Figure 44b along with comparative data for the car and fin mounted powerplant configurations. Power off (or wake propeller off) data is only available for $\delta_e = 0^\circ$ on the wake propeller configuration and a curve is drawn through these points. The curves drawn through the other wake propeller data represent faired curves through the three power or thrust conditions tested to give an indication of the shape of the curve even though propeller off data is not available. It is immediately apparent that the wake propeller configuration data with or without the propeller does not exhibit the same pitching moment characteristics as

JR 2488 (3-52)M

the car and fin mounted powerplant configurations. Extensive plotting and analysis of car and/or fin mounted powerplant pitching moment data has shown that for negative angles of attack the wake propeller data show fairly reasonable agreement (or explainable variations) but no such agreement can be shown for positive angles of attack, especially at $\alpha = +9.5^{\circ}$. The initial reaction to the observed discrepancies was that it might be due to the additional drag of the larger car utilized on the wake propeller configuration since it has already been shown that the lift curves for the various configurations are essentially similar.

In conjunction with tare drag evaluations of both models the drags of the two different cars were measured and the measured drag coefficient of the large car at $\alpha = 0^{\circ}$ was 0.0032 while the small car had a drag coefficient of 0.0010 which gives a change in drag due to the larger car of .0022. This car drag increase would only increase the pitching moment coefficient by approximately 0.0010 compared to the change shown in Figure 44b at $\alpha = 0^{\circ}$ of 0.0130.

Actual total drag data comparisons for the various models at $\alpha = \delta_e = 0$ show a maximum difference between the fin mounted and wake propeller configuration of $\Delta C_D = .0068$. (It should be noted that this represents an extreme value which was discarded as being in error.) This value, assuming it all came from the car, would still only change the pitching moment by a C_m of approximately 0.0032.

Examination of the wake propeller configuration pitching moment tares indicates that they are relatively small, exhibit nearly the same magnitude throughout the attack angle range, and would not change the shape or magnitude of the wake propeller data to any significant degree and might even increase the disagreement at low positive attack angles.

The addition of the tail cone for the wake propeller has been studied and it is considered that this should not affect the lift centroid enough to produce the measured differences in pitching moment coefficient.

Usually, in airship stability analyses the possibility of an upwash from the car affecting the tail surfaces has been considered negligible and various model tests and calculations have supported this assumption. However, since all other attempts to explain the measured differences in pitching moment characteristics have not been successful it is proposed now, without definite proof, that the larger (deeper) car might have resulted in upwash effects on the lower tails which while producing relatively large moment changes, due to the long

JR 2188 (3-52)M

coefficient with angle of attack for the propeller off condition and for the propeller operating at 5000 RPM which approximately gives thrust equal to drag at $\alpha = 0$. It is apparent from this typical plot (others were similar) that the effect of the propeller operation is negligible or within the accuracy of the normal data scatter.

E. BOUNDARY LAYER AND WAKE VELOCITY MEASUREMENTS

1. Non-Dimensional Boundary Layer Velocities

The velocity in the boundary layer was obtained from two rakes mounted on the hull at approximately the 90 and 95 percent stations, with each rake consisting of 14 total head tubes and 4 static pressure tubes spaced along the rake height of 14 inches. These tubes were connected to the same manometer which measured hull static pressures and consequently the data for the propeller off condition were very faint and difficult to read as noted in Section I-B-2-a of this report. Therefore the data was erratic in some instances but enough of the readings appeared reasonable so that curves could be faired through the data with more emphasis attached to points that were near a static pressure tube. This was necessary since the NASA IBM calculation of the data assigned a static pressure reading to be utilized for adjacent total head readings which resulted in apparent errors in velocities determined from total head tubes located some distance from the static tube, due to the variation in static pressure in the boundary layer.

The boundary layer velocity profiles are not necessary for the analysis of the wake propeller but do shed some insight into the flow conditions forward of the wake propeller. In order to illustrate the effects of the wake propeller operation on the non-dimensional boundary layer velocities typical data is presented in Figures 46 and 47 for the propeller off, two freestream velocities, and for three RPM or thrust conditions with the propeller set at the design blade angle of 20 degrees. The power off velocity ratio data for $V_o \cong 140$ ft/sec is more regular and creditable than the measured data for $V_o \cong 94$ ft/sec which exhibits unnatural values between 12" and 14" above the hull for the forward (90%L) rake.

In propeller theories it is generally conceded that the incoming velocities forward of the propeller can be increased as far forward as 1/2 propeller diameter while the forward rake located one propeller diameter in front of the propeller shows increased velocities in this region especially for the higher V_o. However, for this velocity both the forward and aft rakes indicate approximately the same velocity increase which is not justifiable from theoretical considerations. The low velocity data ($V_o \cong$ 94 ft/sec) for both rakes indicate more reasonable differences

JR 2168 (3-52)M

with only small velocity changes for the forward rake and relatively much larger increases for the aft rake.

The curve representing a power-on condition in Figures 46 and 47 is drawn through the data points obtained at the highest thrust condition but except for velocity ratios close to the hull (within 2 or 3 inches) the effect of the variable thrust conditions is negligible with all data for a particular distance from the hull being approximately equal for the various power-on conditions.

2. Velocity Distributions in the Wake

The total and static pressures were measured in the wake of the model one foot aft of the propeller plane for two tunnel velocities (V_o) with power-off and for all conditions with power-on. The rake employed was approximately 24 inches high with 21 total head tubes and 6 static pressure tubes spaced along the rake. As is customary the NASA IBM computation assigned certain static pressure tubes readings to total head tube readings on each side of the static and in many cases two of the total head tubes were 2 inches from the static tube and do not reflect the radial variation in static pressure within the wake. This results in velocity profiles that in certain portions of the wake look like "Steps" instead of smooth curves. Therefore, in this analysis velocity profile curves are faired with the static pressure variation in mind, thus resulting in smooth variations.

a. Static Pressure in the Wake

That a significant variation in wake static pressure does occur is shown in Figures 48 and 49. The exact location of the static pressure tubes was not known since the contractor's information about the rake indicated only five static tubes while test data shows six static pressure readings, but the locations utilized are approximately correct. Figure 48 plots both the variation in the absolute static pressure with distance from the center line of the airship and the variation of the non-dimensional static pressure, for both tunnel velocities employed during the propeller off tests. It is noted that the non-dimensional static pressures (P_L/q_o) vary with tunnel velocity so there can be some error introduced in comparing propeller-off data, obtained at the 16TP and 20TP, and propeller operating data which was obtained at the 12TP and 21TP.

Figure 49 presents a comparison of the propeller-off non-dimensional static pressures along with typical power-on conditions for the GAC wake propeller at β = 20 degrees.

JR 2168 (3-52)M

center line of the airship for three thrust conditions for each of the blade angles and freestream velocities investigated on the GAC wake propeller. These typical variations are indicative of the efficiency of the wake propeller in "filling in" the low velocity region existing behind an airship hull. As was expected, the propeller shows relatively small effects in the region near the center-line of the hull, since the GAC propeller blade has a hub approximately 1.5 inches in radius, and the blunt tail cone occurring forward of the propeller blocks out almost an additional inch of propeller blade. However, even without these limitations it is known that such a propeller is very ineffective at the root in producing thrust and/or slipstream velocity increase. For the lower tunnel velocity ($V_o \cong 94$ ft/sec) the wake velocity ratio for maximum thrust generally reaches 1.0 between 2 and 3 inches from the origin and at $V_o \cong 140$ ft/sec a velocity ratio of 1.0 is obtained between 5 and 6 inches from the center line (origin) for all blade angles.

Therefore, to further improve the efficiency of the wake propeller the emphasis should be placed in this locality with modifications to the tail cone and propeller hub to improve the flow conditions and possible increased effort in the propeller blade design near the root. It was recognized that the model tail cone and propeller arrangement utilized was not the best for attainment of maximum efficiency but it was necessary to reduce fabrication costs and simplify the design. The actual design contemplated for a full-scale application would probably involve an arrangement with the propeller blades intersecting the tail cone with flexible seals to prevent flow into the interior of the tail cone and still provide the ability to change the blade angle if this was desired. The tail cone, faired to a more efficient end, instead of a blunt cut-off, would rotate with the propeller. Such improvements might increase the propulsive efficiency a few percent but this increase would also have to be justified by refined analysis on the basis of the possible added weight and complexity of the system and its effect on range, endurance and cost.

It also appears that a slight increase in the propeller diameter might be beneficial as the wake velocity ratios show that the ratio usually drops below 1.0 around 10 or 11 inches from the center line. However, this is probably due to the contraction of the slipstream and its decrease (or reversal) in ΔV associated near the tips of propellers, so any added diameter might be of doubtful value. It is not due to any tip losses associated with high tip speeds and compressibility as the propeller was not operated at high RPM and the calculated compressibility losses for the maximum RPM tested were zero.

JR 2168 (3-32)M

Figure 54 presents typical variations of the wake velocity ratios for the Transcendental propeller at a blade angle of 20°. Although no analysis of this configuration is performed due to its thrust deficiency, the above variations are given for comparative purposes. It is again noted that curves were faired through the measured velocity ratios with much greater emphasis on values obtained nearest the few static pressure tubes so although points are ignored it is justifiable and more indicative of the true velocity ratios. The Transcendental velocity ratios at $V_o \cong 94$ ft/sec indicate this propeller is not quite as efficient as the GAC wake propeller in "filling in" the wake except at the highest RPM, which incidentally was extended during the tests from a programmed value of 5000 RPM to 8000 RPM to provide sufficient thrust for thrust equals drag. At $V_o \cong 140$ ft/sec the Transcendental propeller deficiency is immediately noticeable as even the curve for the maximum value of 8000 RPM does not attain a velocity ratio of one. As noted previously the Transcendental propeller did not produce sufficient thrust at this velocity for T = D and this is reflected in the plotted wake velocity ratios.

d. Drag Evaluation from Wake Measurements

The evaluation of drag from measurements in the wake is derived from classical theories previously found to give reasonable agreement with conventional drag measurements. The theories and equations have been extensively presented in Reference (b) and only the final equation from this analysis will be utilized to perform the integration of the measured wake velocities and pressures. The equations derived and presented in Reference (b) are

$$C_{D_W} = \frac{4\pi}{\forall^{2/3}} \int_0^{r_w} \sqrt{\frac{P_L - p_L}{q_0}} \left(1 - \sqrt{\frac{H_L - p_0}{q_0}}\right) r\, dr$$

or

$$C_{D_W} = \frac{4\pi}{\forall^{2/3}} \int_0^{r_w} \frac{V_L}{V_0} \left(1 - \sqrt{\frac{H_L - p_0}{q_0}}\right) r\, dr$$

where: C_{D_W} = drag coefficient determined from integration of wake

H_L = local total head or pressure in the wake

P_L = local static pressure in the wake (p_L)

JR 2188 (3-52)M

q_o = freestream dynamic pressure (tunnel q)

p_o = freestream static pressure or static pressure in the wake infinitely far downstream

V_L = local velocity in the wake

V_o = freestream velocity (tunnel V)

r = radial distance from center of wake or extended center line of hull

r_w = limit of integration or radius of wake (taken as 24 inches which is the height of the rake used and generally equal to or greater than r_w)

The second term in the parenthesis within the integral is the correction due the fact that in wake measurements close to a body the local static pressure is not uniform and has not yet attained its freestream value. Unfortunately, the tunnel static pressure utilized in tunnel velocity and dynamic pressure measurements were not measured separately so a reasonable substitution must be made. The best values to which there was ready accessibility were the static pressures measured at the 24 inch location of the wake rake. Although the plotted static pressure evaluations of Figure 48 do not particularly indicate an asymptotical approach at the 24 inch location this value is considered the best available with the realization that some errors could result from its utilization.

Wake integrations were conducted for the two propeller - off conditions available and the results are:

C_{D_W} = .0144 for 16TP, V_o = 112 ft/sec, q_o = 14.90 lbs/ft^2

If the increase in V_L/V_o at radial station 0 is ignored and the curve faired into a more reasonable point the value becomes:

C_{D_W} = .0150 for the 16TP.

C_{D_W} = .0239 for 20TP, V_o = 135.3 ft/sec, q_o = 21.8 #/ft^2

Since the wake measurements were obtained in a region relatively unaffected by the car, support strut, and tails it can be concluded that the wake integration actually gives the value of the bare hull drag coefficient. Therefore, for comparative purposes, the drags obtained from the wind tunnel balance (force data) must be reduced by the magnitude of the car and

JR 2188 (3-52)M

inaccuracies in the wake data and/or the force data, but it is not within the realm or purpose of this report to completely evaluate these differences. The drag of the bare hull obtained from the force data does indicate a logical variation with Reynolds number with no apparent effects of transition or laminar flow at the lower velocity.

JR 2188 (3-52)M

F. Wake Propeller Conclusions

The purpose of the wake propeller tests was to substantiate or prove that such a propeller designed by methods established in Reference (b) would actually produce the efficiencies predicted by these theoretical means and would prove superior to conventional propellers in the propulsion of airships without seriously affecting the stability and control.

The failure of equipment required to measure the drag with the best accuracy hampered the efforts to prove the theories beyond a shadow of a doubt. However, the evaluations substituted show that for the design conditions, the predicted efficiencies ($\eta_e = 98\%$) were attained or exceeded in 3 out of 4 of the substituted evaluations.

It is also concluded that the operation of a wake propeller does not change the stability or control of the airship to any measurable degree for most airship attitudes and flight conditions.

The effect of pitch or angle of attack on the wake propeller efficiency is small (less than $\pm 5\%$) up to $\alpha = 5^\circ$ and at $\alpha = +10^\circ$ the maximum decrease is in the order of 8 to 10 percentage points which would result in an efficiency for the wake propeller that is still higher than conventional propellers at zero angle of attack.

The effect of elevator deflection on the wake propeller efficiencies is negligible for small deflections and are less than a 5% decrease at $\delta_e = \pm 20^\circ$.

The GAC wake propeller is superior to the Transcendental propeller tested in that the latter propeller did not produce sufficient thrust for thrust equal drag at the higher velocities.

CONFIDENTIAL

IV. COMPARATIVE ANALYSIS OF VARIOUS PROPULSIVE ARRANGEMENTS

Aerodynamic tests and evaluations of four propulsive systems for an airship have been completed and an analysis of their comparative characteristics and advantages is necessary to complete the requirements of the subject contract. The results of such an analysis should be the selection of an optimum or best propulsive system for application to future airships or other vehicles of a similar nature. In this respect, it must be noted that the optimum or best propulsive system is also a function of the specific mission that the airship is expected to perform. This report will summarize the aerodynamic qualities of the four configurations investigated with regard to performance, stability, and control.

Since the Transcendental configuration, as noted in previous sections of this report, did not measure up to expectations in that it would not produce the necessary thrust at higher airship velocities it will not be included in this comparative analysis. A redesign of this propeller with greater solidity might possibly result in a configuration that could produce sufficient thrust and efficiencies comparable to the GAC wake propeller.

A. Performance Comparison

It was originally intended to compare the car-mounted powerplant, fin-mounted powerplant, and wake propeller configurations on the basis of a specific mission performance profile similar to a full-scale ZPG-3W airship mission. This concept has been abandoned for two reasons: (1) the effective propeller efficiencies of the GAC wake propeller could not be determined to the degree of accuracy required for such a comparison; and (2) the fact that the best performance for one type of mission (i.e. AEW patrol) might result for one configuration which might not produce the best performance for another type of mission (i.e. ASW search with sonar operations).

Therefore an alternate general method of comparison is utilized to show the relative performance capabilities of the three systems. Performance as utilized in this report is defined as those factors affecting the maximum velocity and the fuel consumption and thus range and/or endurance of the airship. The present comparison will be based on the horsepower required to produce various amounts of thrust and the propulsive efficiencies associated with these thrusts and powers. Data for the conventional (car mounted) and fin-mounted powerplant configurations are obtained from References (a) and (i).

The first step in this analysis is the determination of the effective drag coefficient (C_{D_e}), which has previously been defined in Section I-B-2 of this report, and plotting the variation of C_{D_e}/C_{D_o} against

JR 2186 (3-52)M

V/nD for the three propeller configurations. Figures 55 and 56 present this information for the three propellers at various blade angles and show the lines for various thrust and drag combinations inherent in the definitions of C_{D_e} and C_{D_o}.

The next step is the calculation of the horsepowers required for the various conditions of V/nD, β, T, and D. These results are plotted in a similar fashion in Figures 57 and 58 for the GAC wake propeller, the car-mounted or conventional propeller, and the fin-mounted propeller.

The final items of information necessary for the comparison are the propulsive efficiencies of the various configurations. It is again noted that only relative comparisons are utilized so that the apparent efficiencies are employed in the analysis. The apparent efficiencies of the GAC wake propeller have previously been presented in Figure 20 and the efficiencies for the other configurations are given in Figure 59 as a function of V/nD and blade angle. Figure 60 presents a comparison of the various propellers and their efficiencies for several ratios of T and D.

It might be considered that this last curve is all that would be needed to show the differences in performance of the various configurations as the efficiency of a system is of prime importance. However, because it was necessary to utilize apparent efficiencies rather than effective efficiencies, this parameter is not indicative of the relative performance.

Since the horsepower measured for a certain condition and its resultant apparent efficiency does not change when the effective efficiency is determined it can be used as a comparative parameter for performance purposes. Therefore, Figure 61 is presented which shows the variation of horsepower required with V/nD for various thrust/drag ratios of the three propulsive systems investigated. Only data for values of thrust equal to or less than the drag are presented and these variations are based on data obtained from the preceding figures and from References (a) and (i).

Particular attention is called to the large circles denoting the horsepower required for T = D at the maximum propeller efficiency of each propeller. These points show a 5% reduction in horsepower required for the fin mounted propeller configuration in comparison with the conventional car-mounted propeller, while the GAC wake propeller shows a 30% reduction in horsepower required compared to the conventional arrangement.

If a general comparison of range or endurance is to be performed a few simplifying assumptions must be made.

(1) It is assumed, based on the measured data, that comparable

JR 2185 (3-52)M

CONFIDENTIAL

reductions in horsepower can be attained at all velocities since the above values were given for T = D.

(2) A stern propulsion unit would consist of two normal ZPG-3W airship engines geared together or a single engine of higher horsepower rating having similar fuel consumption characteristics.

Both range and endurance of an airship are functions of the fuel flow in lbs/hr which in turn is a function of the horsepower and the brake specific fuel consumption (B.S.F.C.). The B.S.F.C. variation with horsepower for an engine such as used on the ZPG-3W airship is very slight for normal cruising horsepower and might be assumed as a first approximation to be constant over the range of horsepower considered. Therefore, since the car-mounted and fin-mounted powerplant configurations have practically the same horsepower requirements, it can be concluded that the Wake propeller configuration would have approximately 30% greater range or endurance than the other configurations. With respect to a normal AEW mission for ZPG-3W airship this could represent an increase in endurance in the order of 25 hours.

The full potentialities of a wake propeller configuration can only be realized if it is the sole source of propulsion but this introduces many complicating factors. Although this report is only intended as an Aerodynamic Analysis, which shows a 30 percent advantage in range or endurance, the disadvantages of the system should be noted. The use of the wake propeller as a sole source of propulsion has the following general disadvantages:

(a) Necessity for almost constant blower operation of the air system since the scoops would not have the advantage of slipstream ram pressure.

(b) Loss in reliability, versatility and safety due to the use of only one engine.

(c) Maintenance and inspection problems.

In any actual wake propeller configuration, additional engines would probably be provided in the conventional location to solve some of the above problems. Although these engines and the stern engine could then be smaller (have reduced horsepower requirements) the over all result might possibly be a weight penalty and a reduction in maximum endurance compared to the wake propeller alone even though the wake propeller alone were used for maximum cruise performance. The added cost, complexity and maintenance problems for an actual full-scale vehicle would have to be judged on the basis of the gain in endurance, higher maximum velocity obtainable, and the more efficient and satisfactory crew performance during long missions due to the reduced vibration and noise level associated with the remote propeller and engine location.

CONFIDENTIAL

In regard to the increase in maximum velocity for the wake propeller configuration, it has been shown that the predicted efficiency of $\eta_e = .98$ has essentially been substantiated. Figure 59 indicates a maximum efficiency of approximately 73 percent for the conventional or fin-mounted powerplant configurations. Therefore, assuming equal drag and the same horsepower, the velocity increase would be governed by the ratio of the efficiency changes to the one-third power.

$$\left[V_{MAX}\right]_{\substack{WAKE \\ PROP}} = V_{MAX_{\substack{CONV \\ PROP}}} \sqrt[3]{.98/.73} =$$

$$V_{MAX_{\substack{CONV \\ PROP}}} \sqrt[3]{1.342}$$

$$V_{MAX_{\substack{WAKE \\ PROP}}} \cong 1.10 \quad V_{MAX_{\substack{CONV \\ PROP}}}$$

It could be expected that a maximum velocity increase for a pure wake propeller configuration would be in the order of 10 percent.

In conclusion, the pure wake propeller configuration would produce a 30 percent increase in range or endurance and/or a 10 percent increase in maximum velocity over the corresponding values for the conventional or fin-mounted powerplant configurations.

B. Stability and Control Comparison

It has previously been shown that the aerodynamic characteristics in pitch of the wake propeller configuration are not significantly affected by the propeller operation and that the magnitude and slope of the lift and pitching moment curves are similar to the same curves at zero power for the conventional or fin-mounted powerplant models. Therefore, since the rotary derivatives in pitch would be the same for all models at zero power, it can be concluded that the dynamic stability, as calculated by the stability Index and criterion utilized in Reference (a), is identical to the conventional car-mounted powerplant configuration at zero power.

Reference (a) also shows that the effect of conventional car-mounted propellers on the longitudinal dynamic stability index is negligible or zero and therefore it and the wake propeller configuration have equal longitudinal dynamic stability. The effect of power on the longitudinal dynamic stability index of the fin-mounted powerplant configuration is significant as shown in Reference (a). The following table presents a comparison of the

JR 2188 13-52M

longitudinal dynamic stability for the three configurations with a typical power condition for the fin-mounted configuration utilized.

Longitudinal Dynamic Stability Comparison
Including Power Effects
1/20-Scale Powered Wind Tunnel Model

Powerplant Configuration	Car-Mounted (Any T_c'')	Wake Propeller (All Powers)	Fin-Mounted $T_c'' = 0.5$
C_{m_α} (m')	0.659	0.659	0.459
C_{L_α} (n')	0.716	0.716	0.802
$C_{m_q}(V/V^{1/3})$ (m")	-2.110	-2.110	-2.273
$C_{L_q}(V/V^{1/3})$ (n")	1.180	1.180	1.320
$2\,k_x$	2.175	2.175	2.175
I	-0.393	-0.393	-0.658

In the above table, the longitudinal stability index, I, is given by the following equation:

$$I = m' + \frac{n'm'' - m'n''}{2\,k_x}$$

It is apparent that the dynamic stability (including power effects) of the fin-mounted powerplant configuration is superior to either the conventional or wake propeller configurations at any power.

Since power or propellers did not affect the lift or moment slopes due to elevator deflection for the wake propeller or car-mounted powerplant configurations it can also be concluded, as shown in Section VII-C - Addendum I of Reference (a), that the fin-mounted configuration is also superior in longitudinal control power due to the slipstream effect of the propellers on the control surfaces.

Although lateral aerodynamic characteristics in yaw for the wake propeller configuration were not measured it is not believed that any power effects would be obtained since none were obtained in pitch. Therefore, the fin-mounted powerplant has the same increase in lateral stability and control as shown in Section VII-B and C - Addendum I of Reference (a).

JR 2188 (3-32)M

CONFIDENTIAL

Therefore the effects of power (and/or slipstream effects) result in superior dynamic stability and control characteristics for the fin-mounted powerplant configuration as compared to the conventional car-mounted powerplant configuration or the wake propeller configuration. The degree or magnitude of increased stability and/or control is usually a relative number but based on data from Reference (a) relative values of approximately a 60% increase in longitudinal dynamic stability and a 30 to 40 percent increase in longitudinal control power might be used to illustrate the relative increases, but extreme caution is recommended when quoting such values in order not to imply near perfect stability or completely adequate control power for all conditions of flight.

JR 2168 (3-52)M

CONFIDENTIAL

C. Conclusions and Recommendations

1. An airship powered by a wake propeller only would have approximately 30 percent greater range or endurance than a conventional or fin-mounted powerplant airship of the same size.

2. The maximum velocity of an airship with a wake propeller would be at least 10 percent larger than a similar conventional or fin-mounted powerplant airship.

3. A wake propeller airship would exhibit the same dynamic stability and control characteristics as a conventional airship, and, like it, would not be significantly affected by the propeller operation.

4. The fin-mounted powerplant airship shows superior stability and control characteristics compared to either the wake propeller or the conventional car-mounted configuration.

5. For any future airship, its primary mission would probably dictate the most optimum propulsive configuration, as a wake propeller configuration would be best for missions where long range or endurance is required (i.e. AEW patrol) while a fin-mounted powerplant configuration would be superior where greater control is a prerequisite (i.e. ASW missions or sonar dunking or towing).

6. A detailed design and performance study must be made of any actual full-scale airship wake propeller configuration in order to determine the net gain in endurance or range since the increase quoted in No. 1 would possibly not apply to a mixed-powerplant configuration and it is even possible that the weight of a pure wake propeller configuration might exceed that of a conventional configuration unless considerable effort was applied to solve some of the attendant problems.

7. The superior stability and control qualities quoted for a fin-mounted powerplant configuration are only obtained to the degree noted when an inverted - "Y" empennage is utilized and improvements of this magnitude could not be obtained on an X-tail airship. (This was previously emphasized and explained in Reference (a)).

8. It is recommended that any further studies be directed to the determination of weights and powerplant(s) of an actual full-scale airship with awake propeller so that better information as to the net gain in performance could be better evaluated.

9. The utilization of a wake propellor that could provide directed thrust and/or greater low-speed control, as well as increased endurance, should also be seriously considered for any future airship regardless of its primary mission.

JR 2-58 (3-52)M

CONFIDENTIAL

REFERENCES

a. GER 9461, Rev. A: Aerodynamic Analysis of a 1/20-Scale Powered Wind Tunnel Model of an Airship with Various Propulsive Arrangements-Phase I and II - Fin-Mounted and Car-Mounted Powerplants dated 30 December 1959 BuWeps Contract NOa(s) 54-900c Amendments 5 and 10

b. GER 5128: Aerodynamic Study for Stern Propulsion on XZP5K Airship dated December 1952 BuAer Contract NOa(s) 52-141c

c. GDC Report No. R-502-1 Summary Report - Airship Stern Propulsion 1 July 1953, General Development Corp. report for BuAer Contract NOa(s) 52-103

d. Letter No. 61114418: from Transcendental Aircraft Corporation to Chief, BuAer, Contract NOa(s) 52-107 (AC-7) dated 1 November 1956

e. GER 8446 Rev. 0: Bi-Monthly Progress Reports, 1/20-Scale ZPG-3W Wind Tunnel Model Tests, dated 30 November 1960

f. NASA Report on Wind Tunnel Investigations of Wake Propeller Configurations Unpublished at date of this report but to be released in approximately one month

g. NASA RM SL56C12: Tabulated Pressure Coefficient Data from a Tail Loads Investigation on a 1/15-scale Model of the Goodyear XZP5K Airship TED No. NACA DE-211, 15 February 1956

h. DTMB Aero Report 914: Wind Tunnel Investigation of the Drag of a Proposed Boundary-Layer Controlled Airship, dated March 1957

i. NASA Memorandum Report No. 7-1-59L: Results of a Wind Tunnel Investigation of a 1/20-scale Model of the Goodyear ZPG-3W Airship with Fin-Mounted and Conventional Car-Mounted Engines TED No. NASA AD-3141

j. DGAI Report of May 1947: Stern Propulsion Tests on an Airship Model with Counter-Rotating Propellers (Daniel Guggenheim Airship Institute)

JR 2188 (3-52)M

PREPARED
CHECKED
DATE
REV DATE

FIGURE 1
DESCRIPTIVE ARRANGEMENT - WAKE PR
1/20 - SCALE WIND TUNNEL MODEL OF A MO

NOTE: BASIC DIMENSIONS OF HULL AND
IDENTICAL TO THOSE GIVEN IN REF
ALL DIMENSIONS ARE IN INCHES.

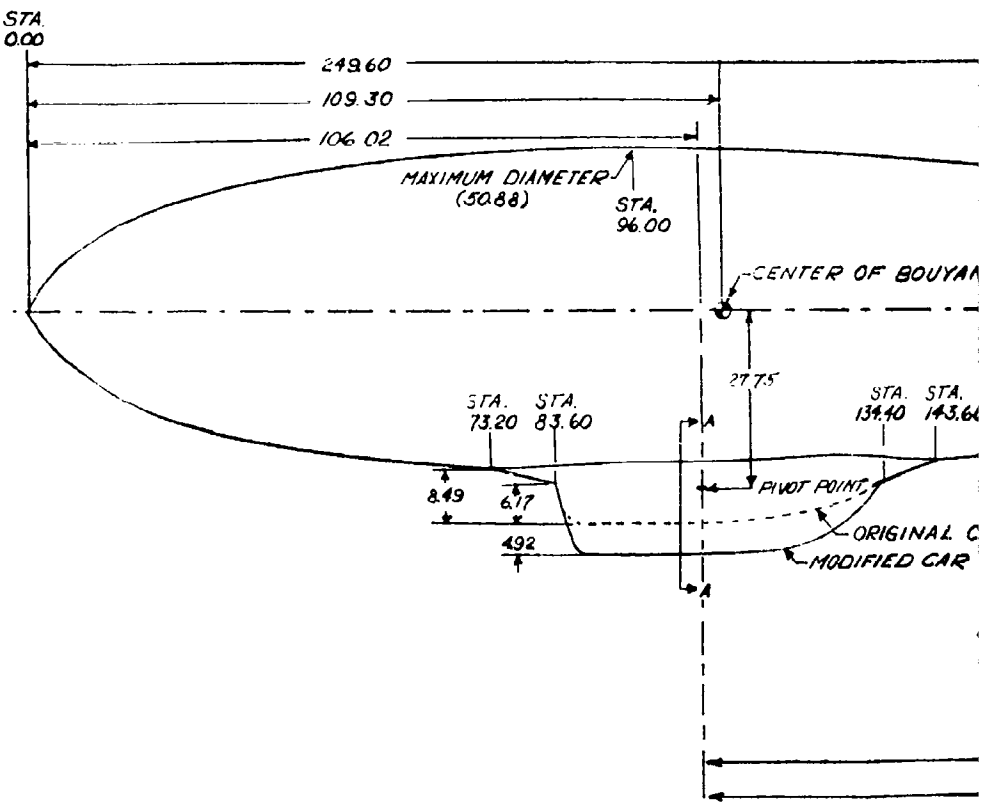

1

CONFIDENTIAL

FIGURE 1

RIPTIVE ARRANGEMENT - WAKE PROPELLER CONFIGURATIONS
E WIND TUNNEL MODEL OF A MODIFIED ZPG-3W AIRSHIP

BASIC DIMENSIONS OF HULL AND TAIL ARE IDENTICAL TO THOSE GIVEN IN REFERENCE 1. ALL DIMENSIONS ARE IN INCHES.

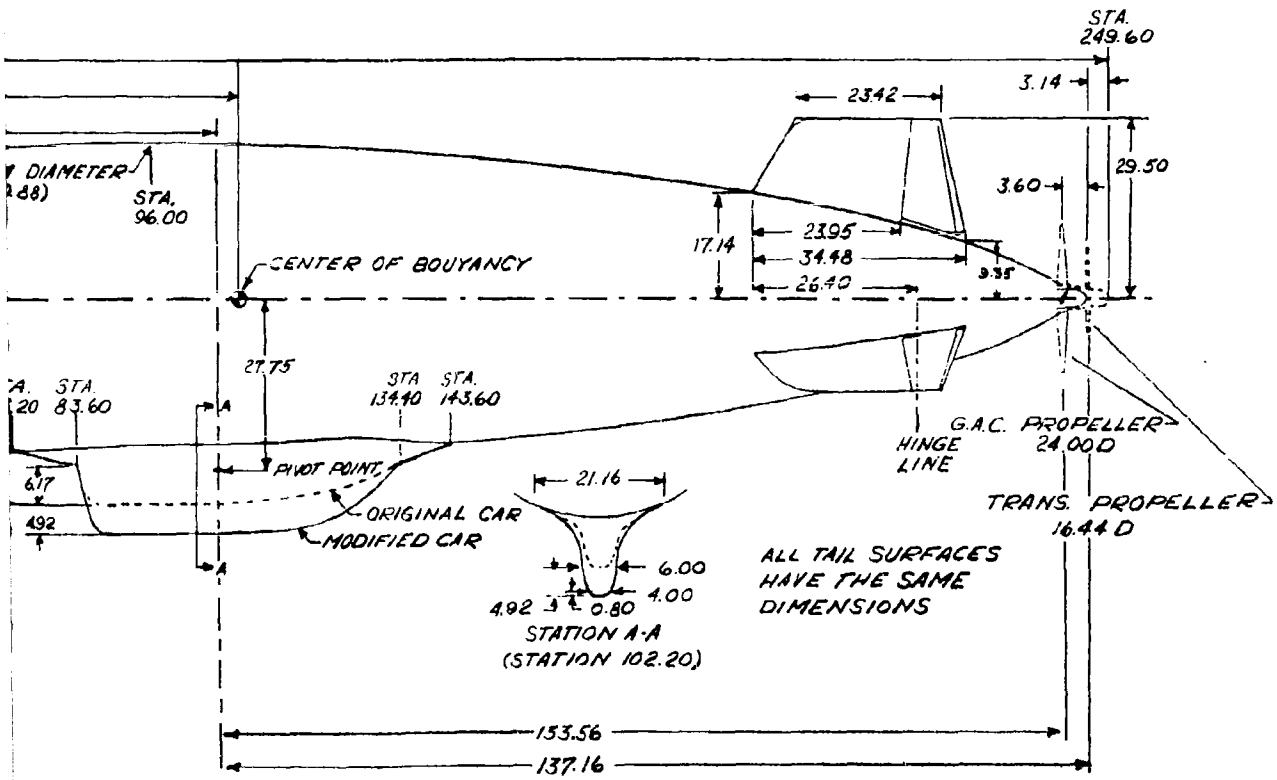

2

CONFIDENTIAL

CONFIDENTIAL

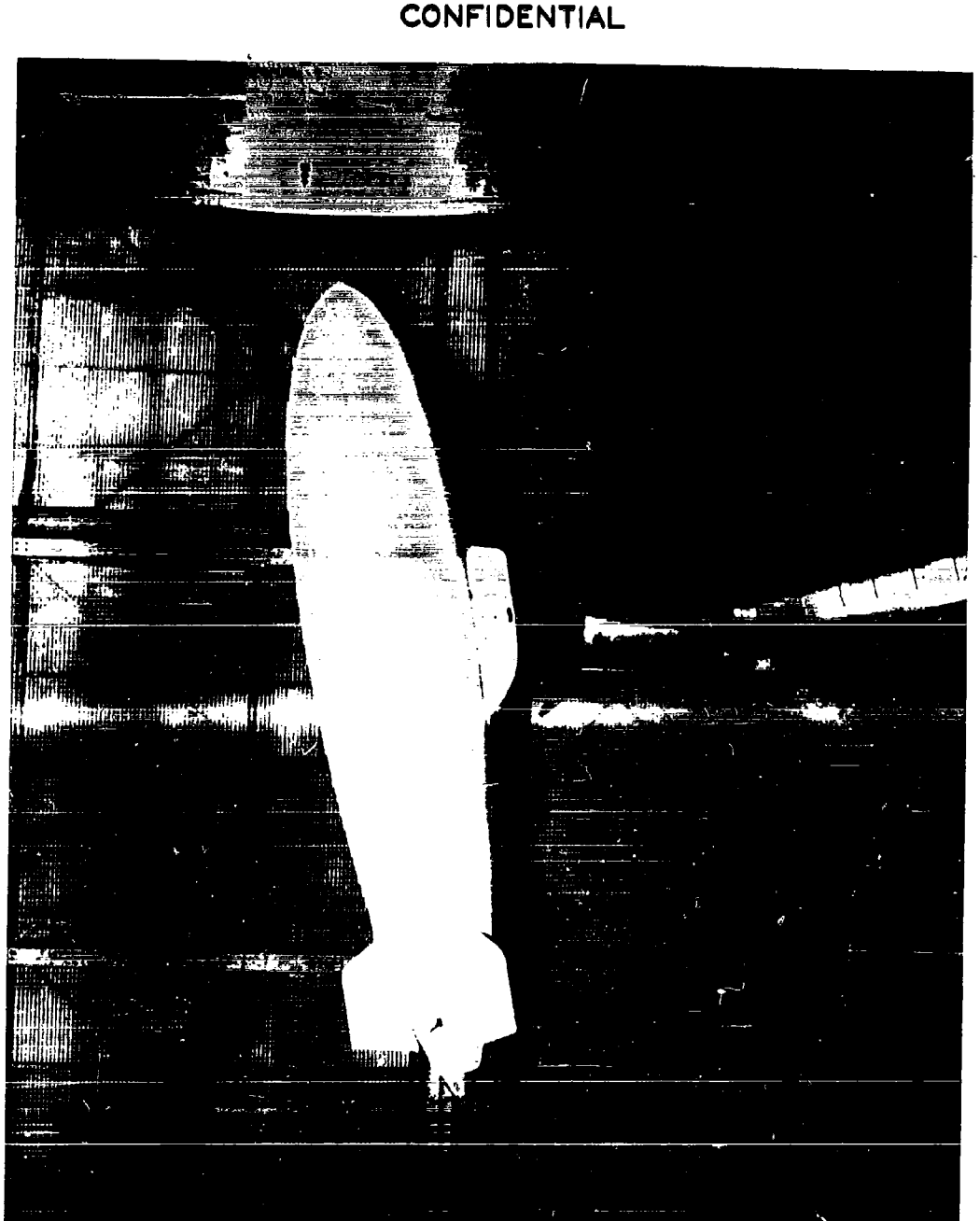

Figure 2 - GAC Make Propeller Configuration in the NASA-Langley Full-Scale Tunnel

CONFIDENTIAL

CONFIDENTIAL

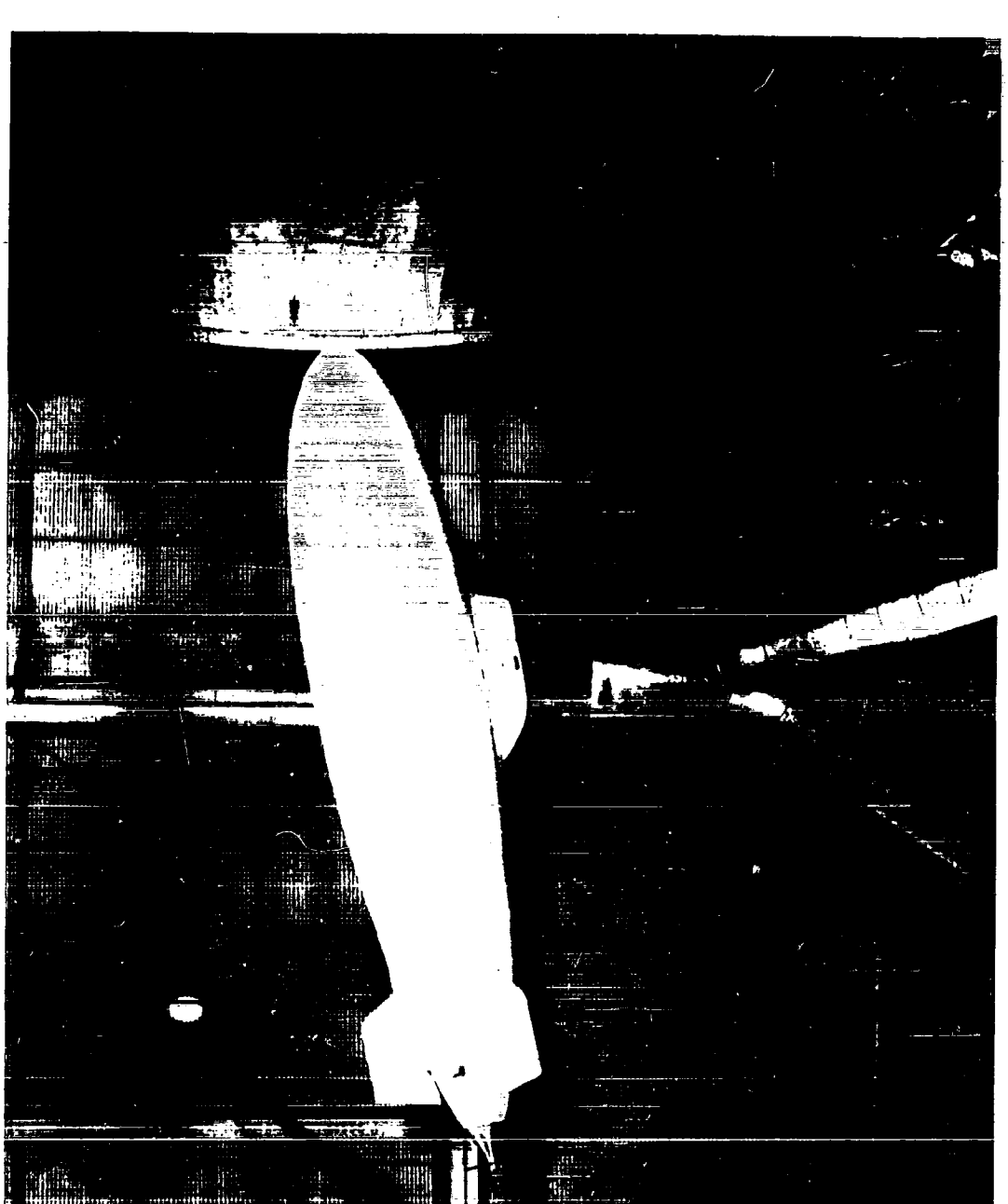

Figure 3 - Transcendental Wake Propeller Configuration in the NASA-Langley Full-Scale Tunnel

CONFIDENTIAL

CONFIDENTIAL

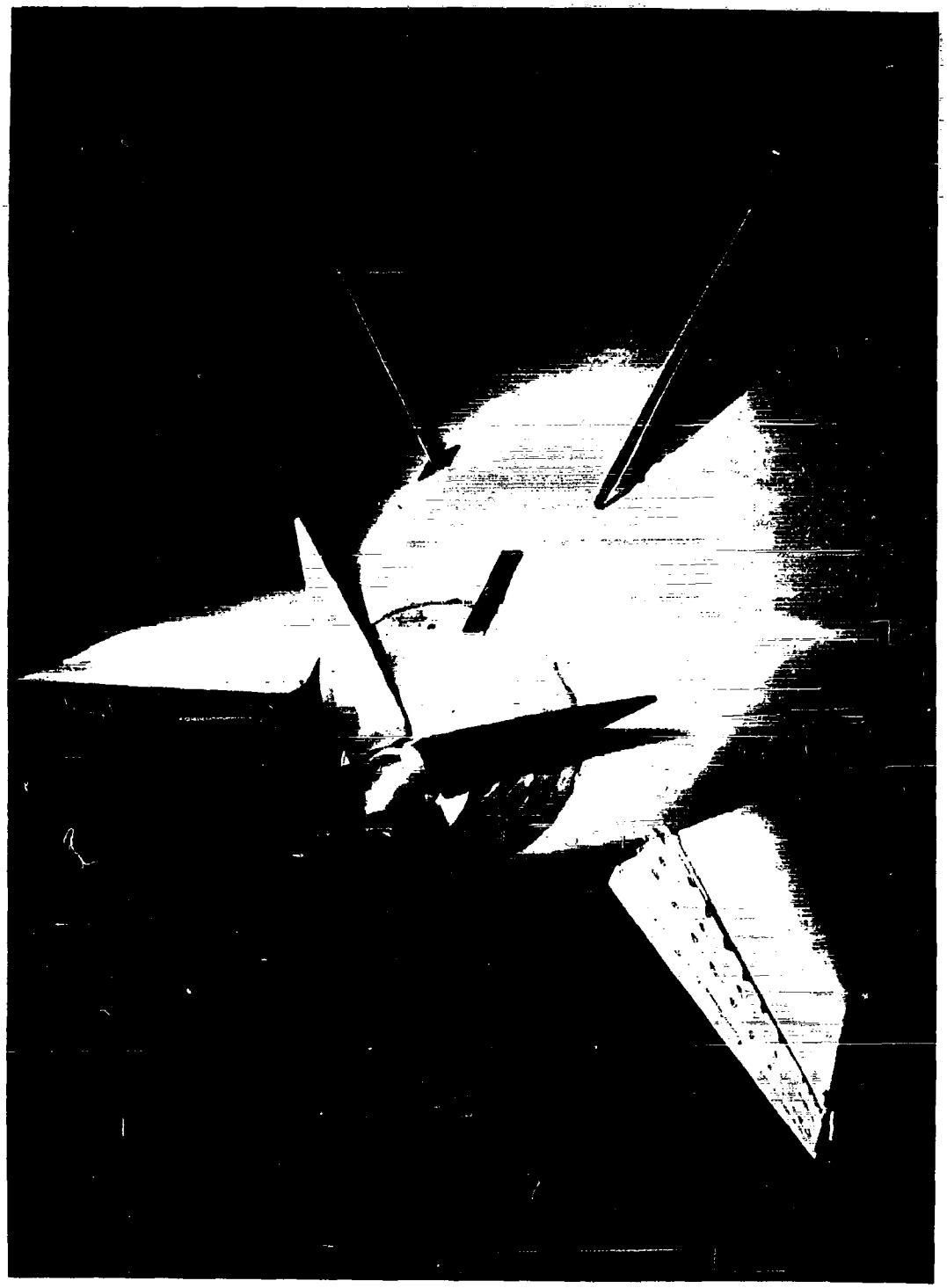

Figure 4 - GAC Wake Propeller

CONFIDENTIAL

CONFIDENTIAL

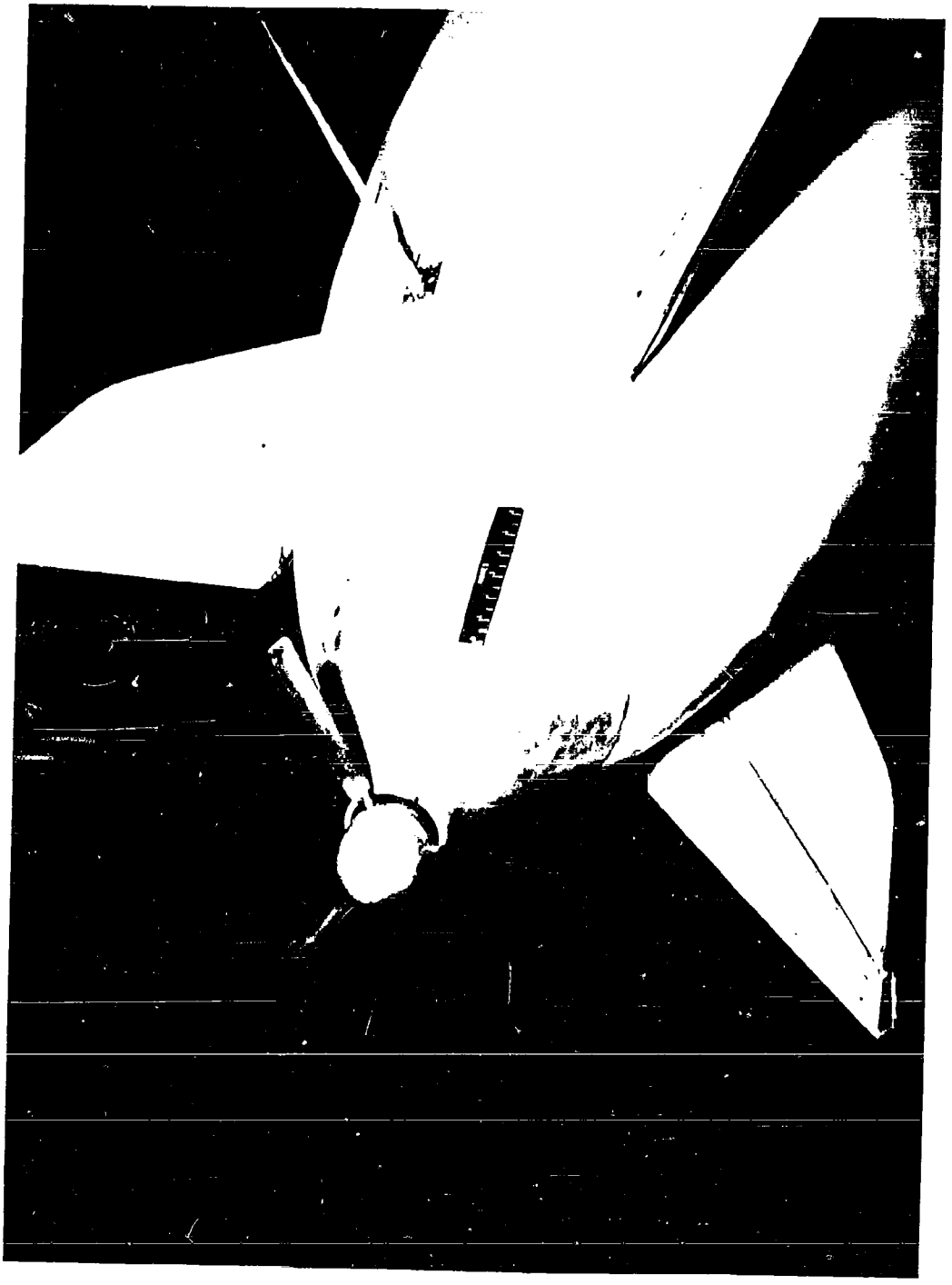

Figure 5 - Transcendental Wake Propeller

CONFIDENTIAL

CONFIDENTIAL

FIGURE 6

1/20 SCALE ZPG-3W AIRSHIP (MODIFIED)
GAC WAKE PROPELLER
PRESSURE RATIOS MEASURED AT PLANE OF PROPELLER

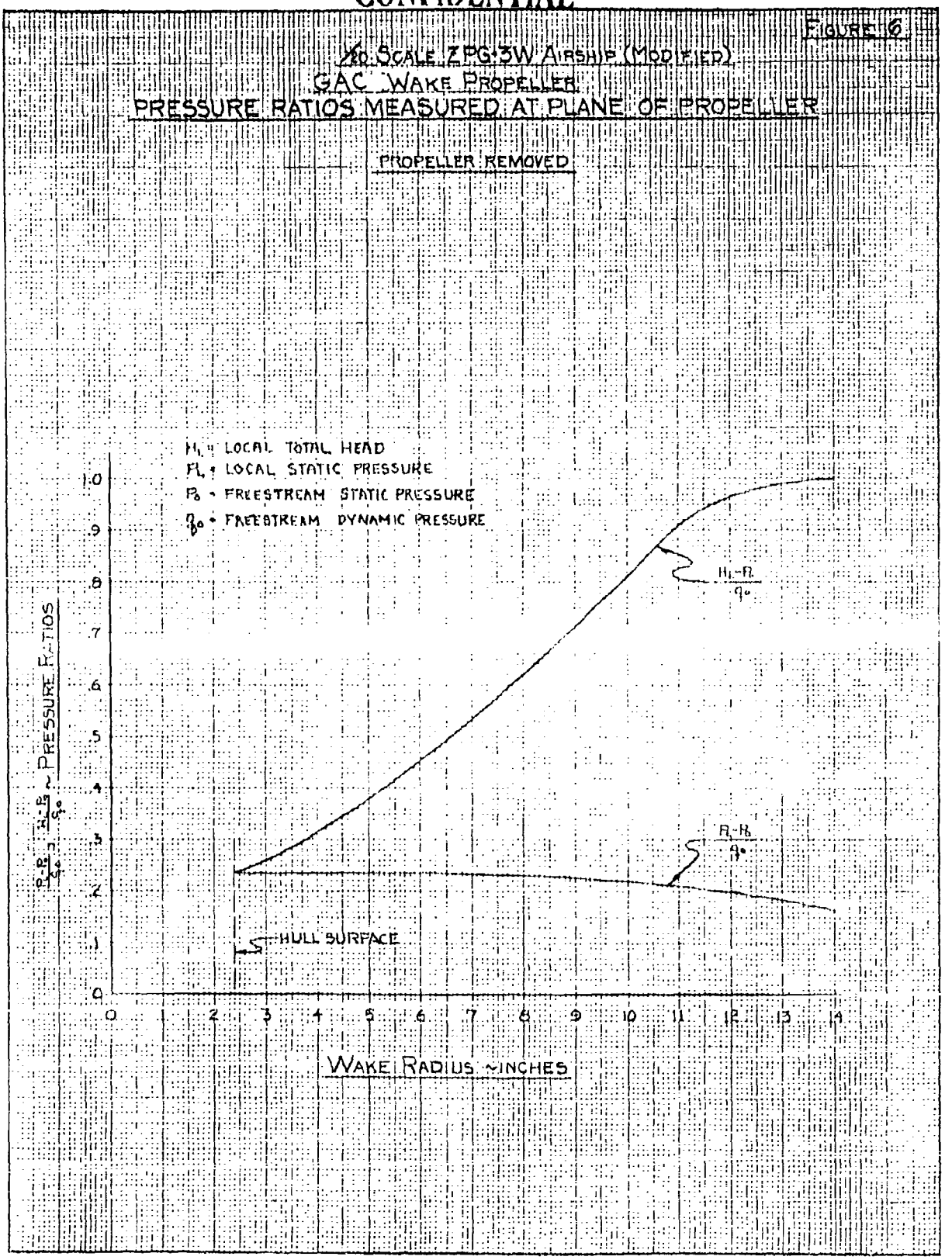

JR 220 3-59

CONFIDENTIAL

FIGURE 7

1/20 SCALE ZPG-3W AIRSHIP
STERN PROPELLER
WAKE VELOCITY

(PROPELLER OFF)

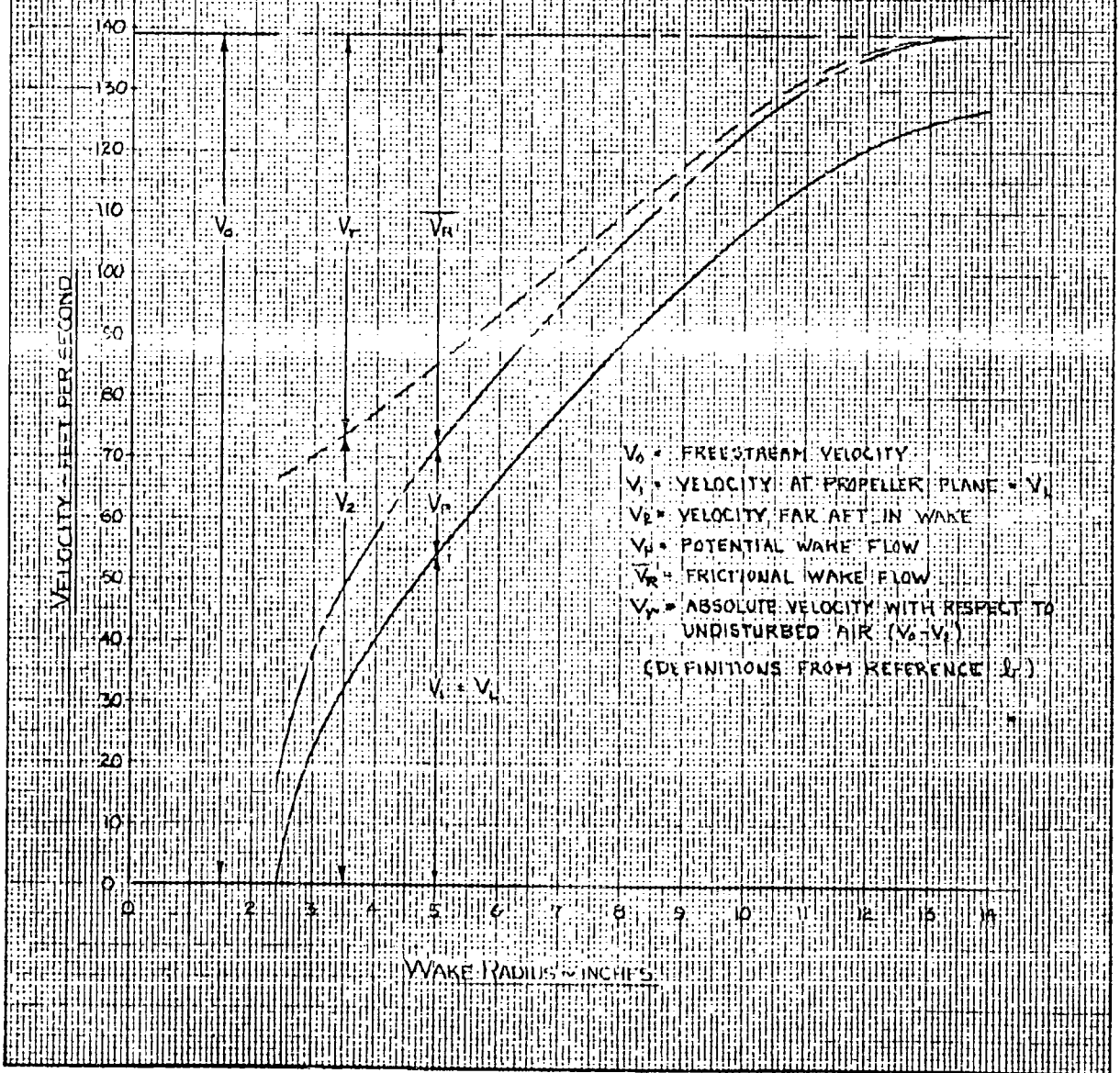

CONFIDENTIAL

JR 220 (3-59).

FIGURE 8

1/20 SCALE ZPG-3W AIRSHIP
STERN PROPELLER
AXIAL VELOCITY INCREASE IN SLIPSTREAM
GAC WAKE PROPELLER

BHP = 5.06
RPM = 4500
ϵ = 0.025
$\Delta\eta_a$ = 50%
η_i = 98%
RADIUS = 12 INCHES
4 BLADES

ϵ = RATIO OF PROFILE DRAG TO LIFT FOR THE PROPELLER
$\Delta\eta_a$ = LOCAL RING ELEMENT (SECTION) EFFICIENCY
$\eta_T = \eta_a$ = TOTAL OR EFFECTIVE EFFICIENCY
(SEE REF 4 FOR COMPLETE NOTATIONS AND DERIVATIONS)

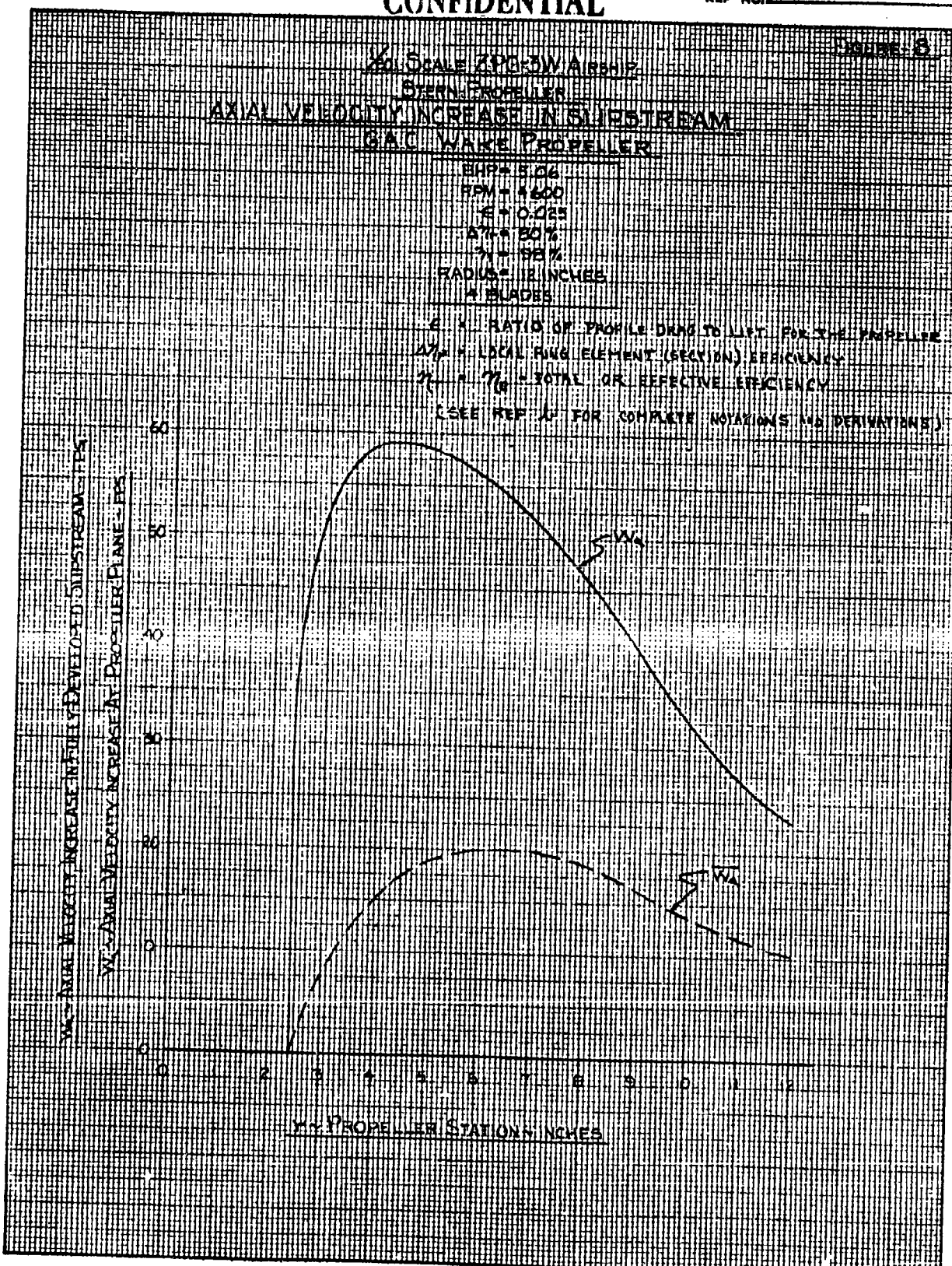

AR 220 (3-59)

FIGURE 9

1/20 SCALE ZPG-3W AIRSHIP
STERN PROPELLER
TANGENTIAL VELOCITY DISTRIBUTION IN SLIPSTREAM
GAC WAKE PROPELLER

V_0 = 139 FPS
BHP = 5.06
RPM = 4600
C_T = 0.025
$A_{7/4}$ = 80%
η = 98% = η_0
RADIUS = 12 INCHES
4 BLADES

(SEE FIG. 8 AND REFERENCE 4 FOR COMPLETE NOTATIONS AND DERIVATIONS.)

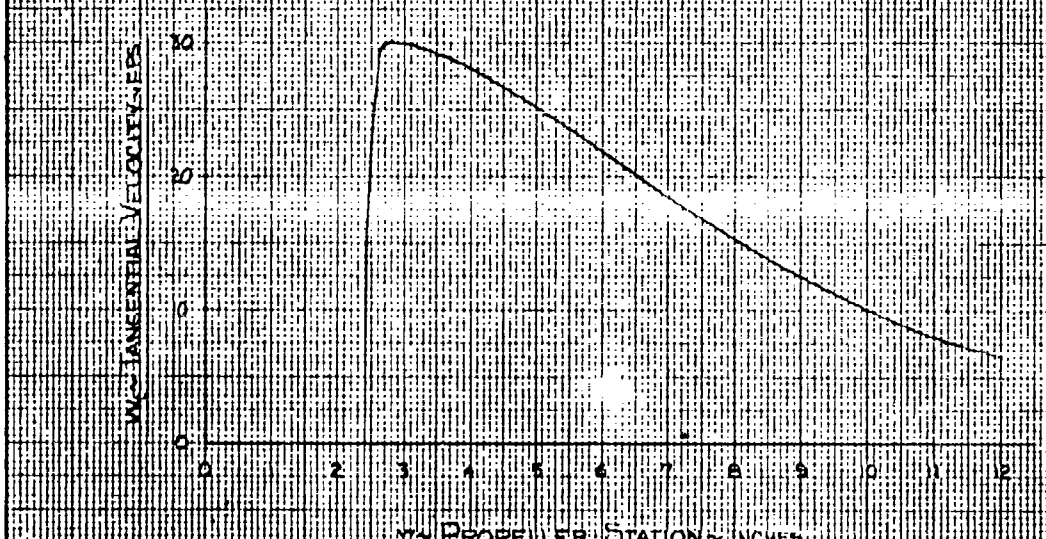

JR 220 (3-59)

FIGURE 6

1/20 SCALE ZPG-3W AIRSHIP
STERN PROPELLER
GAC PROPELLER CHARACTERISTICS

CLARK-Y AIRFOIL
4 BLADES
BHP = 5.06
RPM = 4600
ϵ = 0.025
A% = 80%

(SEE FIG. 8 AND REF. 1 FOR COMPLETE NOTATIONS AND DERIVATIONS)

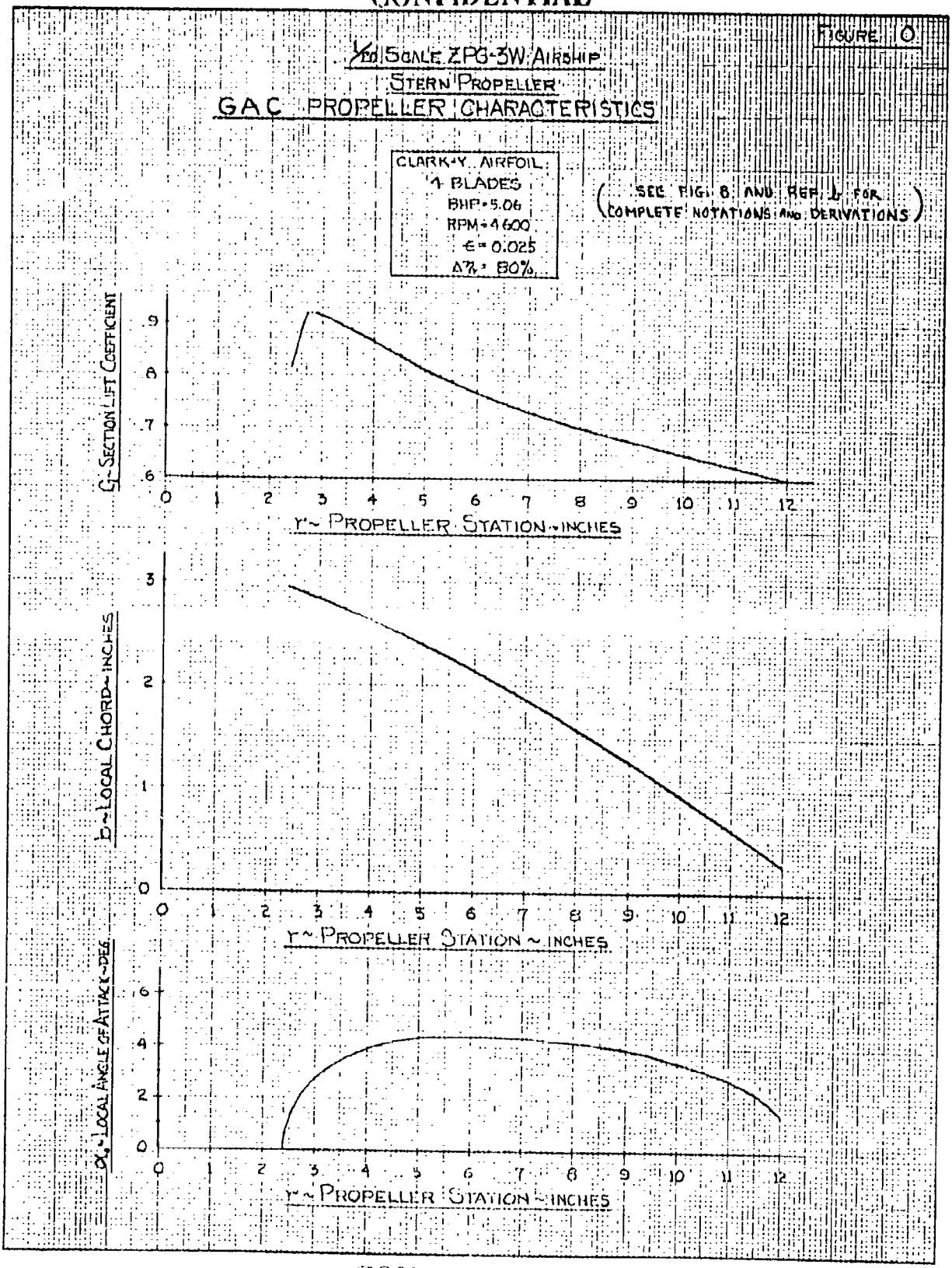

JR 220 3-57

CONFIDENTIAL

FIGURE 11

1/20 SCALE ZPG-3W AIRSHIP
STERN PROPELLER
AERODYNAMIC PITCH ANGLE, BLADE ANGLE AND BLADE THICKNESS RATIO FOR GAC PROPELLER

(SEE REFERENCE 4 FOR COMPLETE NOTATIONS AND DERIVATIONS)

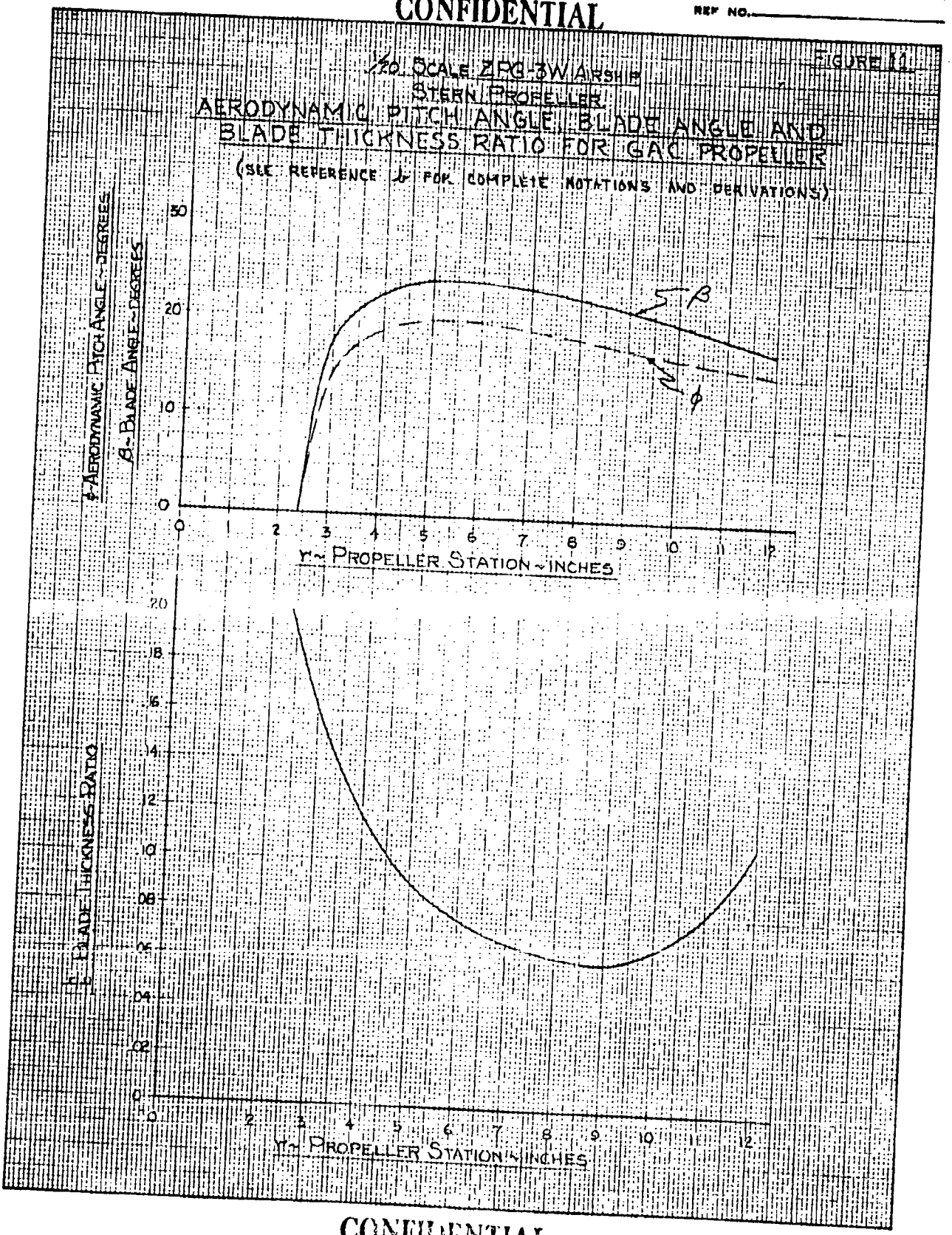

JB 220 (3-39)

CONFIDENTIAL

PREPARED BY O.D.B.
CHECKED BY R.J.P.
DATE APRIL 15, 1961
REVISED

GOODYEAR AIRCRAFT

PAGE 49
MODEL 1/20-ZPG-3W (MODIFIED)
GER- 10176
REF NO.

CONFIDENTIAL

FIGURE 12

1/20 SCALE ZPG-3W AIRSHIP
STERN PROPELLER
AERODYNAMIC PITCH ANGLE
GAC WAKE PROPELLER

V_o = 139 FPS
BHP = 5.06
RPM = 4600
ϵ = 0.025
$\Delta\eta_h$ = 80%
η_t = 98%
RADIUS = 12 INCHES
4 BLADES

(SEE FIG 8 AND REF 4 FOR COMPLETE NOTATIONS AND DERIVATIONS)

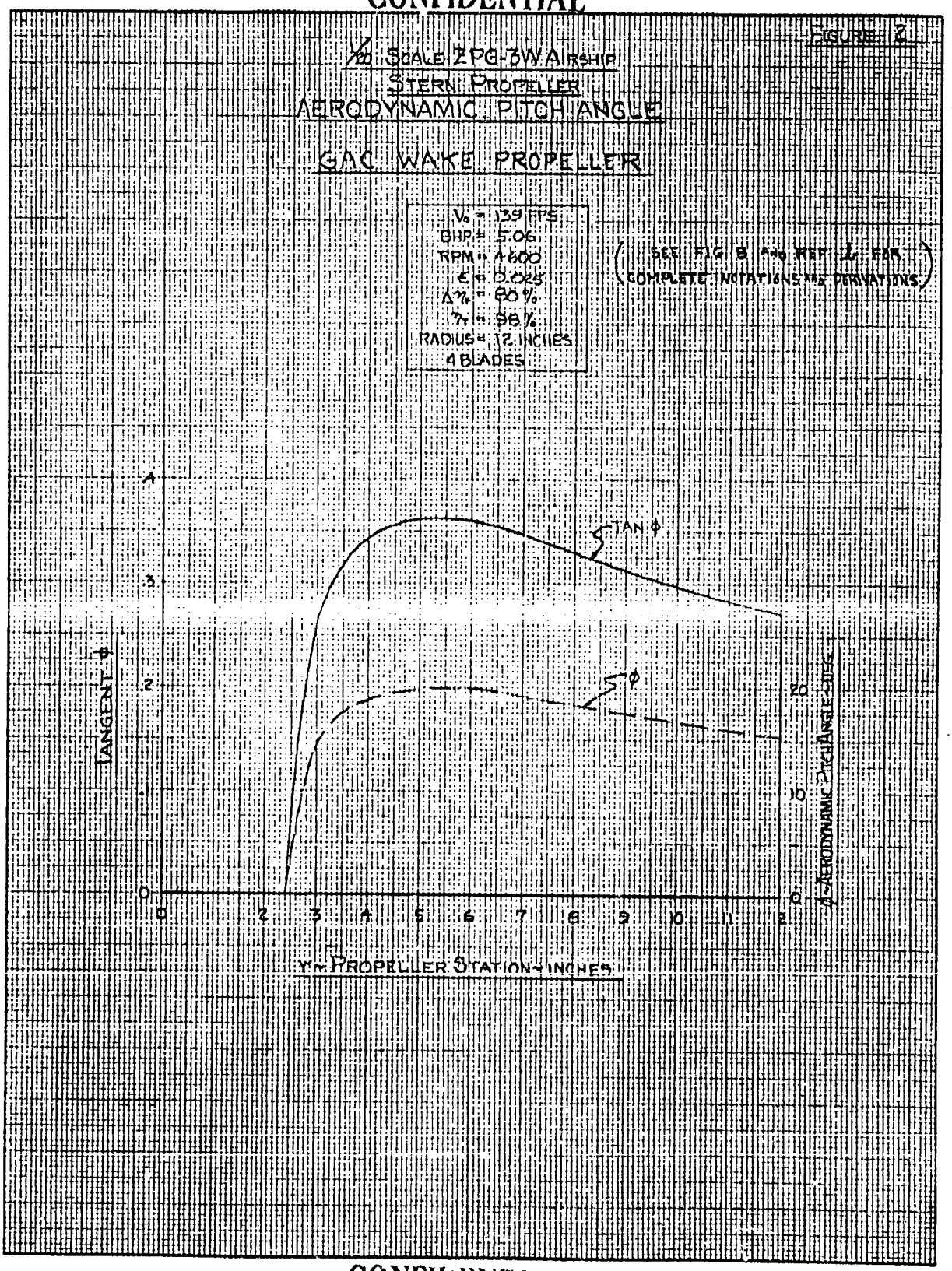

CONFIDENTIAL

AR 220 (3-60)

CONFIDENTIAL

FIGURE 13

1/20 SCALE ZPG-3W AIRSHIP
STERN PROPELLER
PROPELLER BLADE WIDTH FACTOR

GAC WAKE PROPELLER

BHP = 5.06
RPM = 4,600
ϵ = 0.025
A_{γ} = 80%
η_{γ} = 96%
RADIUS = 12 INCHES
4 BLADES

(SEE FIG. 8 AND REF. 4 FOR COMPLETE NOTATIONS AND DERIVATIONS)

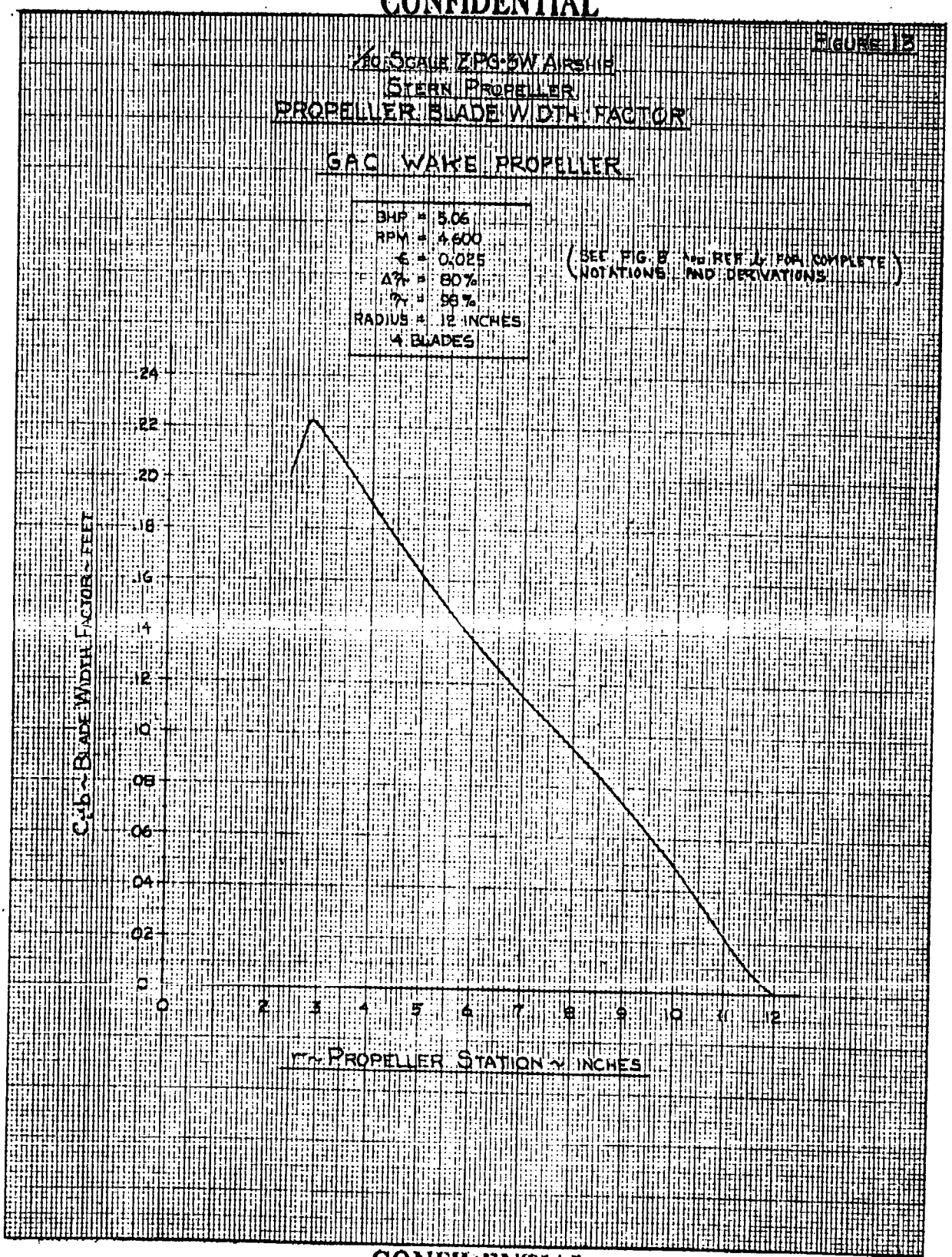

CONFIDENTIAL

CONFIDENTIAL

FIGURE 14

1/20 SCALE ZPG-3W AIRSHIP
STERN PROPELLER
PROPELLER POWER LOADING

GAC WAKE PROPELLER

V = 139 FPS
BHP = 5.06
RPM = 4600
ε = 0.025
Δη/η = 80%
RADIUS = 12 INCHES

(SEE FIG. 8 AND REF. 1 FOR COMPLETE NOTATIONS AND DERIVATIONS)

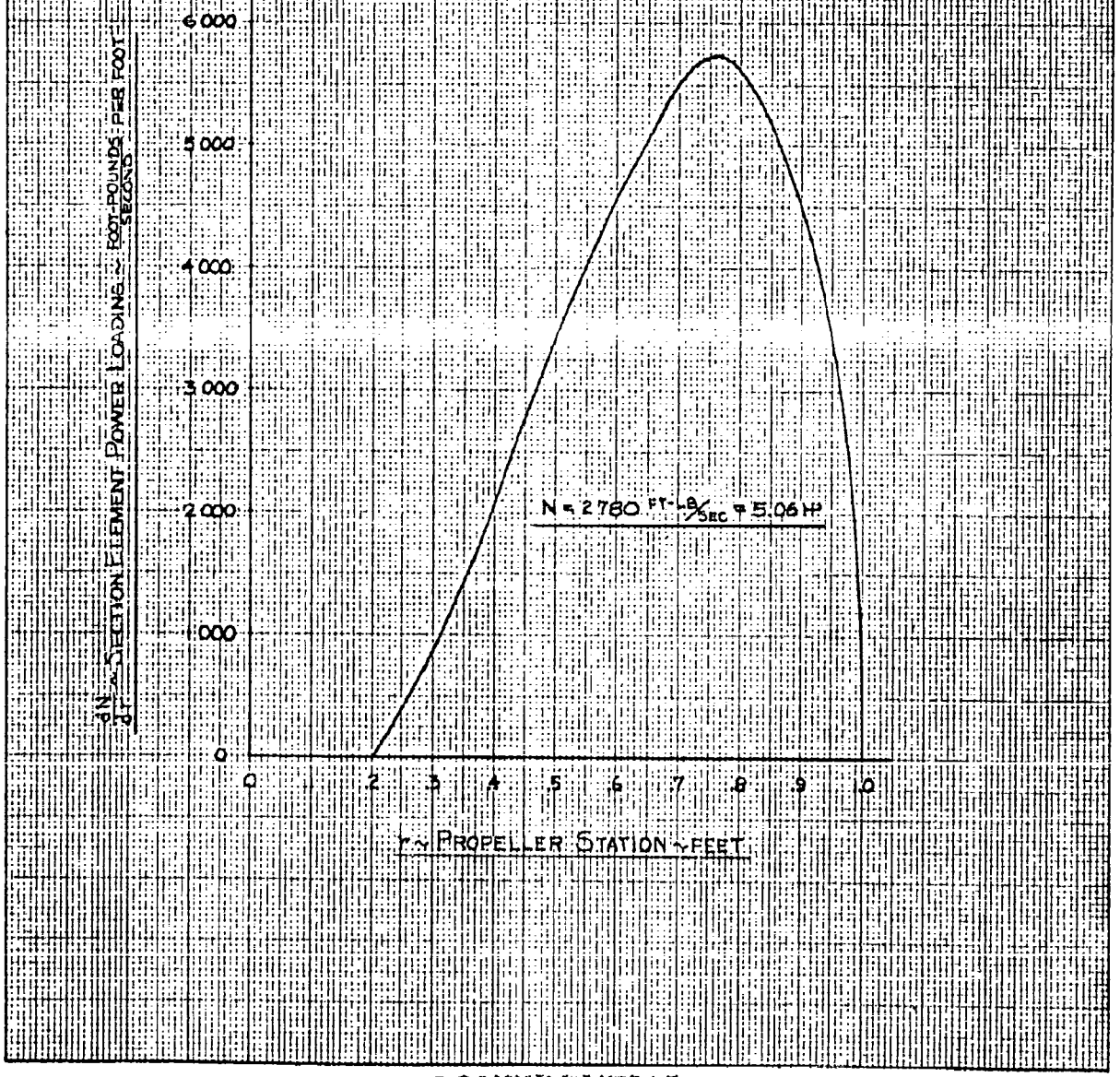

CONFIDENTIAL

FIGURE 5

1/20 SCALE ZPG-3W AIRSHIP
STERN PROPELLER
PROPELLER THRUST LOADING
GAC WAKE PROPELLER

V_o = 139 FPS
BHP = 5.05
RPM = 4600
ϵ_F = 0.025
$\Delta\eta$ = 80%
RADIUS = 12 INCHES

(SEE FIG. 8 AND REF. 1 FOR COMPLETE NOTATIONS AND DERIVATIONS)

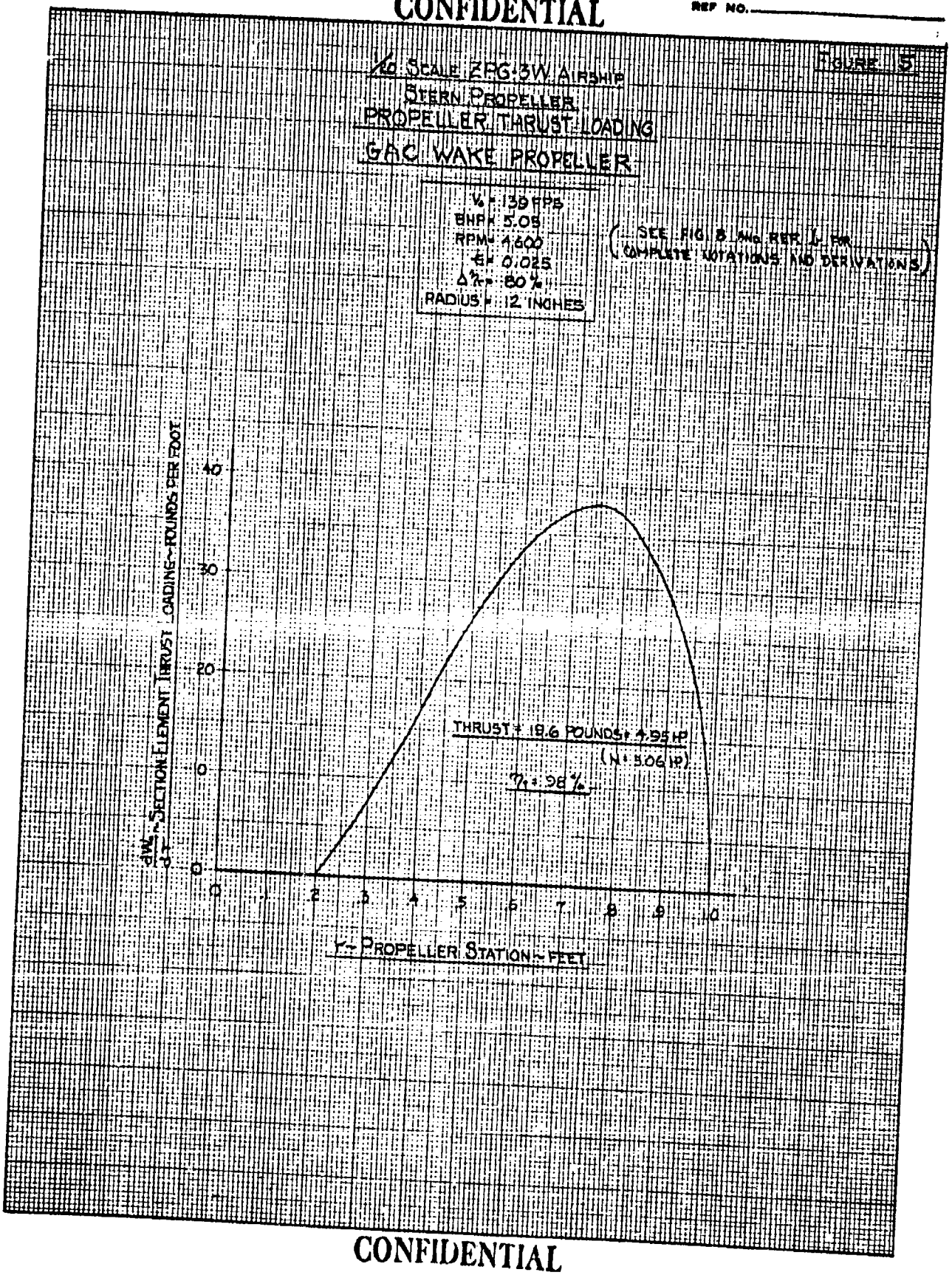

CONFIDENTIAL

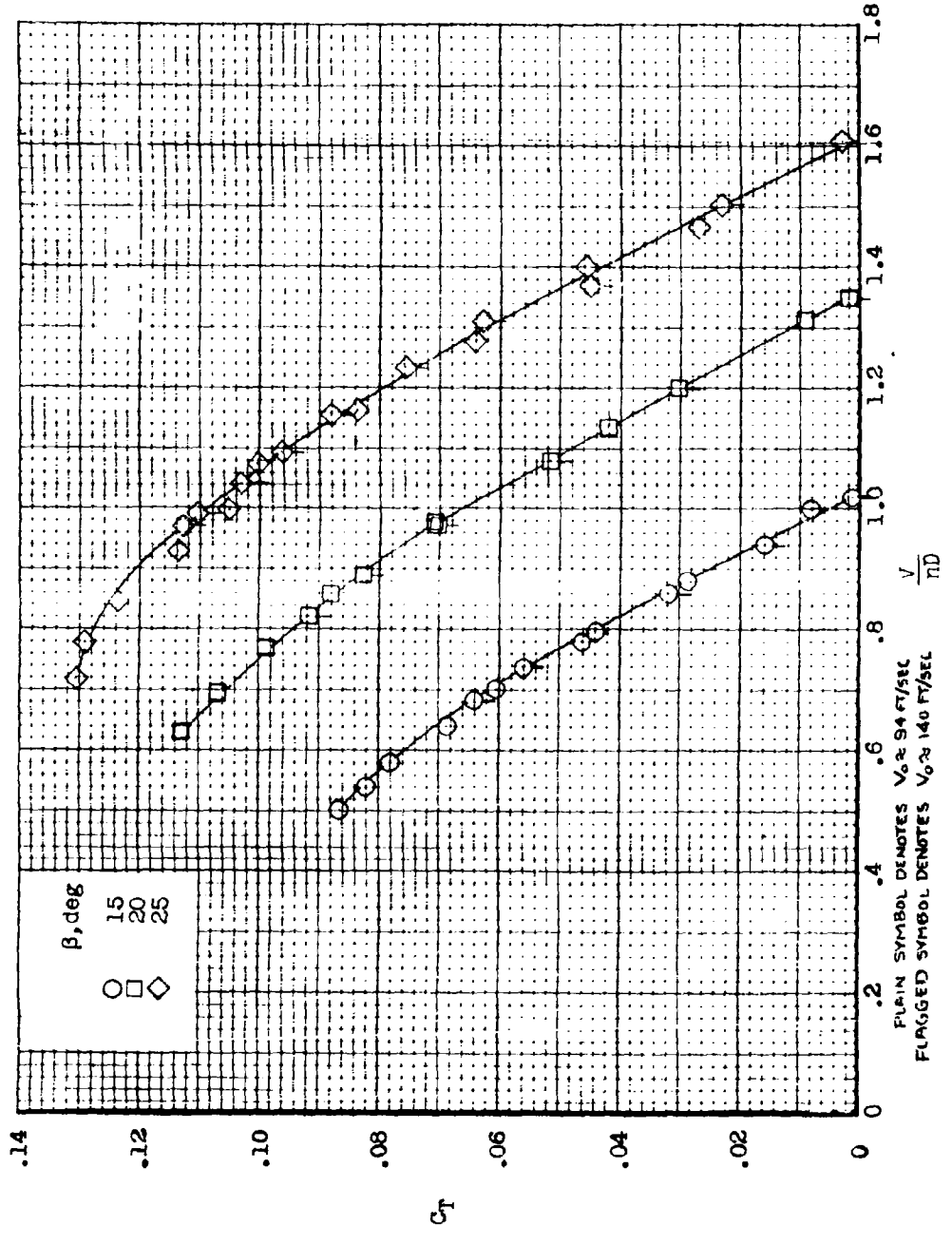

Figure 16 - Variation of Propeller Thrust Coefficient with Advance Ratio-GAC Wake Propeller

CONFIDENTIAL

CONFIDENTIAL

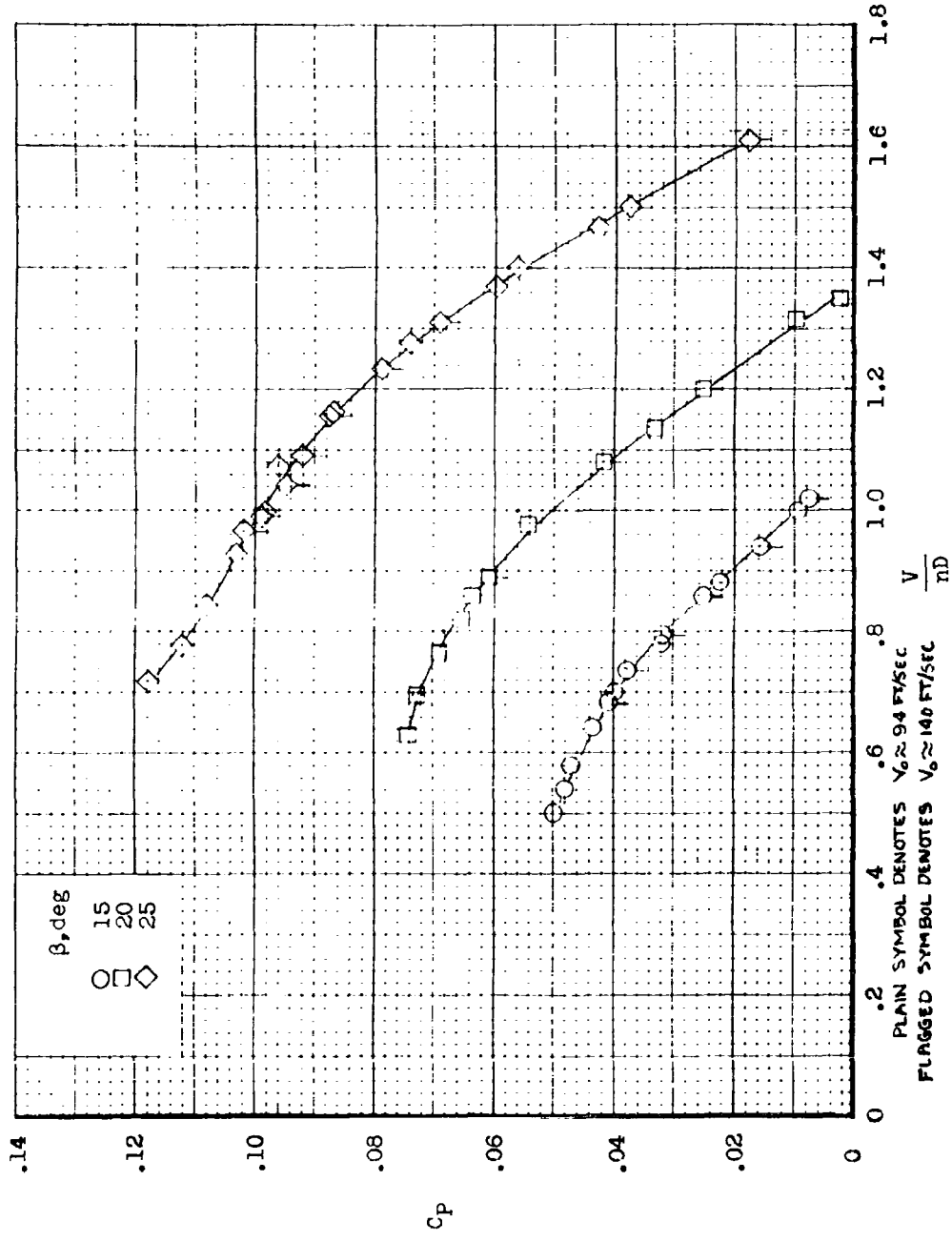

Figure 17 - Variation of Propeller Power Coefficient with Advance Ratio-GAC Wake Propeller

CONFIDENTIAL

CONFIDENTIAL

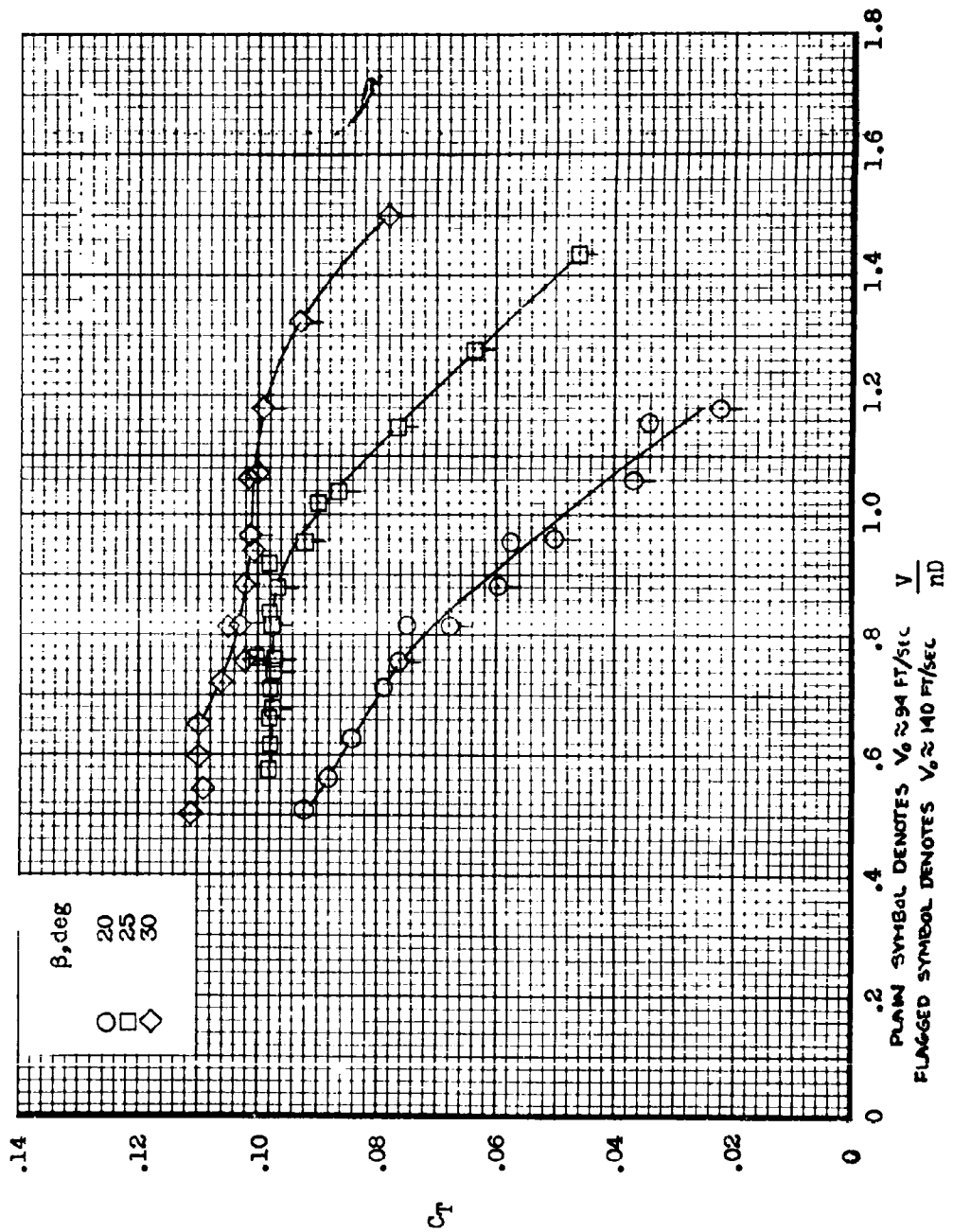

Figure 13 - Variation of Propeller Thrust Coefficient with Advance Ratio-Trans. Propeller

CONFIDENTIAL

CONFIDENTIAL

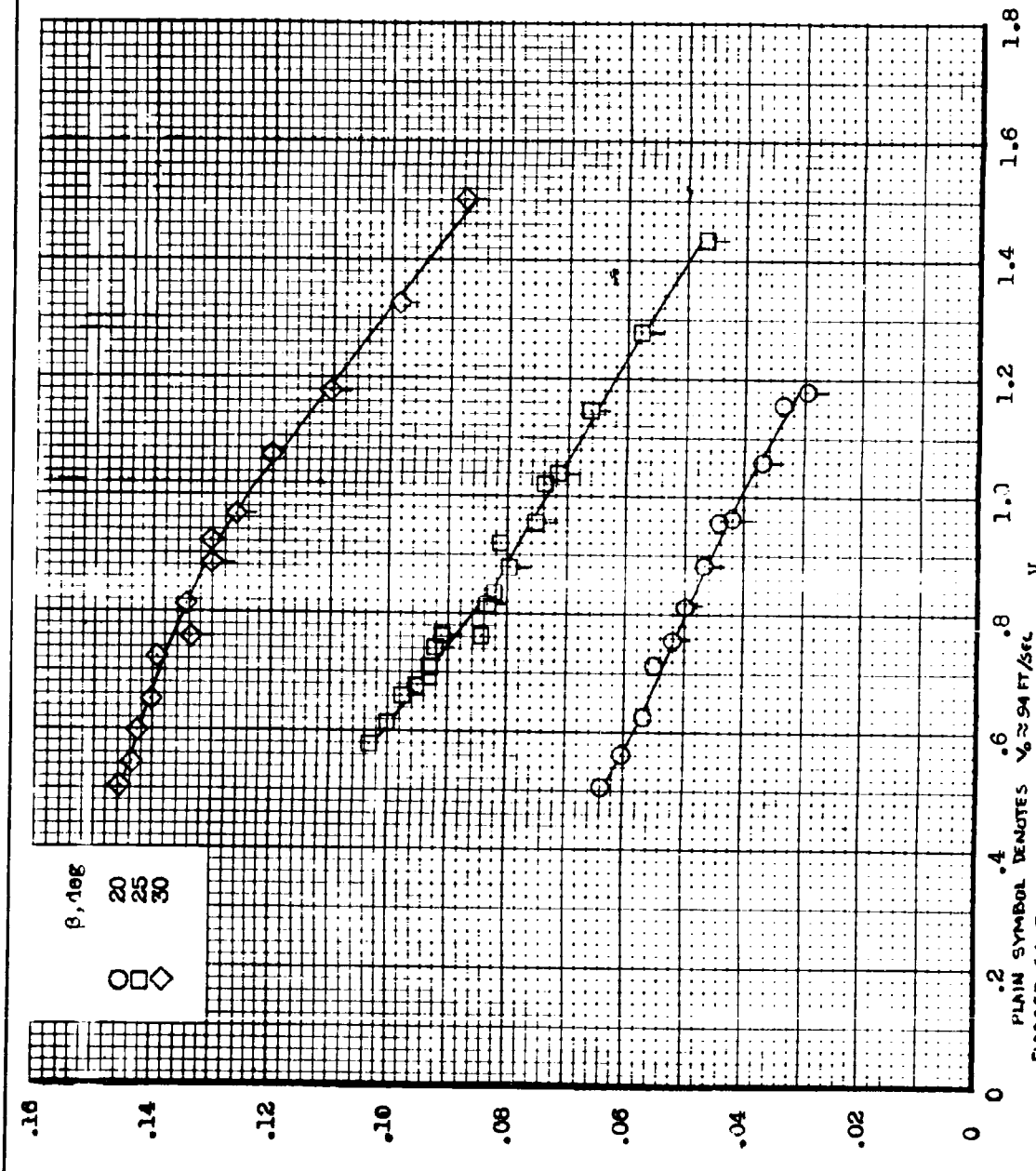

Figure 19 - Variation of Propeller Power Coefficient with Advance Ratio-Trans. Propeller

CONFIDENTIAL

CONFIDENTIAL

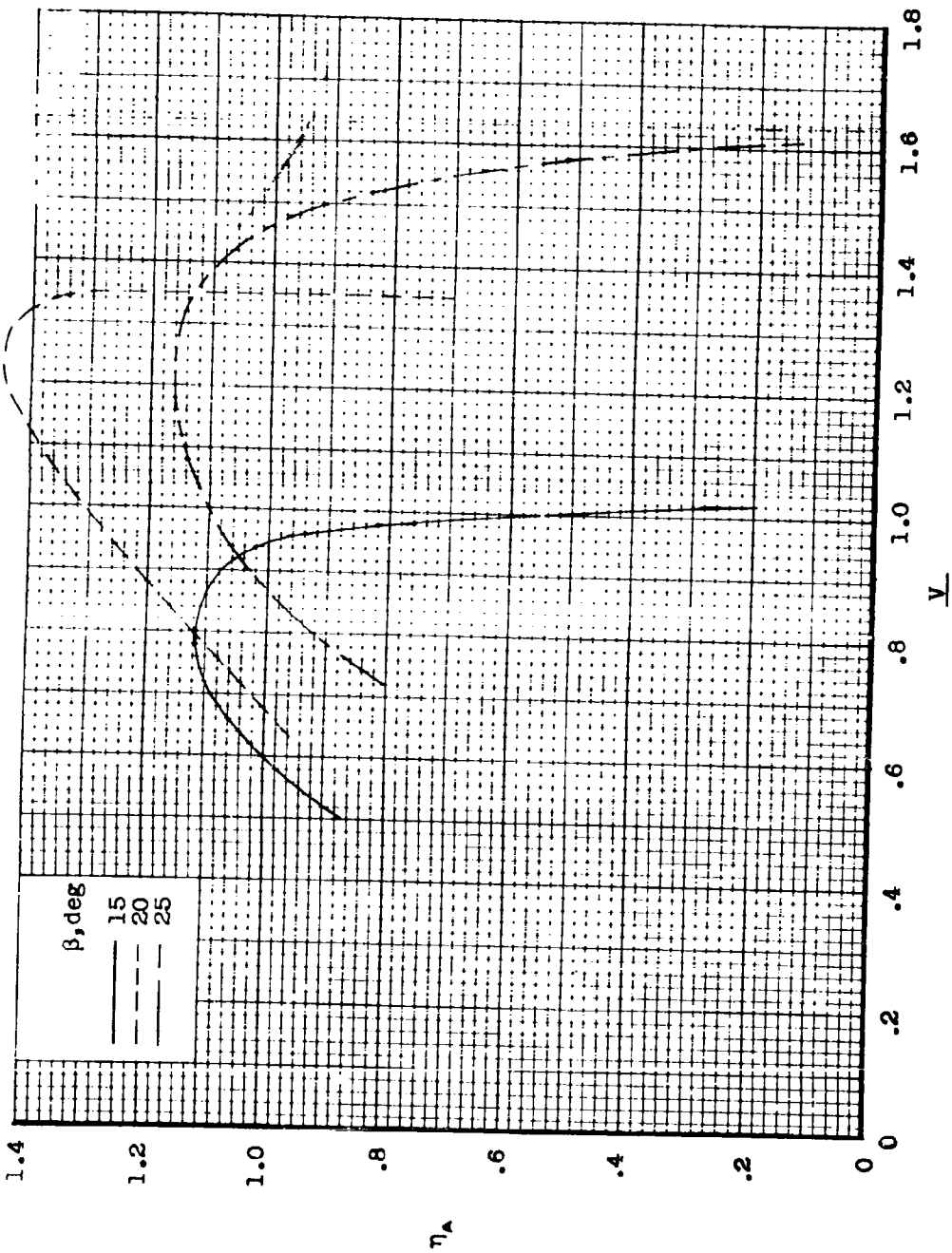

Figure 20 - Variation of Apparent Propeller Efficiency with Advance Ratio and Blade Angle - 2AC Wake Propeller

CONFIDENTIAL

CONFIDENTIAL

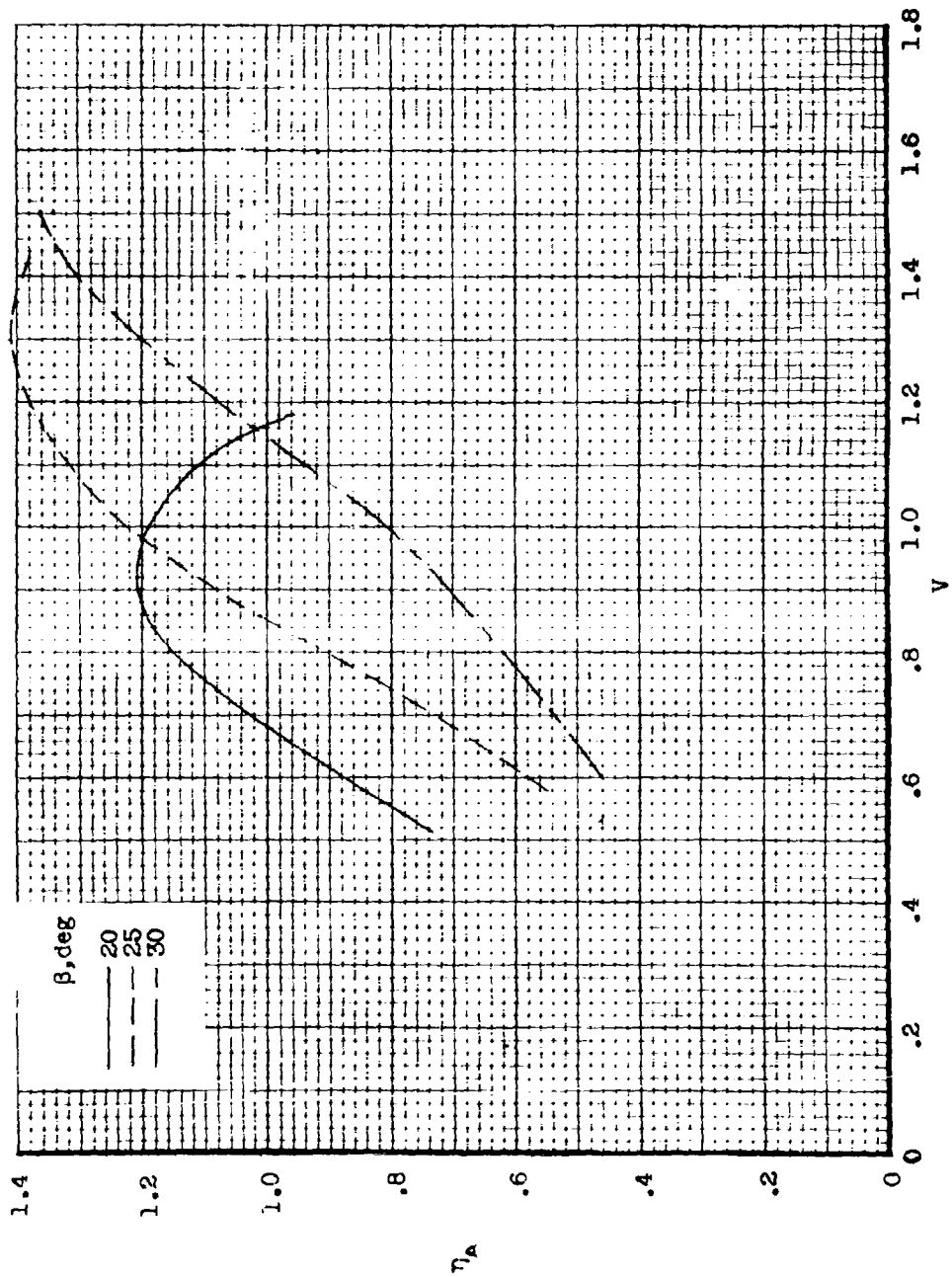

Figure 21 - Variation of Apparent Propeller Efficiency with Advance Ratio and Blade Angle - Trans. Propeller

CONFIDENTIAL

PREPARED BY BPS
CHECKED BY K.A.Y
DATE APRIL 15, 1961
REVISED

GOODYEAR
GOODYEAR AIRCRAFT CORPORATION
AKRON, OHIO

PAGE 59
MODEL 1/20-EPG-3W (MODIFIED)
GER- 10176
REF NO.

CONFIDENTIAL

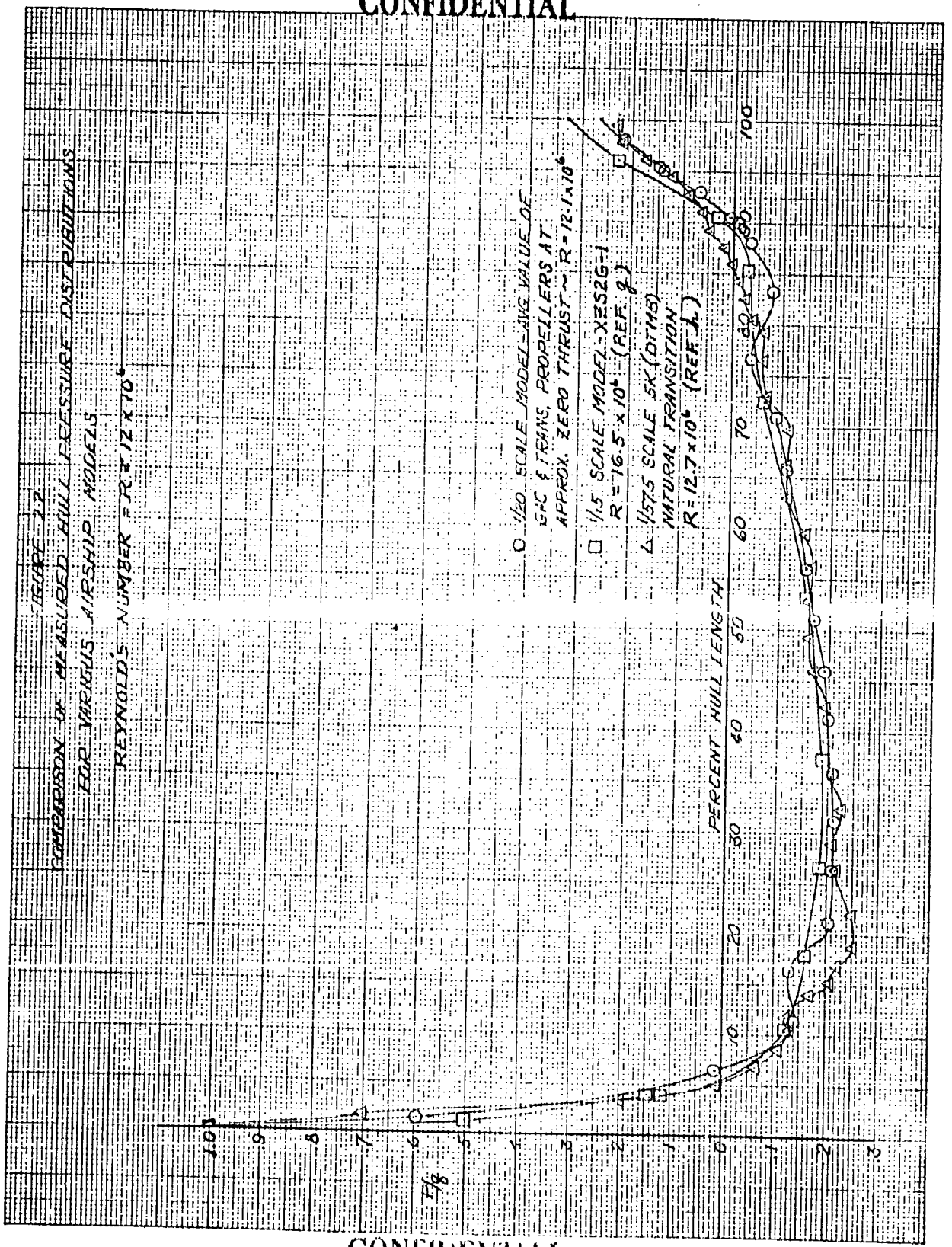

Fig 8

CONFIDENTIAL

JR 220 (12-60)

PREPARED BY BPS
CHECKED BY K.A.Y.
DATE APRIL 15, 1961
REVISED

GOODYEAR
GOODYEAR AIRCRAFT CORPORATION
AKRON, OHIO

PAGE 60
MODEL 1/20 - ZPG-3W (MODIFIED)
GER- 10176
REF NO.

CONFIDENTIAL

FIGURE 23
COMPARISON OF MEASURED HULL PRESSURE DISTRIBUTIONS
FOR VARIOUS AIRSHIP MODELS
REYNOLD'S NUMBER = R ≅ 18 x 10⁶

Fig 8

CONFIDENTIAL

JR 120 (12-60)

CONFIDENTIAL

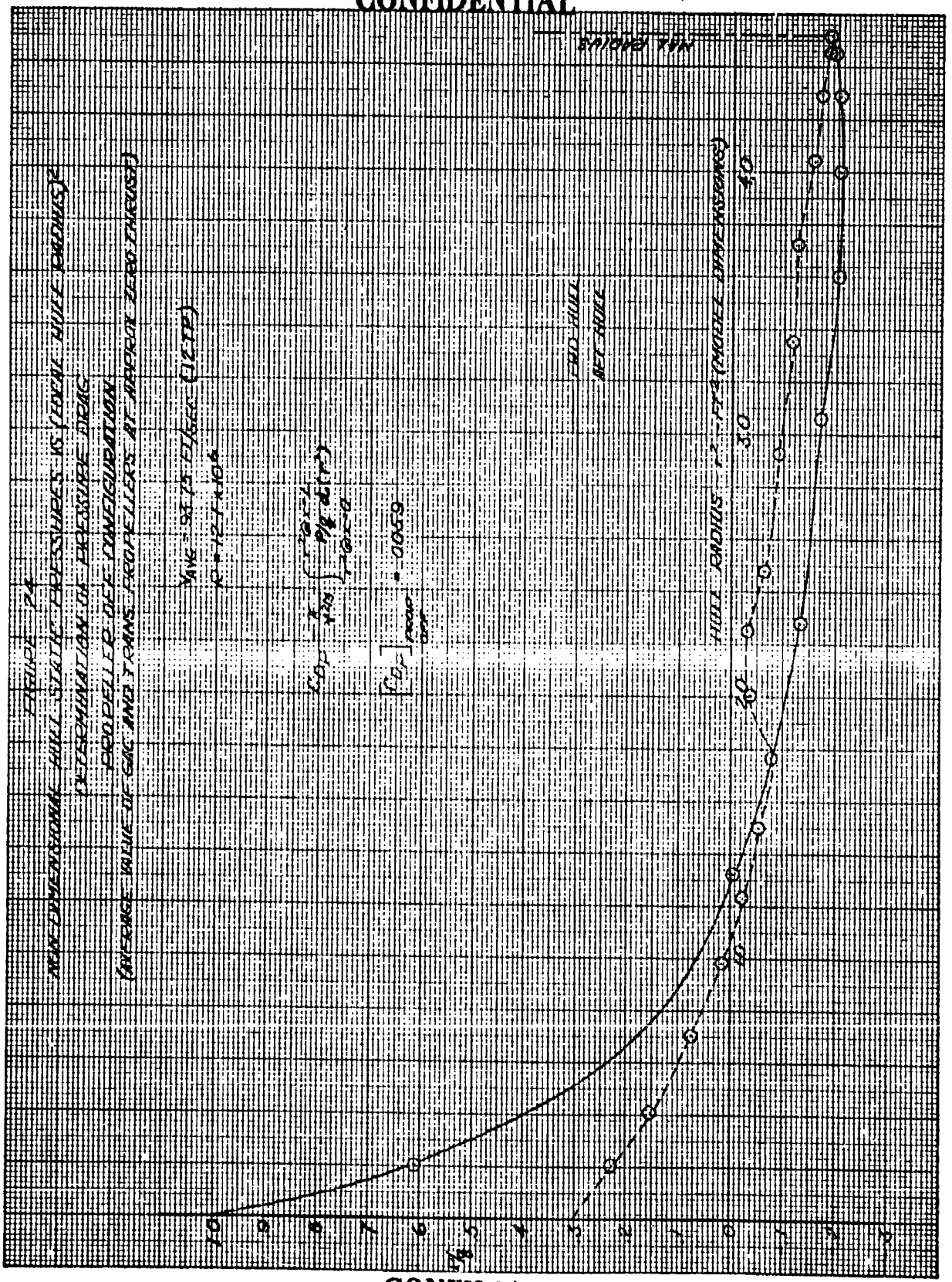

CONFIDENTIAL

CONFIDENTIAL

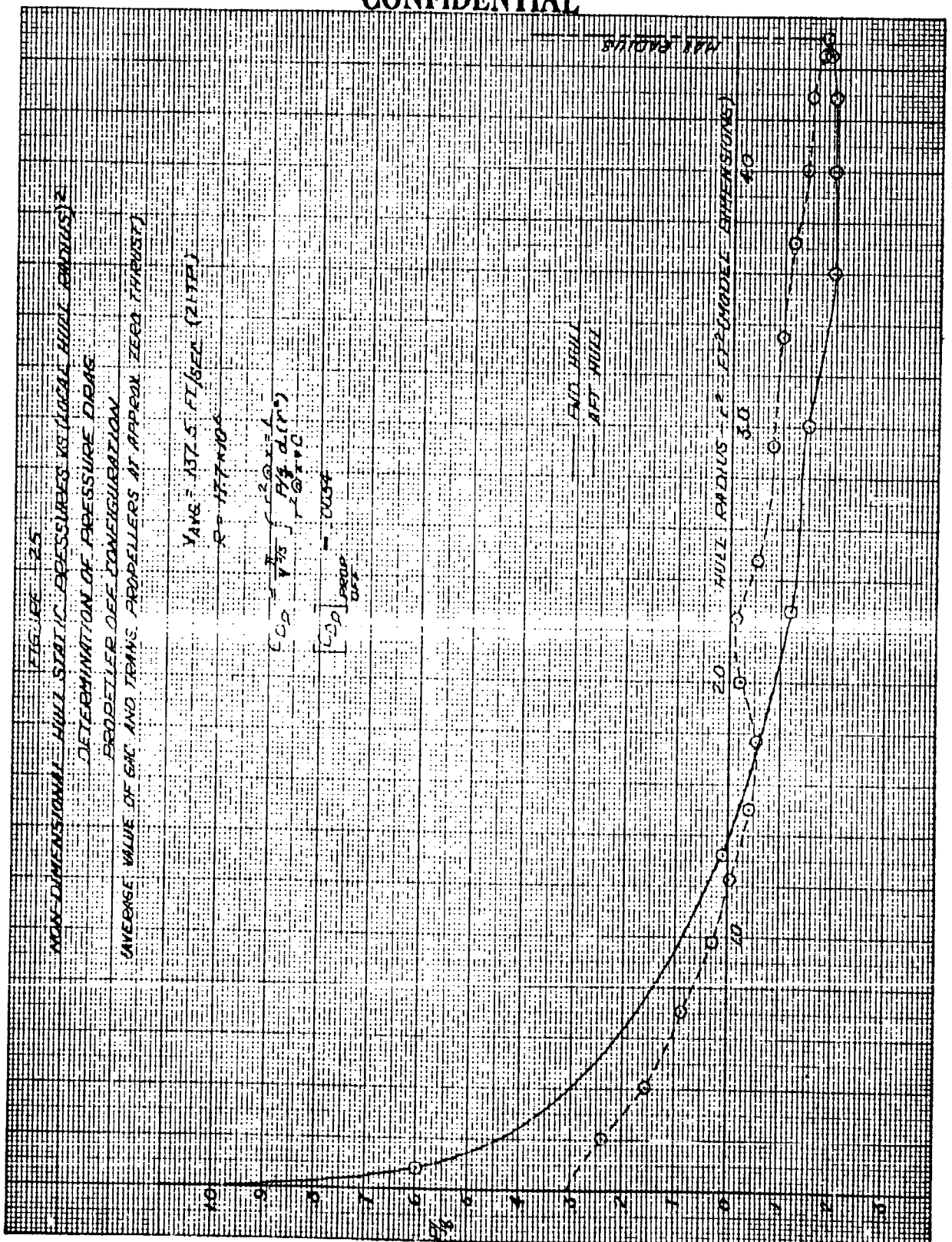

FIGURE 25

NON-DIMENSIONAL HULL STATIC PRESSURES VERSUS HULL RADIUS (STATION 170)

DETERMINATION OF PRESSURE DRAG

PROPELLER DEE CONFIGURATION

AVERAGE VALUE OF GAC AND TRANS. PROPELLERS AT APPROX. ZERO THRUST

$V_{AVG} = 137.5$ FT/SEC (21 KTS)

$\rho = .002404$

$C_{D_{PROP}} = \frac{T}{\frac{1}{2}\rho V^2 A} = \frac{P/S \, d(r^2)}{\frac{1}{2}\rho V^2 \pi r^2 @ x=1} + 0$

$C_{D_{PROP}} = .0034$

AR 220 (12-60)

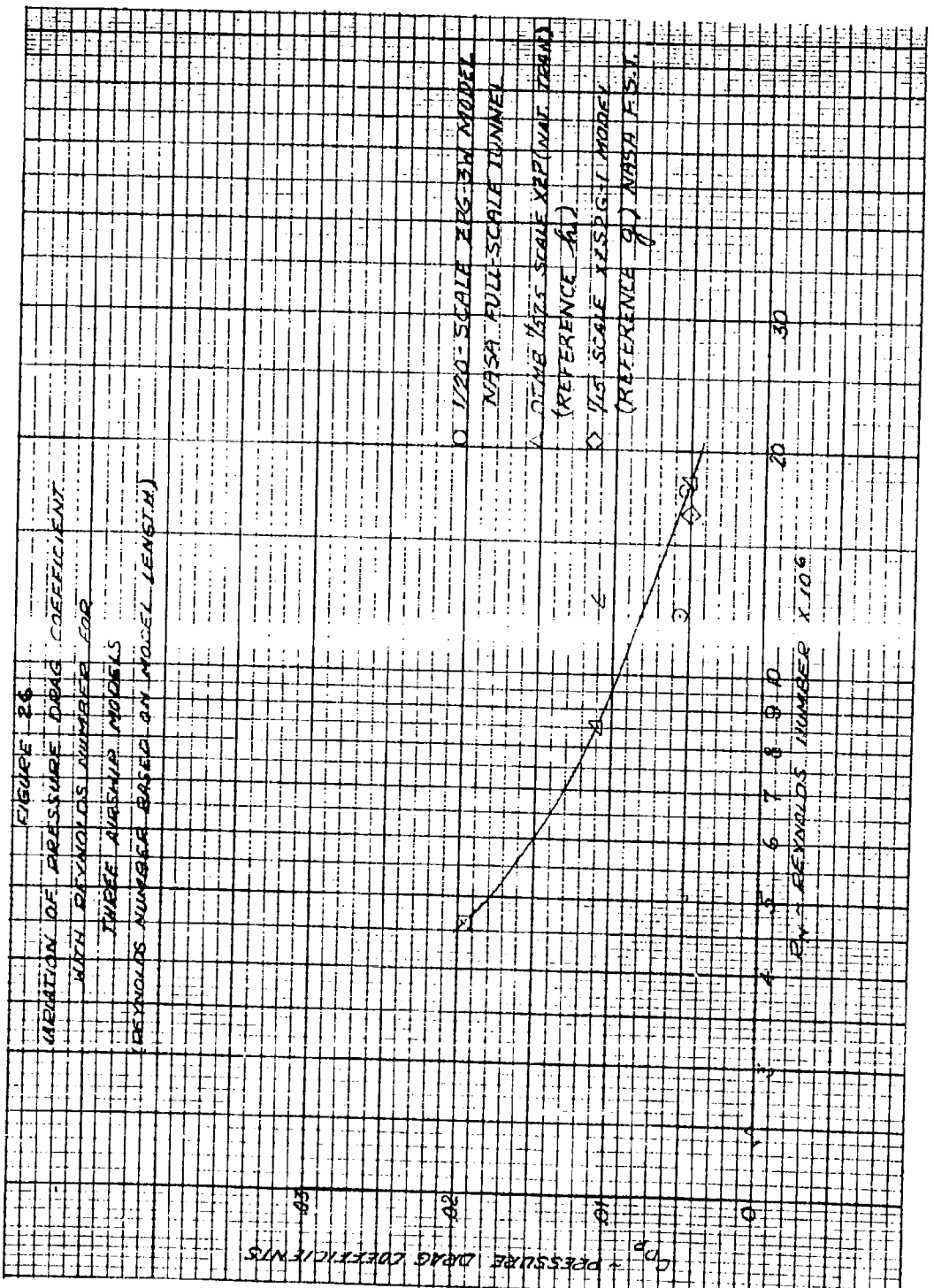
FIGURE 26
VARIATION OF PRESSURE DRAG COEFFICIENT
WITH REYNOLDS NUMBERS FOR
THREE AIRSHIP MODELS
(REYNOLDS NUMBERS BASED ON MODEL LENGTH)
1/20-SCALE ZPG-3W MODEL
NASA FULL-SCALE TUNNEL
(REFERENCE 41)
1/15 SCALE XZP(WAF TEST)
(REFERENCE 41)
1/15 SCALE XZP(NAF) MODEL
(REFERENCE 9) NASA F.S.T.
C_{D_p} = PRESSURE DRAG COEFFICIENTS
.03
.02
.01
0
1
2
3
4
5
6
7
8
9
10
20
30
R_N - REYNOLDS NUMBER
X 10⁶

PREPARED BY BCS
CHECKED BY K.A.Y.
DATE APRIL 15, 1961
REVISED

GOODYEAR
GOODYEAR AIRCRAFT CORPORATION
AKRON, OHIO

PAGE 64
MODEL 1/30 - ZPG-3W - (MODIFIED)
GER- 10176
REF NO.

CONFIDENTIAL

DETERMINATION OF PRESSURE DRAG
MONOCOQUE HULL STATIC PRESSURES VS LOCAL RUN OF HULL
FIGURE 27

VAC. PROPELLER
V = 94.6 FT/SEC.
V/nD = 1.187
THRUST = 2.75 LBS.
B = 20°
RPM = 2600
BHP = 0.324
C_T = 0.042

$C_{D_P} = C_{D_F} = \left[C_{D_B}\right]_{REPORT}$
$-0.0060 - 0.0059$
$C_{D_P} = 0.0021$

FWD HULL
AFT HULL

HULL RADIUS - r² - FT.² (MODEL DIMENSIONS)

STATION X/L

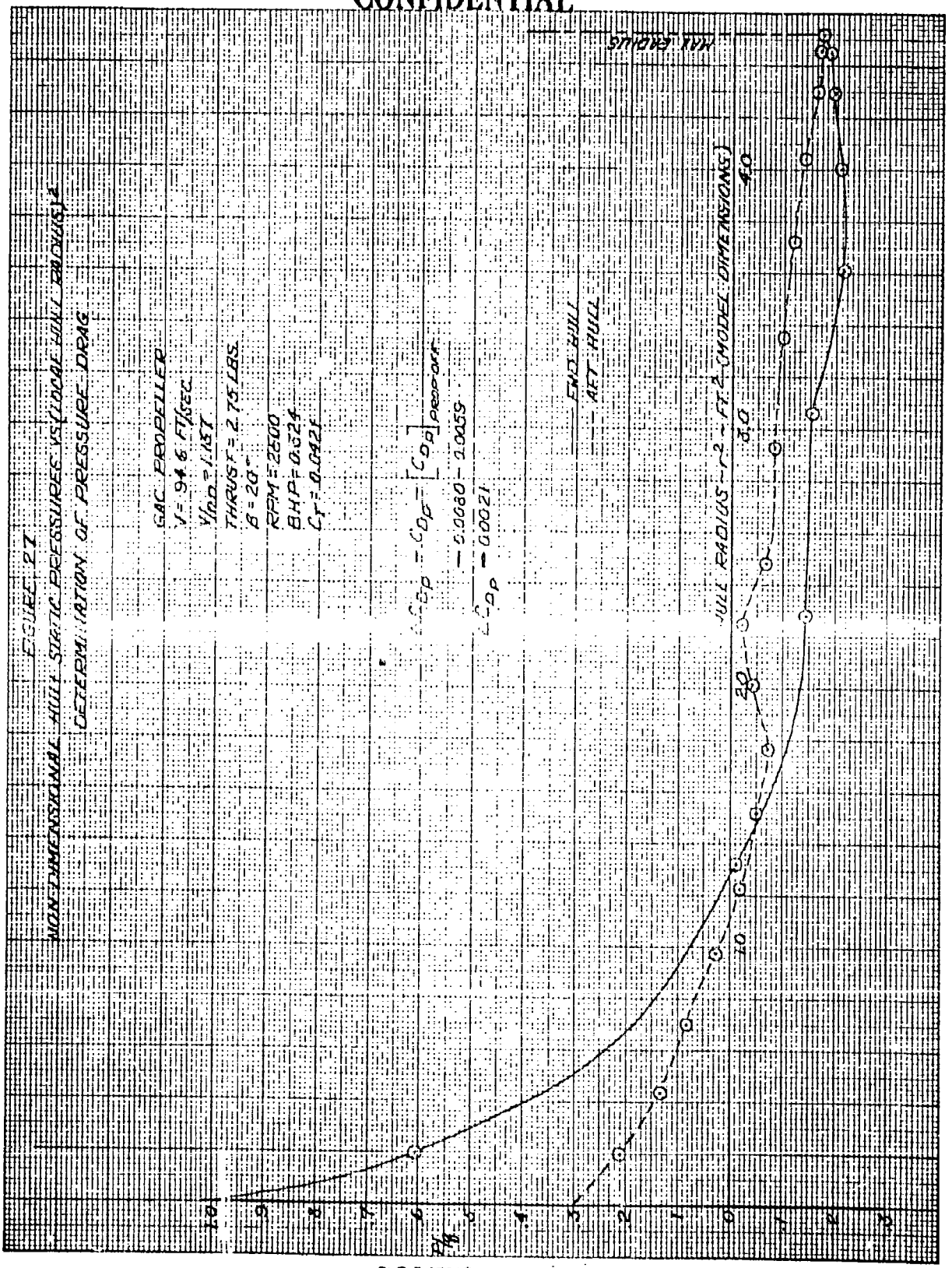

CONFIDENTIAL

JR 230 (12-60)

PREPARED BY G'K'S
CHECKED BY K.A.Y.
DATE APRIL 15, 1961
REVISED

GOODYEAR
GOODYEAR AIRCRAFT CORPORATION
AKRON, OHIO

PAGE 65
MODEL 1/20 - ZPG-3W - (MODIFIED)
GER- 10176
REF NO.

CONFIDENTIAL

FIGURE 28
NON-DIMENSIONAL HULL STATIC PRESSURES VS (LOCAL HULL RADIUS)^2
DETERMINATION OF PRESSURE DRAG

GAC PROPELLER
V= 94.6 FT/SECS
V/nD = 0.860
THRUST = 16.05 LBS.
β = 20°
RPM = 3300
BHP = 1.450
C_T = 0.0882

$\Delta C_{D_p} = C_{D_p} - [C_{D_p}]_{\text{SEP. OFF}}$
= 0.0125 - 0.0059
ΔC_{D_p} = 0.0066

FWD. HULL
AFT. HULL

STATION MAX. RADIUS
HULL RADIUS - r^2-FT^2 - (MODEL DIMENSIONS)

P_{H_2}

CONFIDENTIAL

JB 220 (12-60)

PREPARED BY JRS
CHECKED BY K.A.Y.
DATE APRIL 15, 1961
REVISED

GOODYEAR
GOODYEAR AIRCRAFT CORPORATION
AKRON, OHIO

PAGE 66
MODEL YEA-2PG-2N-(MODIFIED)
SER. 10176
REF NO.

CONFIDENTIAL

CONFIDENTIAL

AR 250 (12-60)

PREPARED BY B.V.S
CHECKED BY K.A.Y.
DATE APRIL 15, 1961
REVISED

GOODYEAR
GOODYEAR AIRCRAFT CORPORATION
AKRON, OHIO

PAGE 67
MODEL 1/20 - ZPG-3W-(MODIFIED)
GER- 10176
REF NO.

CONFIDENTIAL

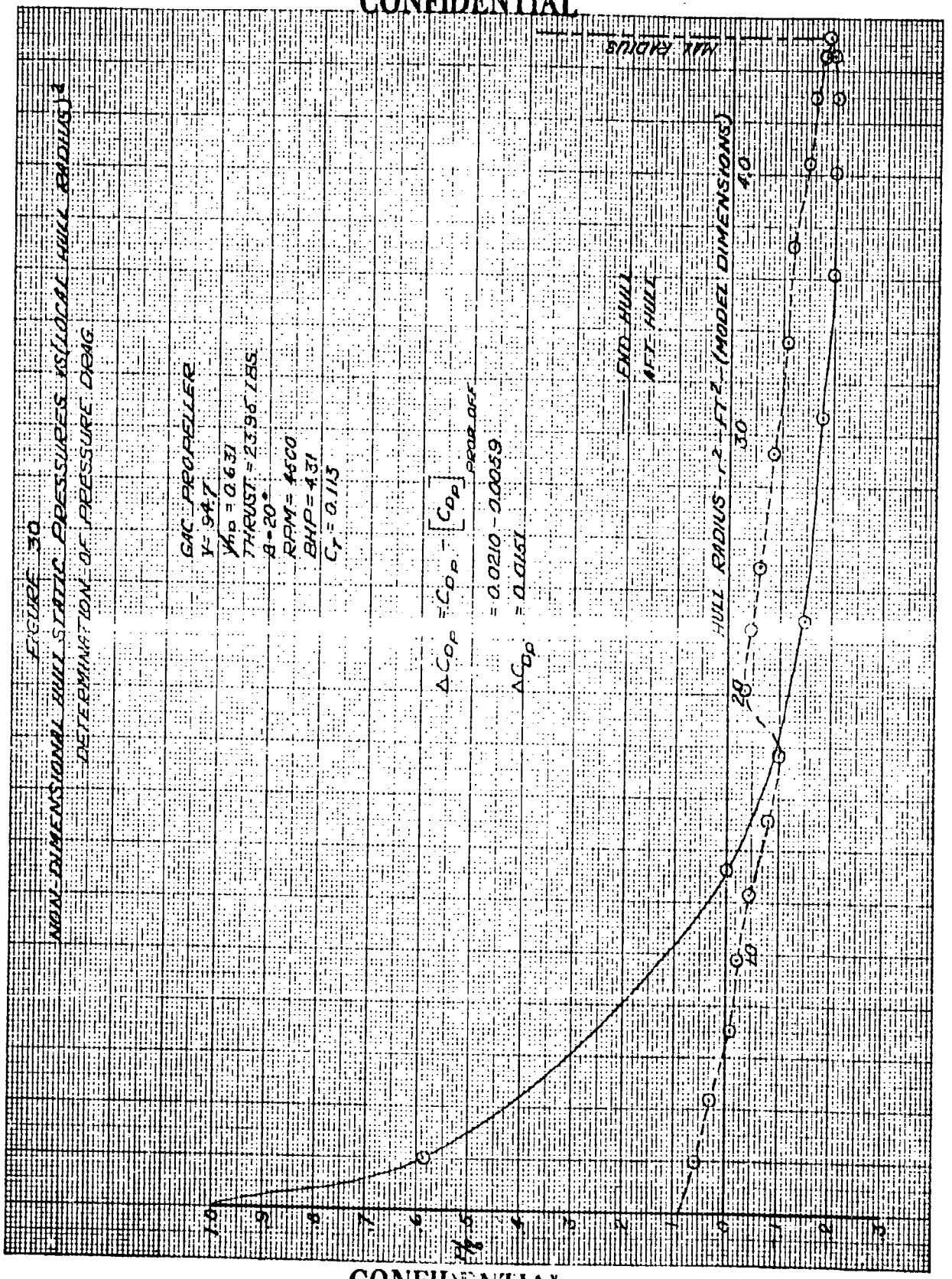

CONFIDENTIAL

AR 220 (12-60)

PREPARED BY BES
CHECKED BY K.A.Y.
DATE APRIL 15, 1961
REVISED

GOODYEAR
GOODYEAR AIRCRAFT CORPORATION
AKRON, OHIO

PAGE 68
MODEL 1/20 - ZPG-3W (MODIFIED)
GER- 10176
REF NO.

CONFIDENTIAL

FIGURE 31
NON-DIMENSIONAL HULL STATIC PRESSURES (LOCAL HULL RADIUS)^2
DETERMINATION OF PRESSURE DRAG

GAC PROPELLER
$V = 140.3$ FT/SEC
$M_\infty = 1.202$
THRUST = 3.90 LBS.
$\beta = 20°$
RPM = 3500
BHP = 0.692
$C_T = 0.0304$

$\Delta C_{Dp} = C_{Do} - \left[C_{Do}\right]_{PROP\ OFF}$
$= 0.0067 - 0.0054$
$\Delta C_{Dp} = 0.0013$

FWD HULL
AFT HULL

MAX. RADIUS

HULL RADIUS - r^2 - FT^2 - (MODEL DIMENSIONS)

Fig. 5

CONFIDENTIAL

JB 220 (12-60)

PREPARED BY BRS
CHECKED BY K.A.Y.
DATE APRIL 15, 1961
REVISED

GOODYEAR
GOODYEAR AIRCRAFT CORPORATION
AKRON, OHIO

PAGE 69
MODEL 1/20 - ZPG-3W (MODIFIED)
GER- 10176
REP NO.

CONFIDENTIAL

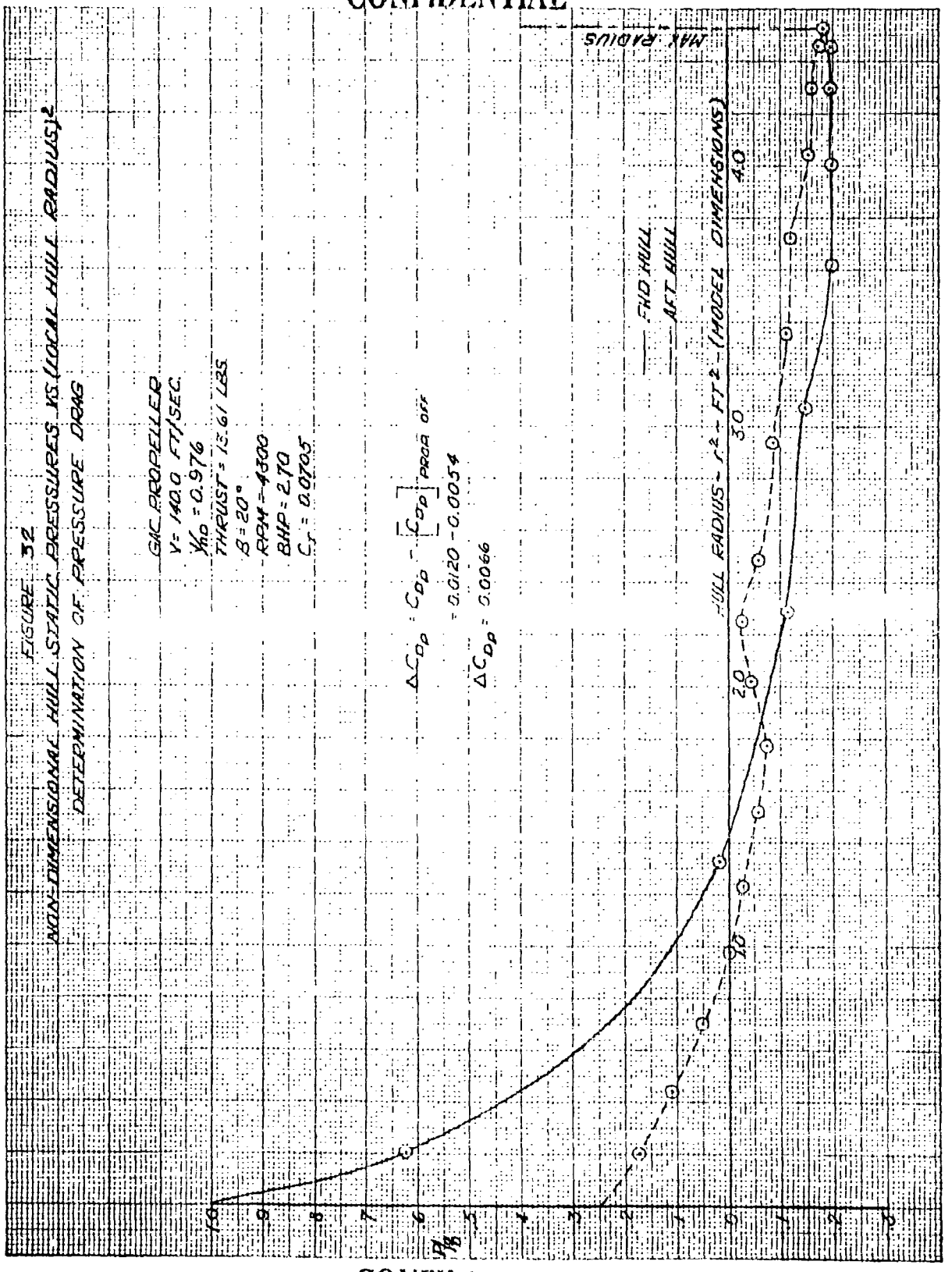

CONFIDENTIAL

JB 220 (12-60)

CONFIDENTIAL

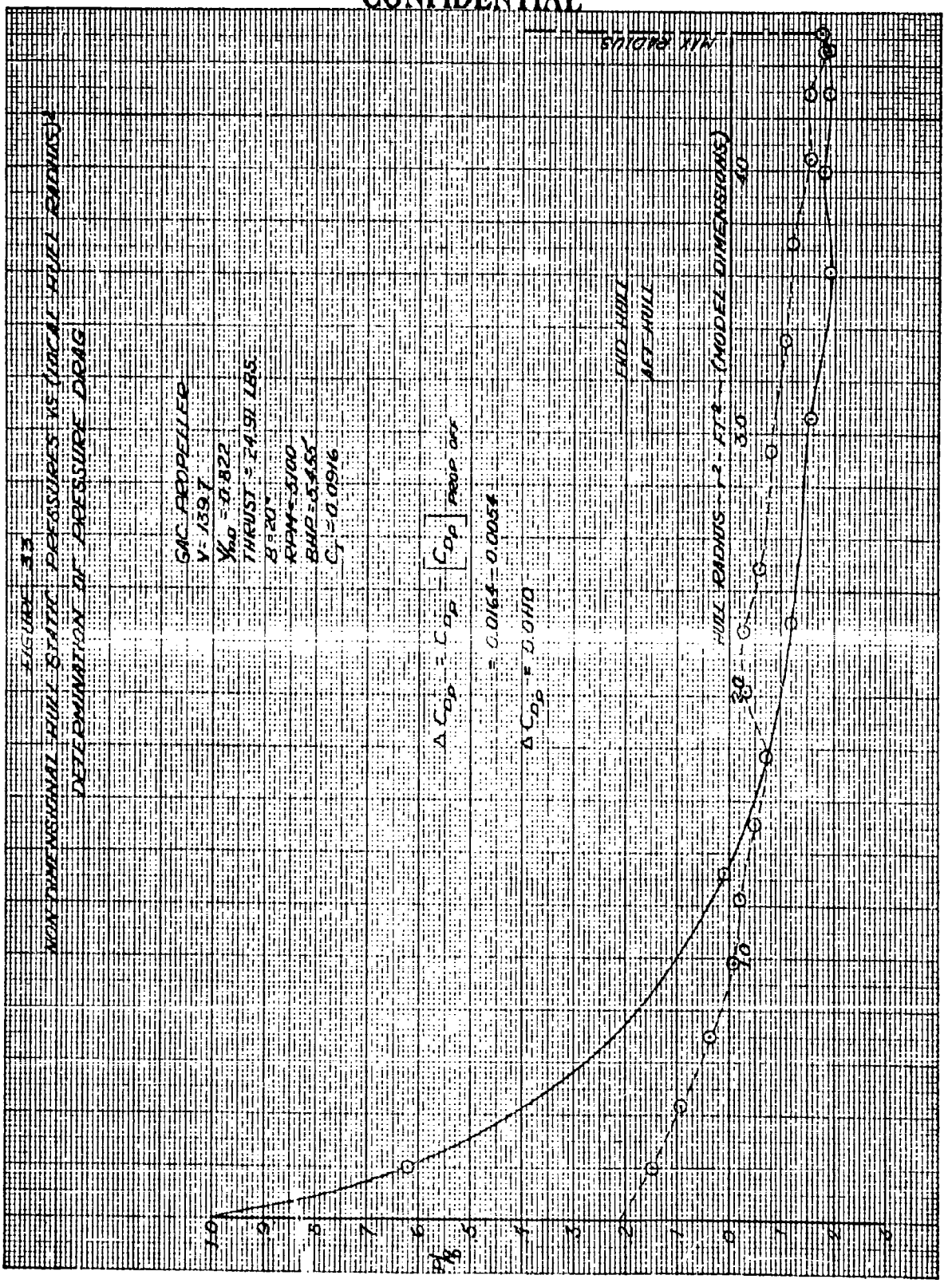

CONFIDENTIAL

JB 220 (12-60)

CONFIDENTIAL

FIGURE 34
NON-DIMENSIONAL HULL STATIC PRESSURES VS (LOCAL HULL RADIUS)^2
DETERMINATION OF PRESSURE DRAG

TRANS. PROPELLER
V = 92.8 FT/SEC
K_{H_0} = 0.508
THRUST = 13.65 LBS.
β = 20°
RPM = 8000
BHP = 3.185
C_T = 0.0907

$\Delta C_{D_p} = C_{D_0} - \left[C_{D_0}\right]_{PROP\ OFF}$
= 0.0161 - 0.0059
ΔC_{D_p} = 0.0102

MAX RADIUS
FWD. HULL
AFT. HULL

HULL RADIUS - r^2 - FT.^{2} - (MODEL DIMENSIONS)

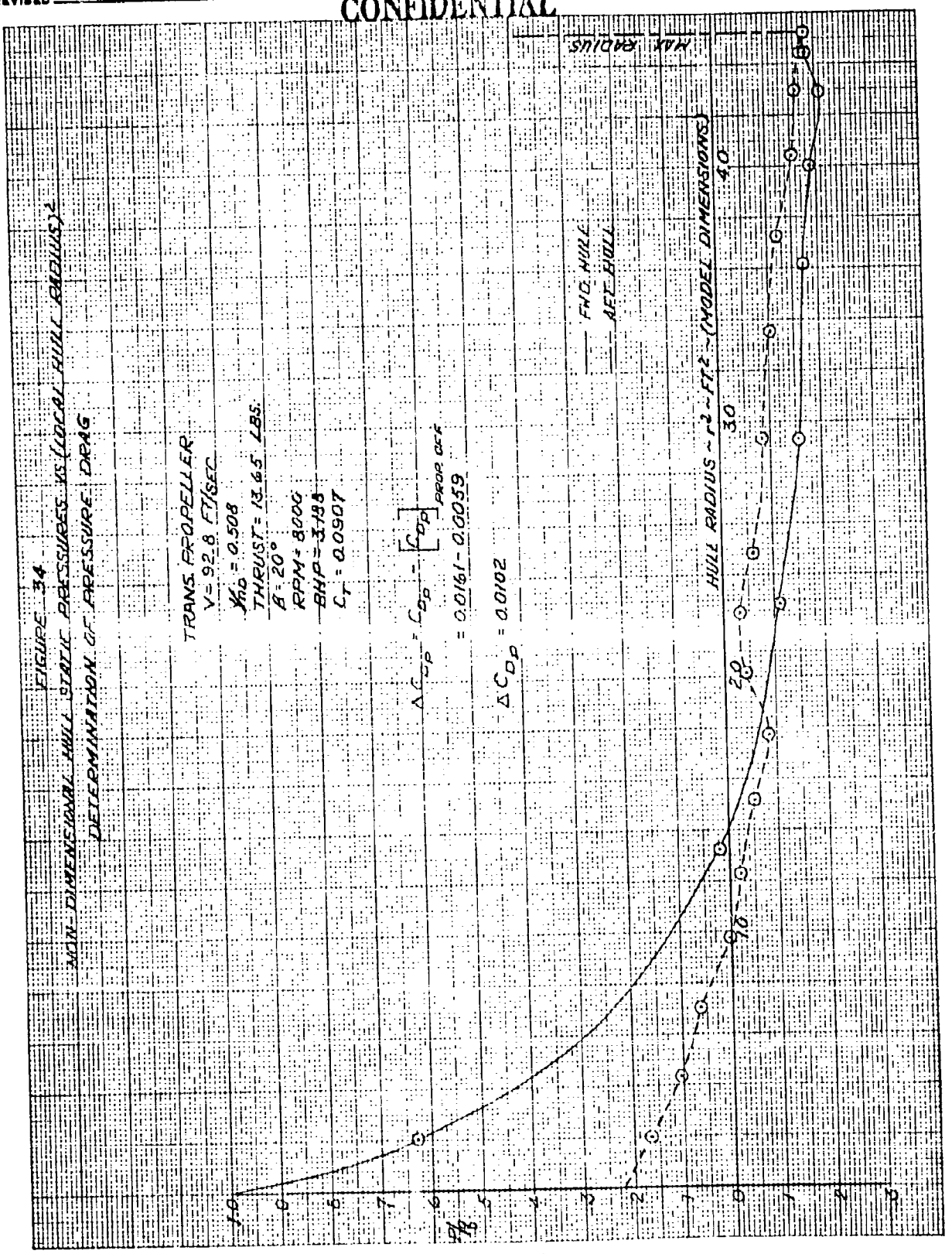

CONFIDENTIAL

JR 220 (12-60)

PREPARED BY BLS
CHECKED BY K.A.Y.
DATE APRIL 15, 1961
REVISED

GOODYEAR
GOODYEAR AIRCRAFT CORPORATION
AKRON, OHIO

PAGE 72
MODEL 1/20-ZPG-3W (Modified)
GER- 10176
REF NO.

CONFIDENTIAL

FIGURE 35

NONDIMENSIONAL HULL STATIC PRESSURES VS (LOCAL HULL RADIUS)^2

DETERMINATION OF PRESSURE DRAG

TRANS. PROPELLER
V = 136.3 FT/SEC
$V_{/D}$ = 0.757
THRUST = 11.35 LBS
β = 20°
RPM = 8000
BHP = 2.567
C_T = 0.0761

$\Delta C_{DP} = C_{DP} - [C_{DP}]_{PROP\ OFF}$
= 0.0135 - 0.0054
ΔC_{DP} = 0.0081

— FWD HULL
--- AFT HULL

SHROUD MAX

HULL RADIUS^2 - FT^2 - (MODEL DIMENSIONS)

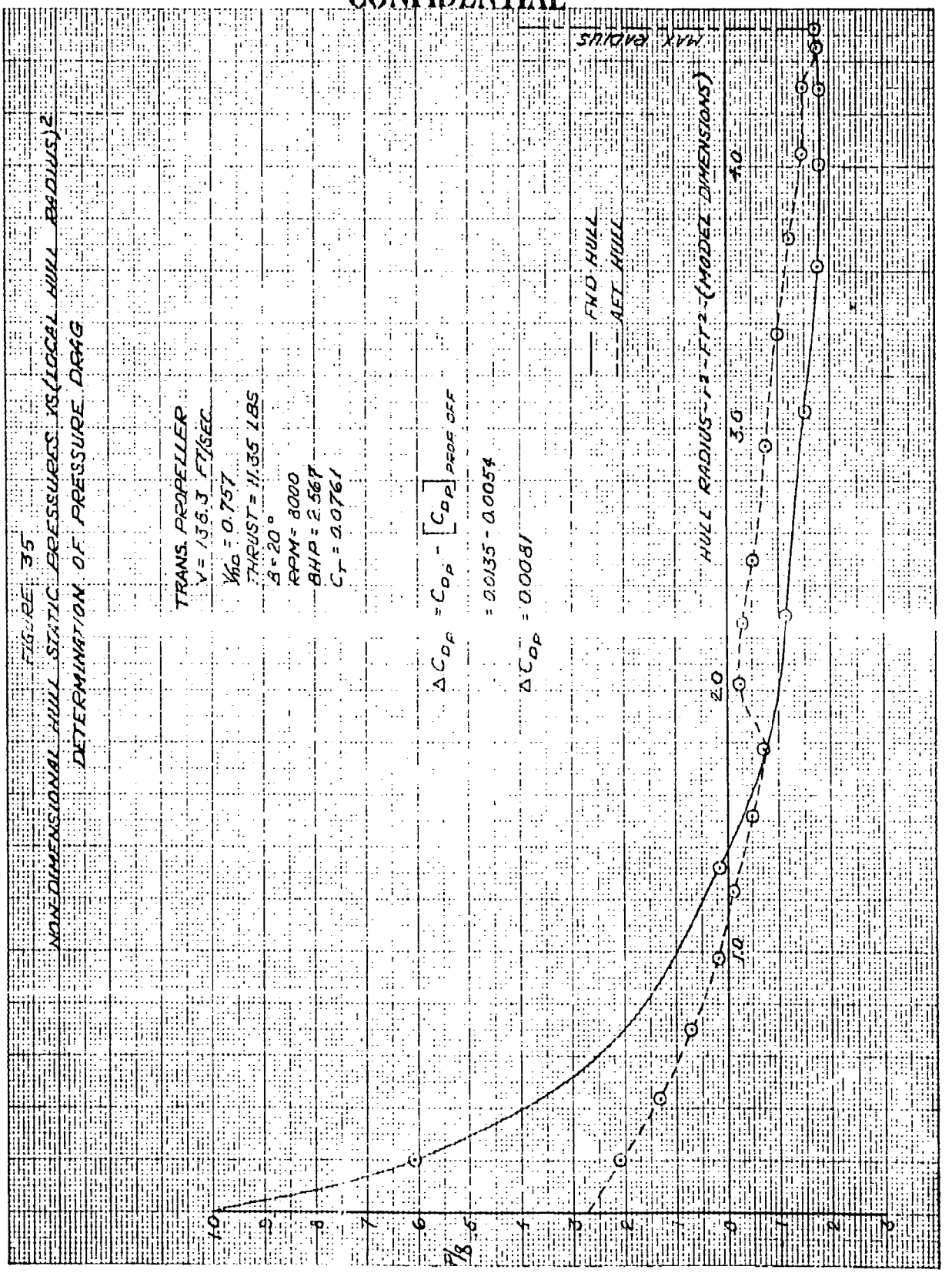

CONFIDENTIAL

JR 220 (12-60)

PREPARED BY E
CHECKED BY A
DATE APRIL
REVISED

FIGURE 36
VARIATION OF THE CHANGE IN PRESSURE DU
OPERATION, WITH THRUST COE
GAC WAKE PROPELLE

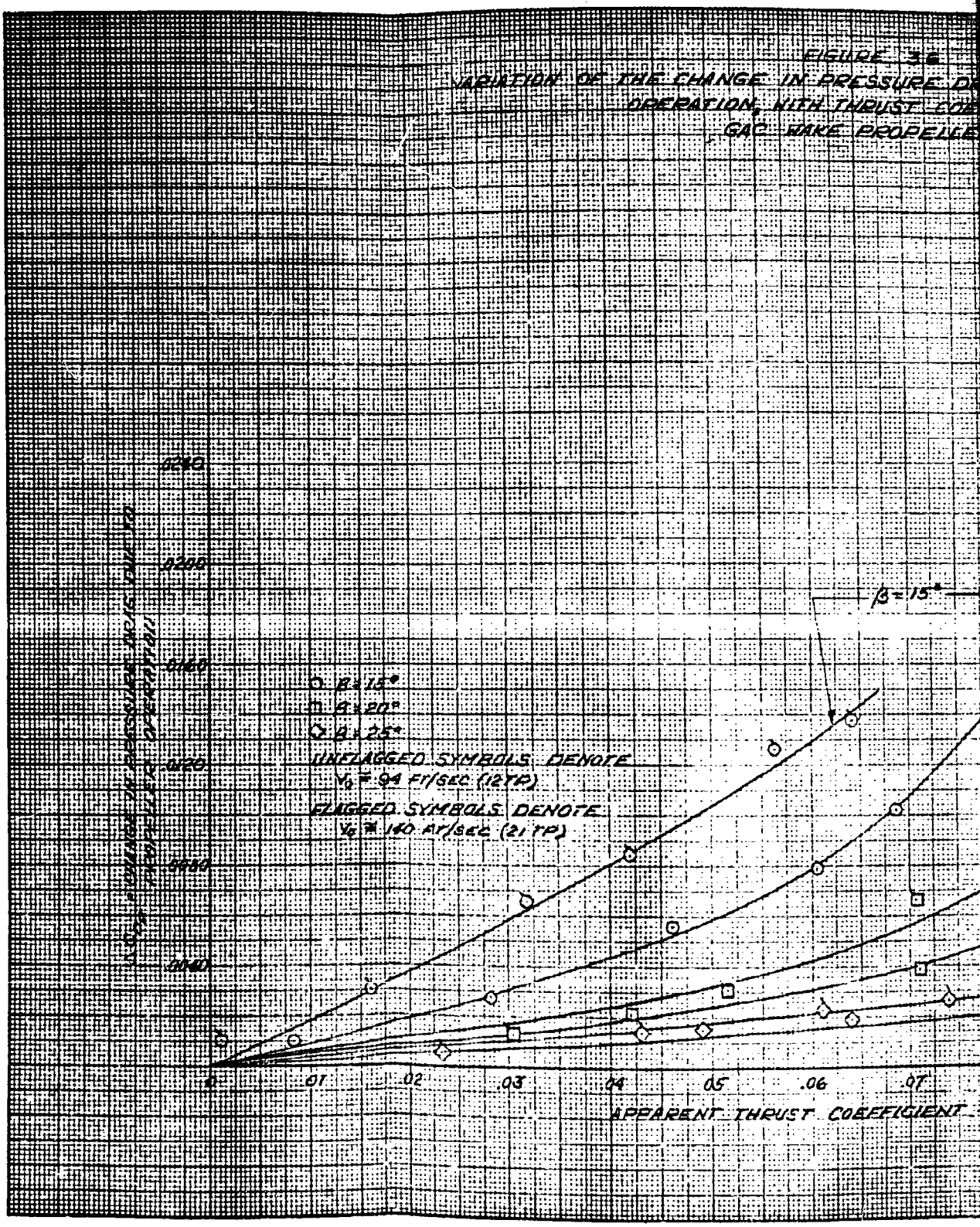

1

CONFIDENTIAL

FIGURE 36
CHANGE IN PRESSURE DRAG, DUE TO WAKE PROPELLER
RATION, WITH THRUST COEFFICIENT
GAC WAKE PROPELLER

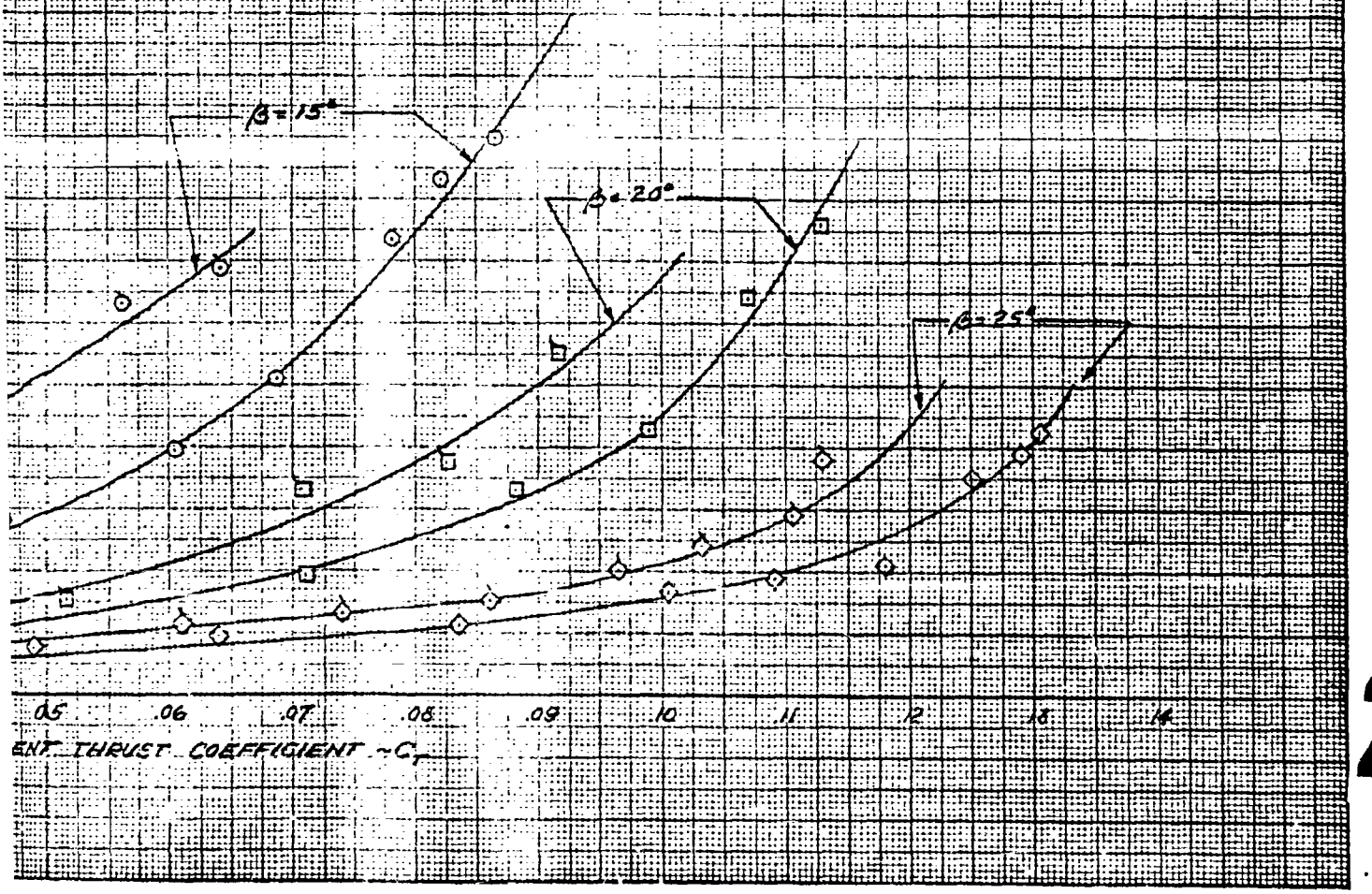

2

CONFIDENTIAL

PREPARED BY TBPS
CHECKED BY K. A. Y.
DATE APRIL 15, 1961
REVISED

GOODYEAR
GOODYEAR AIRCRAFT CORPORATION
AKRON, OHIO

PAGE 74
MODEL 120 - ZPG-3W (MODIFIED)
GER- 10176
REF NO.

CONFIDENTIAL

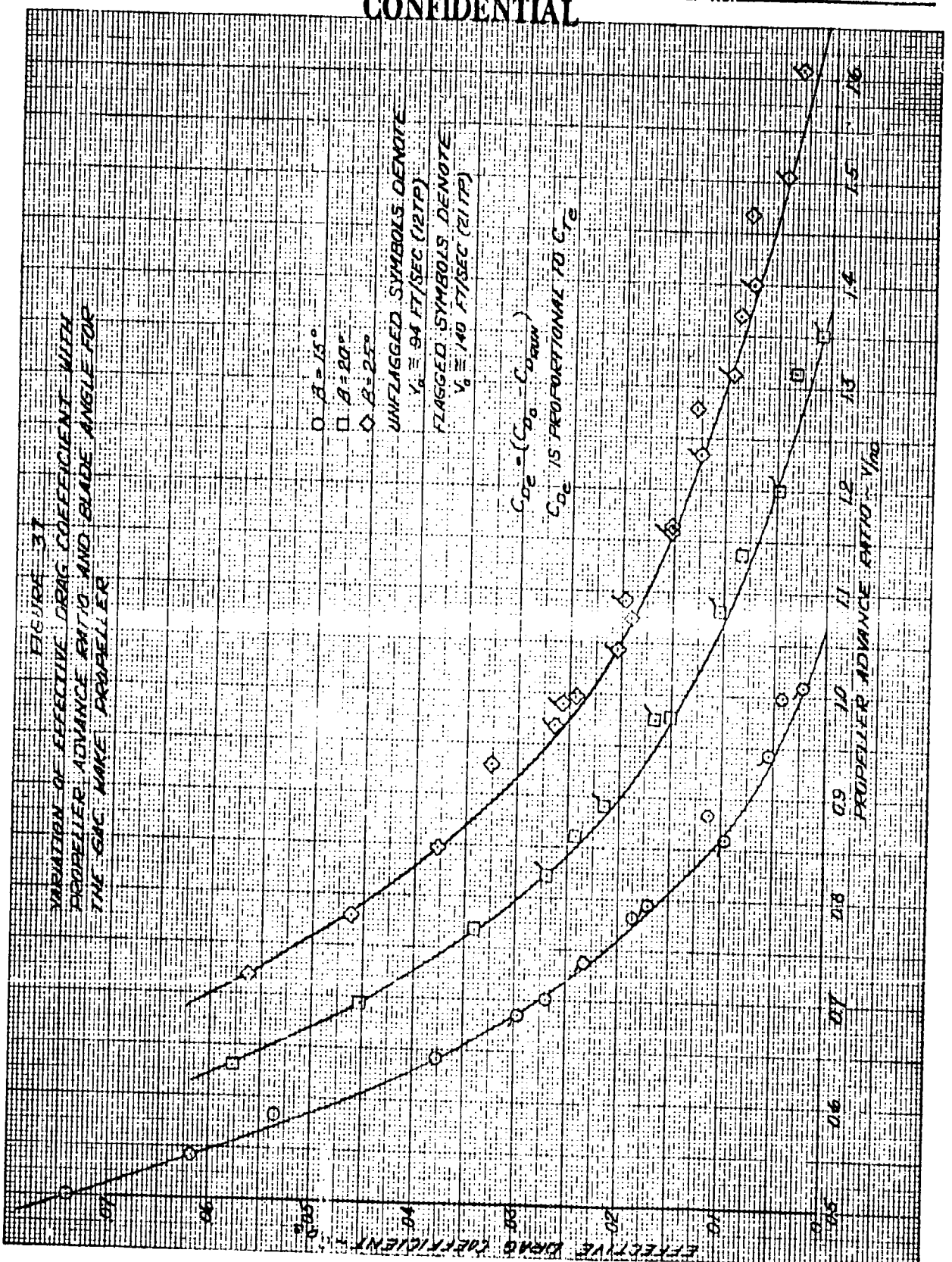

FIGURE 37
VARIATION OF EFFECTIVE DRAG COEFFICIENT WITH PROPELLER ADVANCE RATIO AND BLADE ANGLE FOR THE GAC WAKE PROPELLER

CONFIDENTIAL

JR 220 (12-60)

PREPARED BY BPS
CHECKED BY K.A.Y.
DATE April 15, 1961
REVISED

FIGURE 3.8
COMPARISON OF APPARENT EFFICIENCY AND
AS DETERMINED BY SEVERAL ME

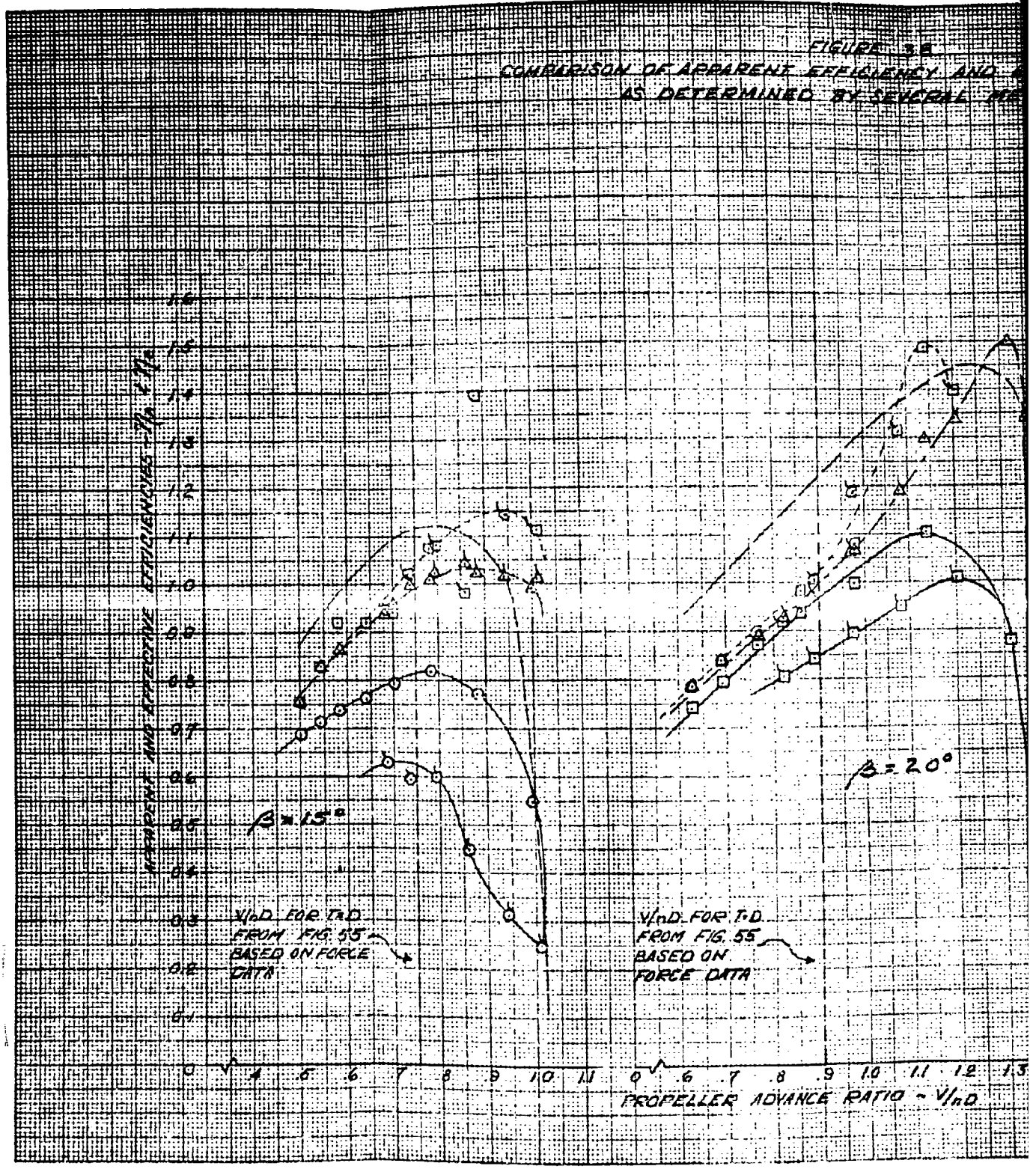

1

CONFIDENTIAL

FIGURE 38
APPARENT EFFICIENCY AND EFFECTIVE EFFICIENCY DETERMINED BY SEVERAL METHODS

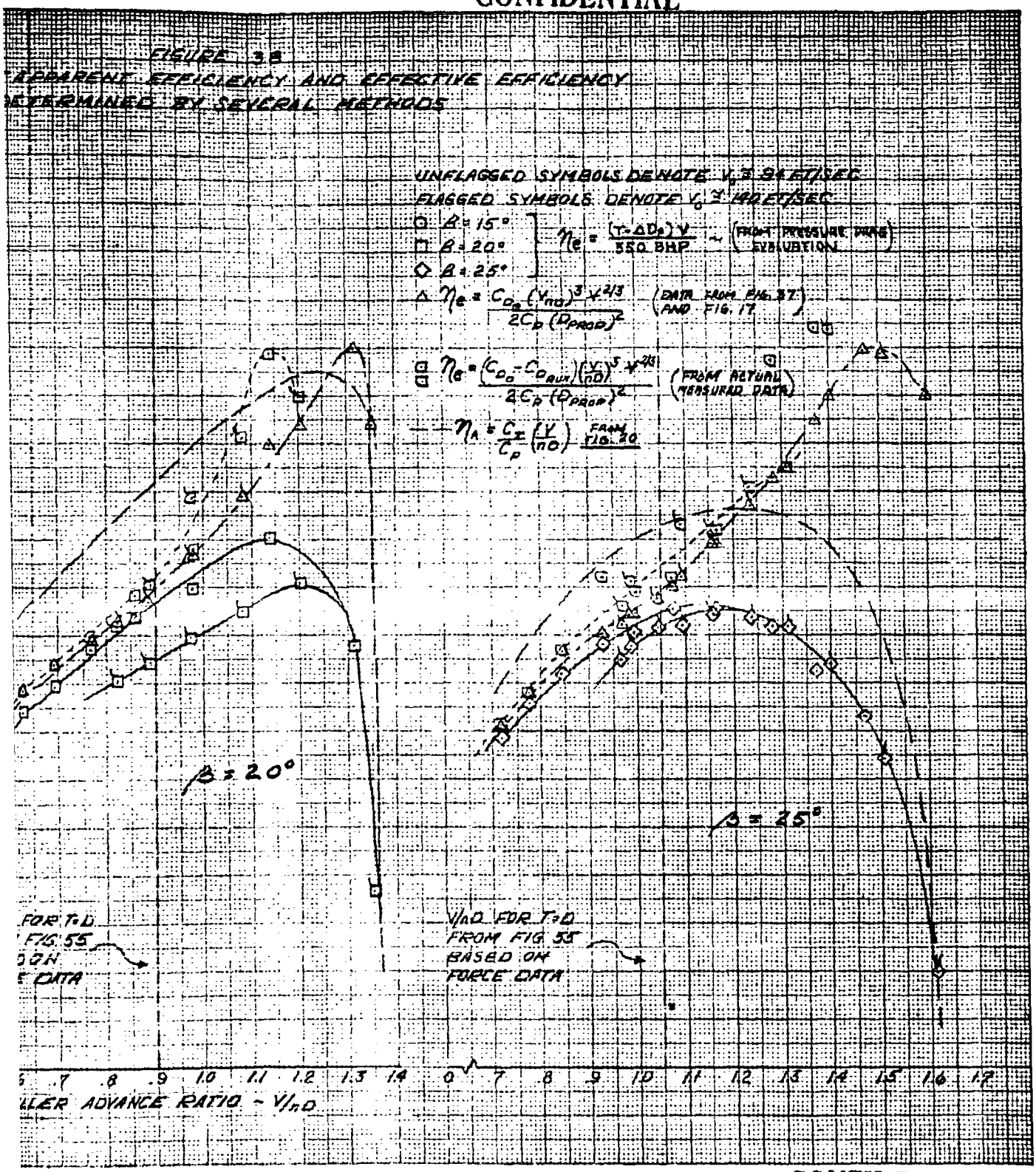

2

CONFIDENTIAL

JR 220 (12-60)

PREPARED BY JJ&S
CHECKED BY K.A.Y.
DATE APRIL 15, 1961
REVISED

GOODYEAR
GOODYEAR AIRCRAFT CORPORATION
AKRON, OHIO

PAGE 76
MODEL GA-ERG-3W (Mod)
GER- 12126
REF NO.

CONFIDENTIAL

FIGURE 39

η_A vs. V/nD

COMPARISON OF APPARENT EFFICIENCY DETERMINED DURING PROPELLER EVALUATION AND AERODYNAMIC CHARACTERISTICS EVALUATIONS.

GAC WAKE PROPELLER

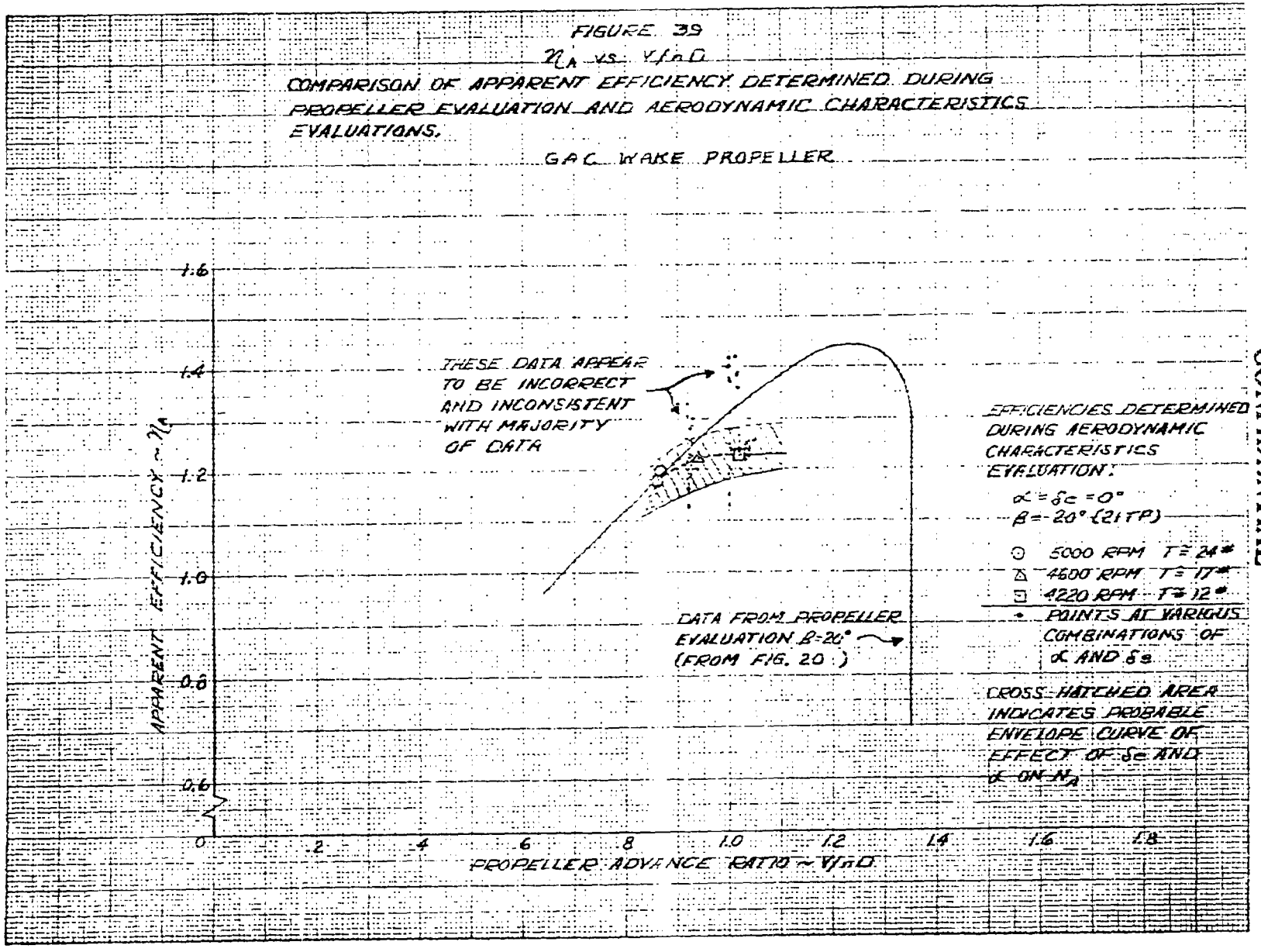

CONFIDENTIAL

PREPARED BY XRS
CHECKED BY K.A.Y.
DATE AUGUST 15, 1961
REVISED

GOODYEAR
GOODYEAR AIRCRAFT CORPORATION
AKRON, OHIO

PAGE 77
MODEL V-20-J PG-3W (MODIFIED)
GER- 10176
REF NO.

CONFIDENTIAL

FIGURE 40
EFFECT OF ANGLE OF ATTACK ON APPARENT EFFICIENCY
FOR THREE POWER CONDITIONS
G.A.C. WAKE PROPELLER

η_a

$\xi = 0°$
$\beta = 20°$
$V_0 = 141.78$ FT/SEC

□ $V/nD = 0.850$ (AVG. VALUE @ 5000 RPM)
□ $V/nD = 0.924$ (AVG. VALUE @ 4600 RPM)
△ $V/nD = 1.015$ (AVG. VALUE @ 4220 RPM)

ACTUAL DATA CURVE WHICH APPEARS TO BE INCORRECT

POSSIBLE VARIATION BASED ON OTHER CURVES AND PREVIOUSLY CALCULATED-NA

1.50
1.40
1.30
1.20
1.10

12 10 8 6 4 2 0 -2 -4 -6 -8 -10

ANGLE OF ATTACK = α - DEGREES

CONFIDENTIAL

JE 210 (12-60)

PREPARED BY B.L.S.
CHECKED BY K.A.Y.
DATE APRIL 15, 1961
REVISED

GOODYEAR
GOODYEAR AIRCRAFT CORPORATION
AKRON, OHIO

PAGE 78
MODEL 1/20-SCALE 2PG-3W (MODIFIED)
GER- 10176
REF NO.

CONFIDENTIAL

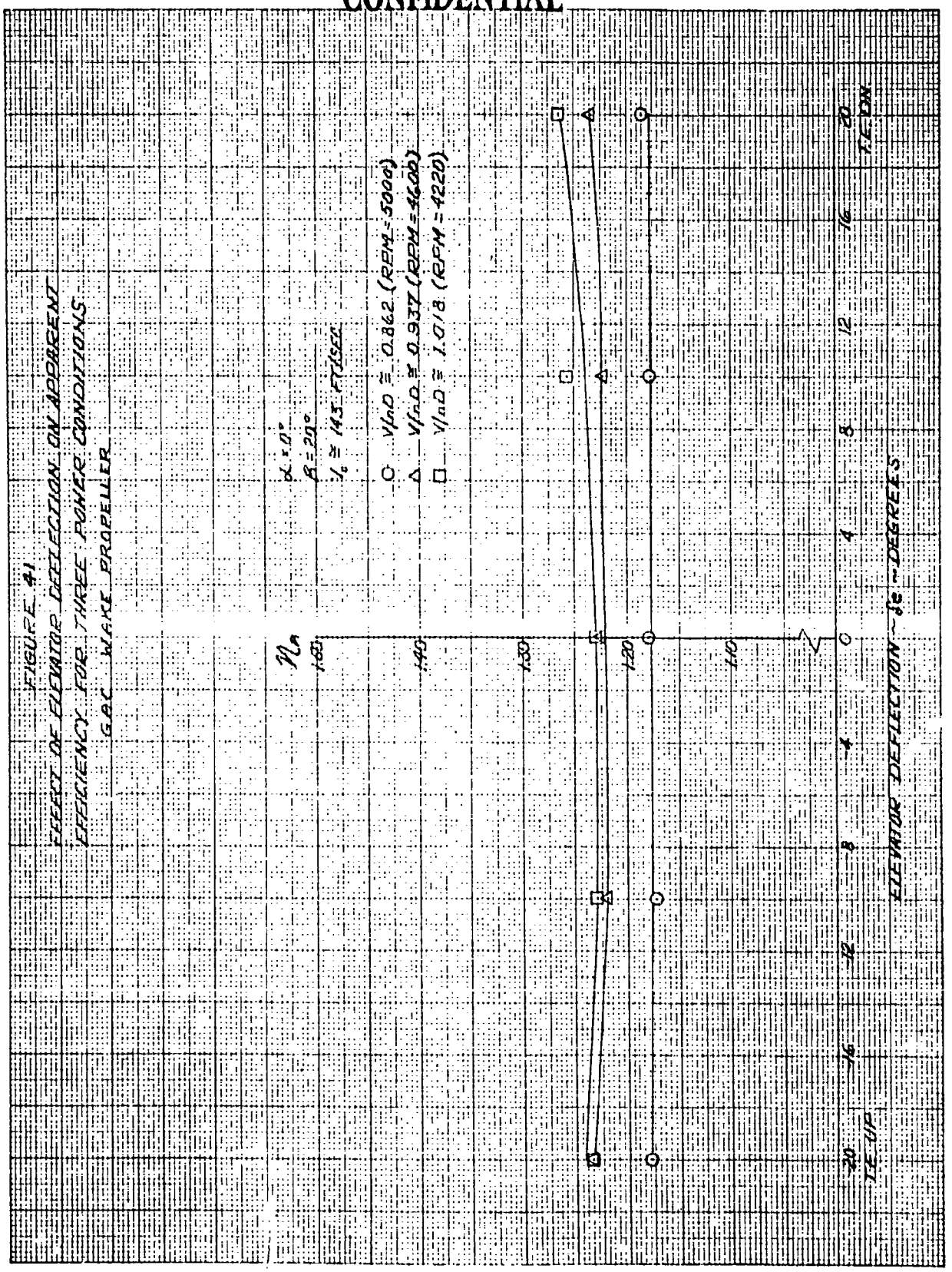

CONFIDENTIAL

JR 220 (12-60)

PREPARED BY BPS
CHECKED BY K.A.Y.
DATE APRIL 15, 1961
REVISED

GOODYEAR
GOODYEAR AIRCRAFT CORPORATION
AKRON, OHIO

PAGE 79
MODEL 1/20 - 7.PG-3W (MODIFIED)
GER- 10176
REF NO.

CONFIDENTIAL

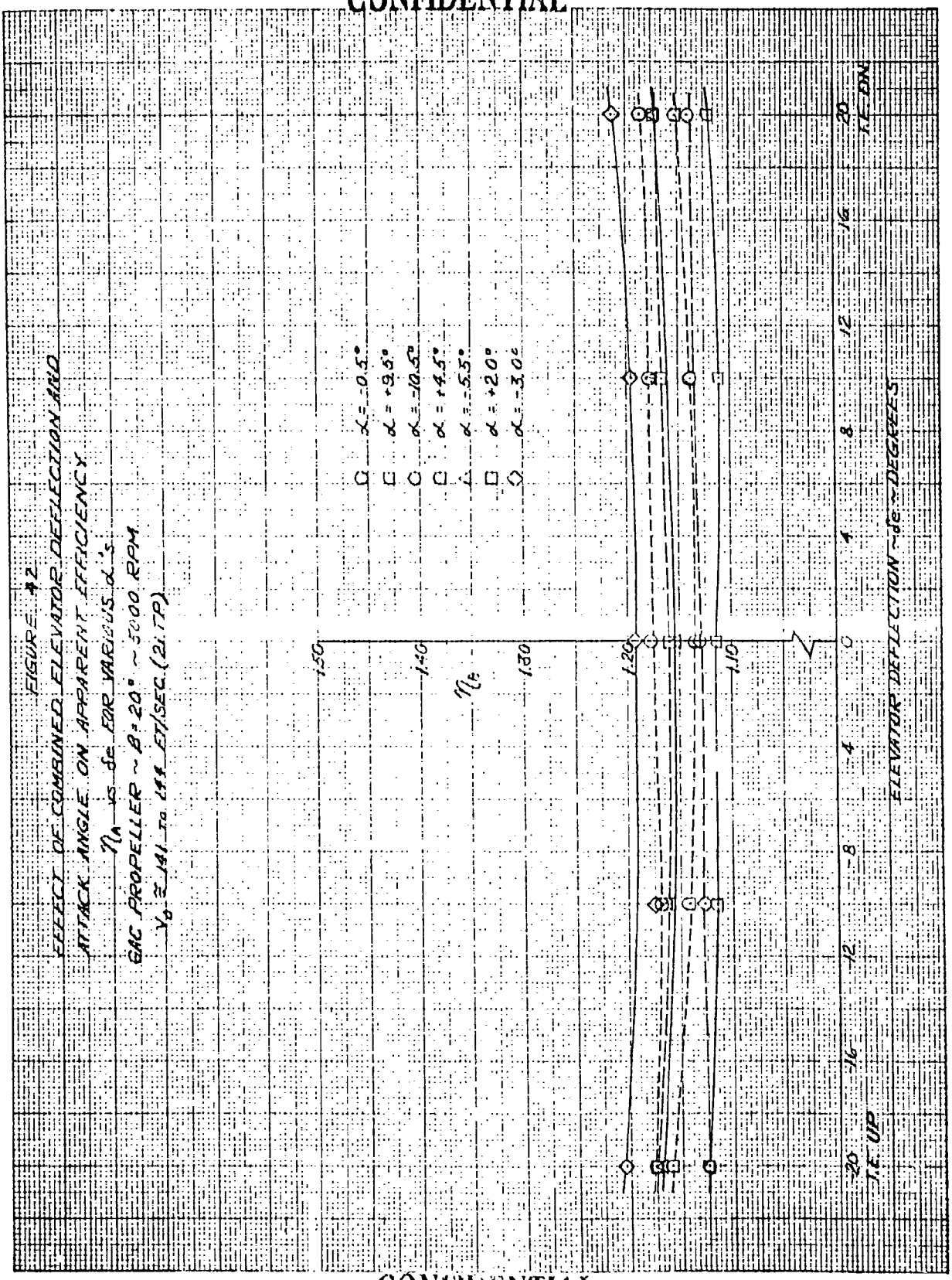

CONFIDENTIAL

JR 220 (12-60)

CONFIDENTIAL

FIGURE 43
EFFECT OF COMBINED ATTACK ANGLE AND ELEVATOR DEFLECTION ON APPARENT EFFICIENCY
η_a vs α FOR VARIOUS δ_e's
GAC PROPELLER - $\beta = 20°$
V_∞ = 141 TO 144 FEET/SEC (21 TO 22)

5000 RPM
○ $\delta_e = 0$
□ $\delta_e = +20°$
◇ $\delta_e = -20°$

4600 RPM
△ $\delta_e = 0$
□ $\delta_e = +20°$
◇ $\delta_e = -20°$

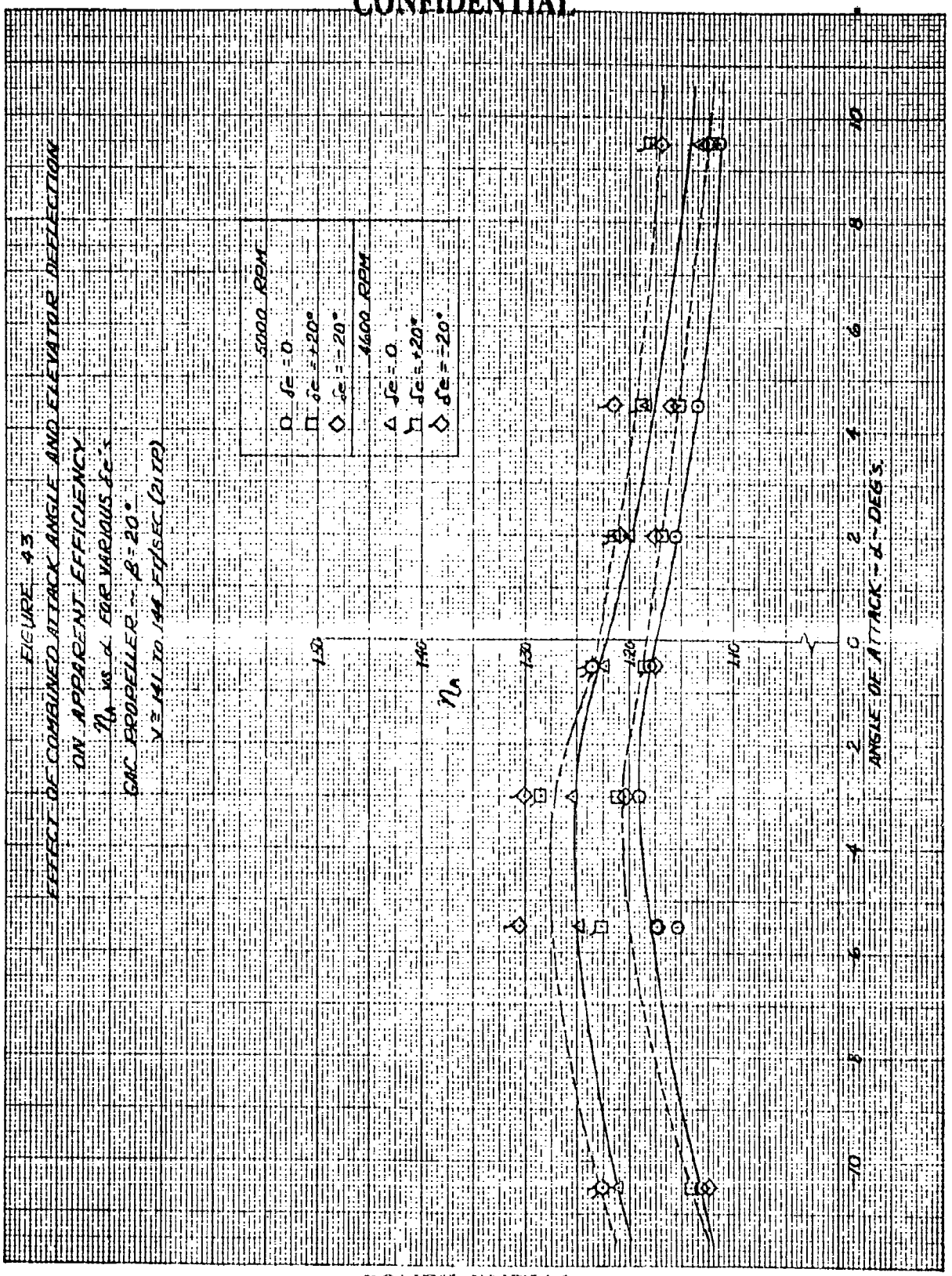

CONFIDENTIAL

PREPARED BY B.P.S.
CHECKED BY K.A.K.
DATE APRIL 15, 1961
REVISED

B.R.S.
K.A.K.
APRIL 15, 1961

GOODYEAR

GOODYEAR AIRCRAFT CORPORATION
AKRON, OHIO

PAGE 81
MODEL 1/20 - 3PG - 5W (MODIFIED)
GER 10176
REF NO.

CONFIDENTIAL

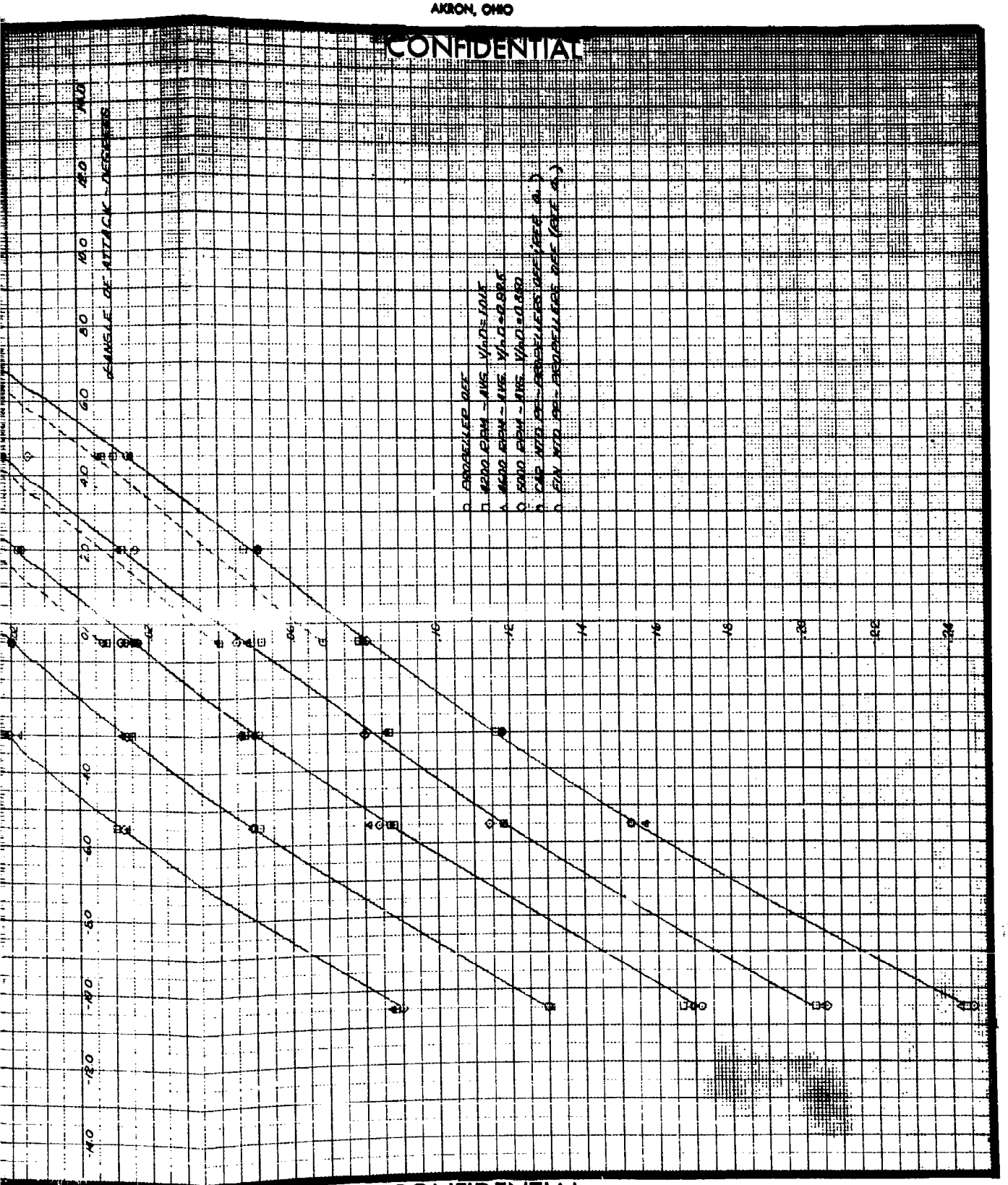

2

CONFIDENTIAL

PREPARED BY TRS
CHECKED BY K.A.Y.
DATE APRIL 15, 1961
REVISED

GOODYEAR
GOODYEAR AIRCRAFT CORPORATION
AKRON, OHIO

PAGE 82
MODEL 1/20-ZPS-3W (MODIFIED)
GAC 10176
REF NO.

CONFIDENTIAL

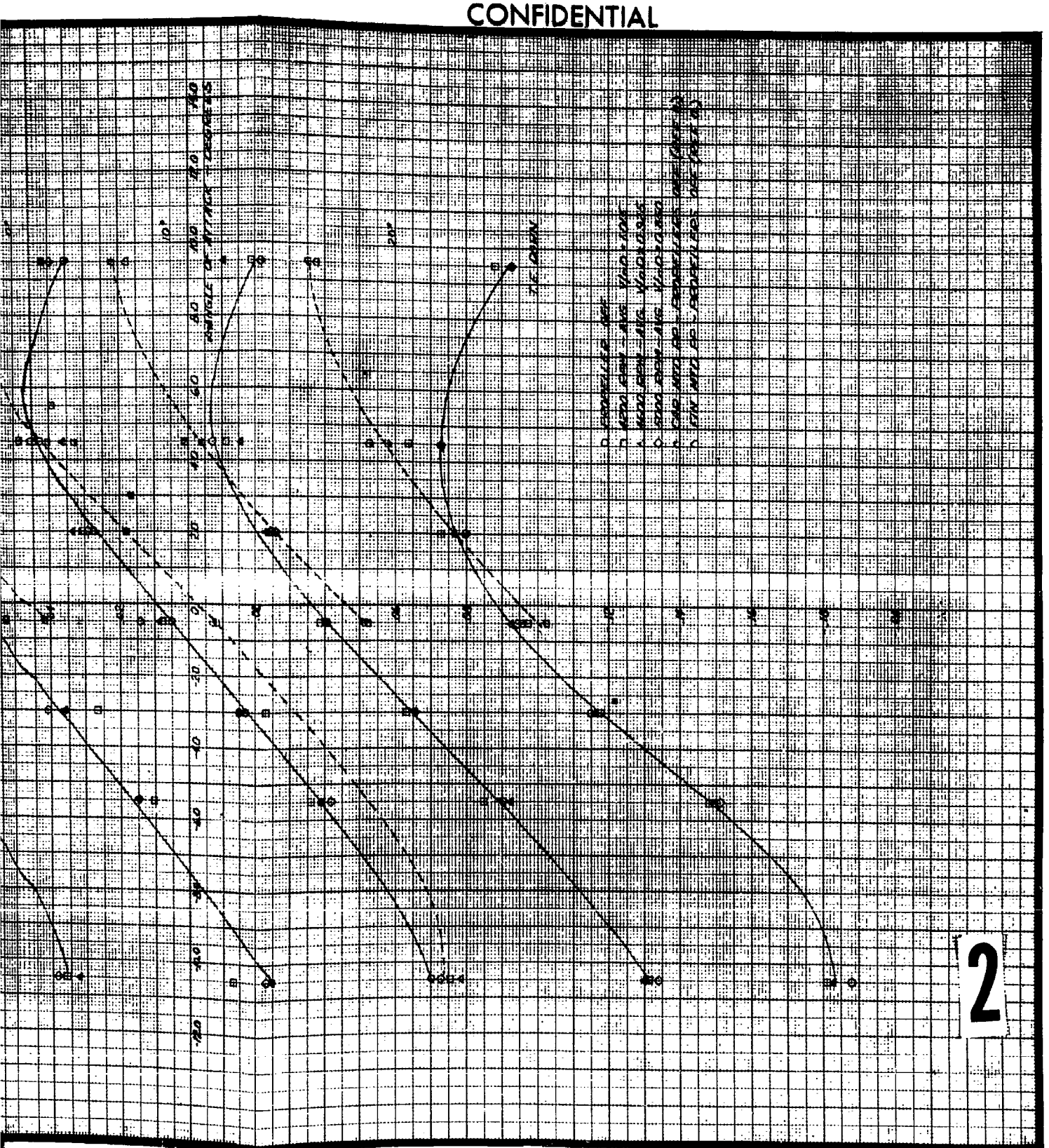

PREPARED BY BLS
CHECKED BY K.A.Y.
DATE APRIL 15, 1
REVISED

FIGURE 44 (C
EFFECT OF WAKE PROPELLER
THE LONGITUDINAL AERODYNAMIC CHARA
C_D DRAG COEFFICIENT
G.A.C. PROPELLER ~ β = 20
V_o = 141 TO 144 FT/SEC (21 T

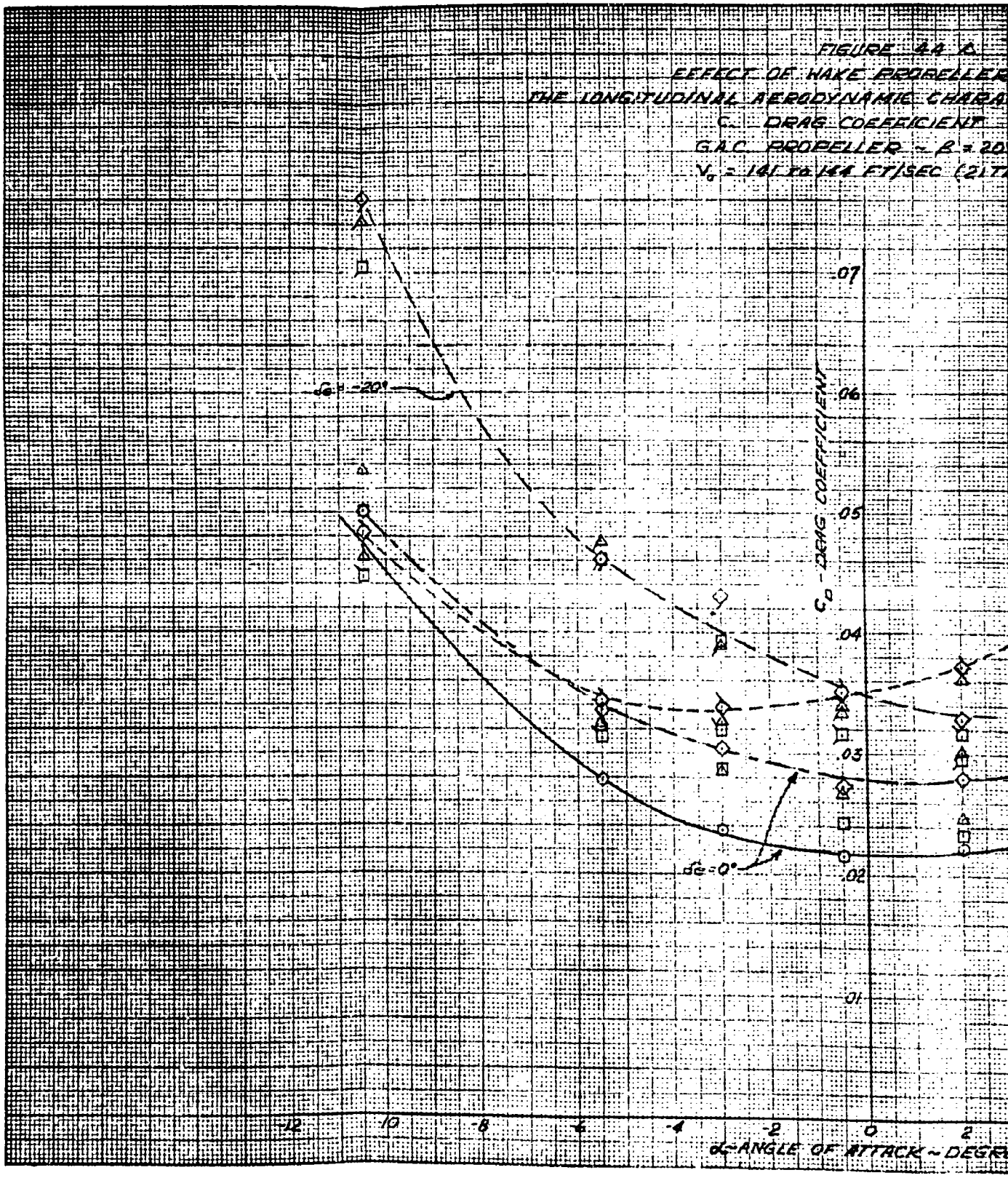

1

PREPARED BY BRS
CHECKED BY K.A.Y.
DATE APRIL 15, 1961
REVISED

GOODYEAR AIRCRAFT

PAGE 83
MODEL 1/20-ZPG-3W (MOD)
GER 10176
REF NO.

CONFIDENTIAL

FIGURE 44 C
EFFECT OF WAKE PROPELLER ON
TUDINAL AERODYNAMIC CHARACTERISTICS IN PITCH
C_D DRAG COEFFICIENT
G.A.C. PROPELLER - B = 20°
V_o = 141 to 144 FT/SEC (21 TP)

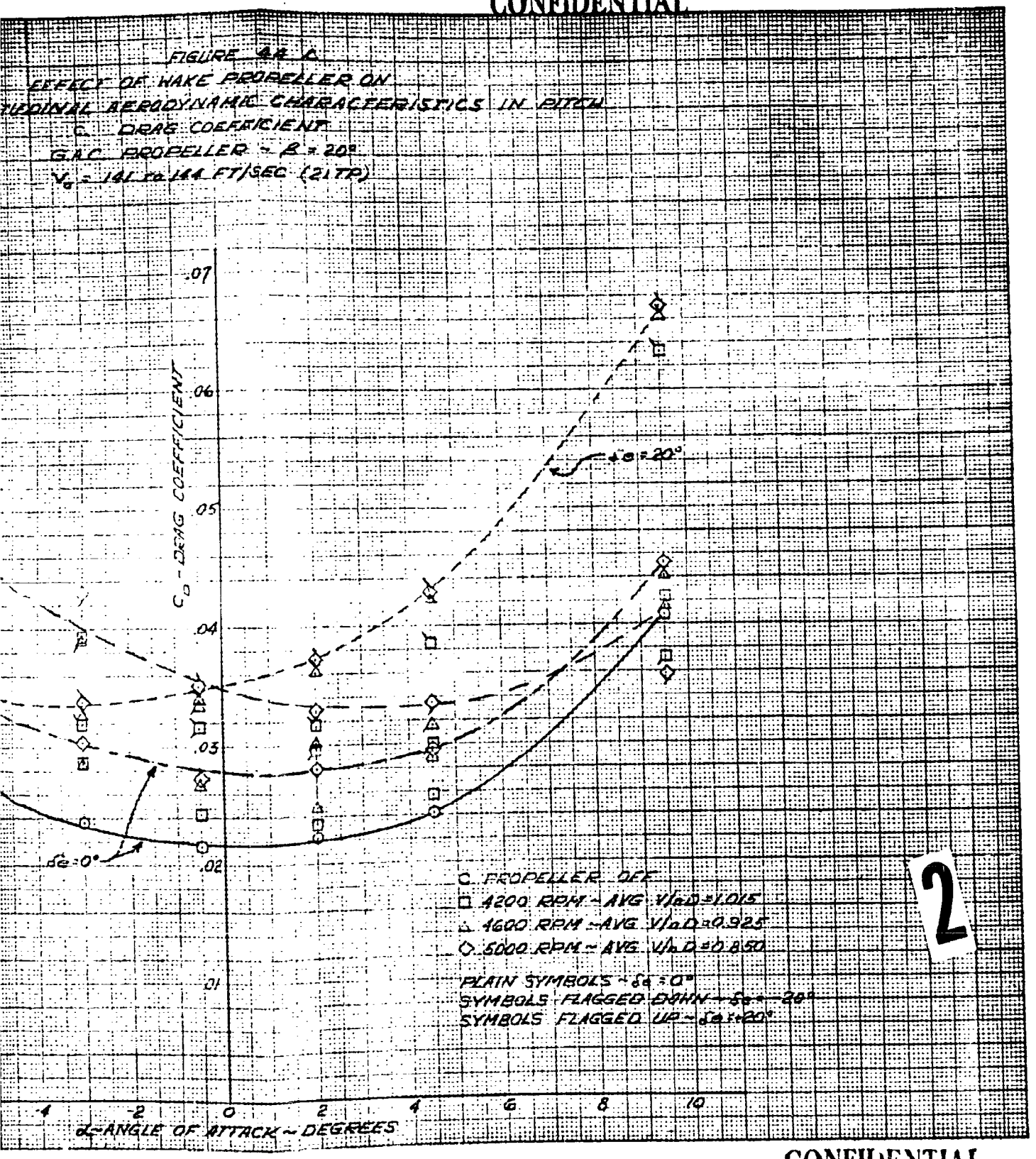

2

CONFIDENTIAL

CONFIDENTIAL

FIGURE 45

TYPICAL EFFECT OF WAKE PROPELLER ON THE LATERAL AERODYNAMIC CHARACTERISTICS IN PITCH (CROSS-COEFFICIENTS)

GAC PROPELLER + β = 20° V_o = 141 TO 144 FT/SEC (ELTA)

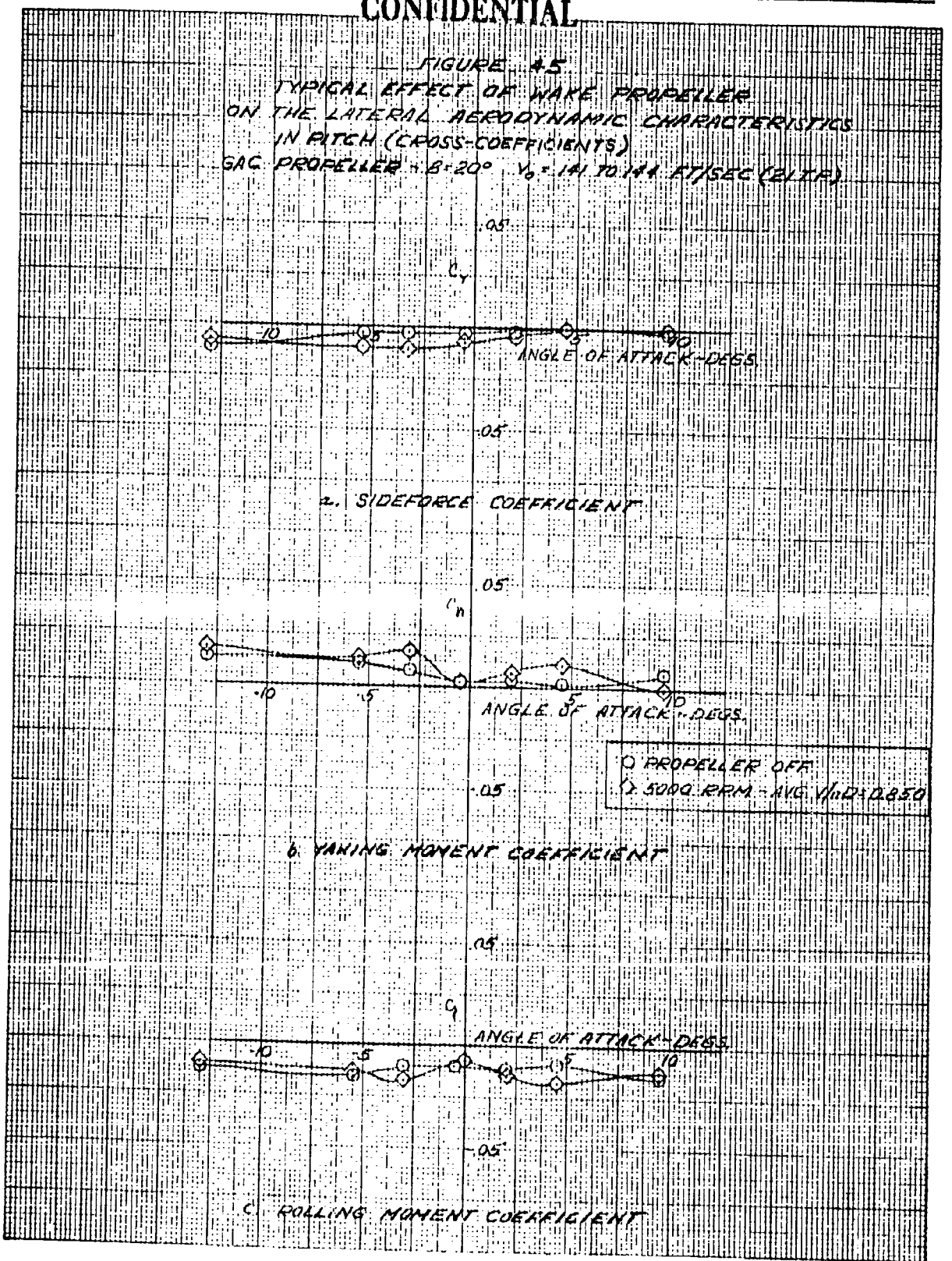

JR 230 (12-60)

CONFIDENTIAL

FIGURE 46
TYPICAL EFFECT OF WAKE PROPELLER ON
BOUNDRY LAYER VELOCITY PROFILES AT TWO HULL STATIONS
S.A.C. PROPELLER - β=20°
V_o = 94 FT/SEC (12 T.P.)

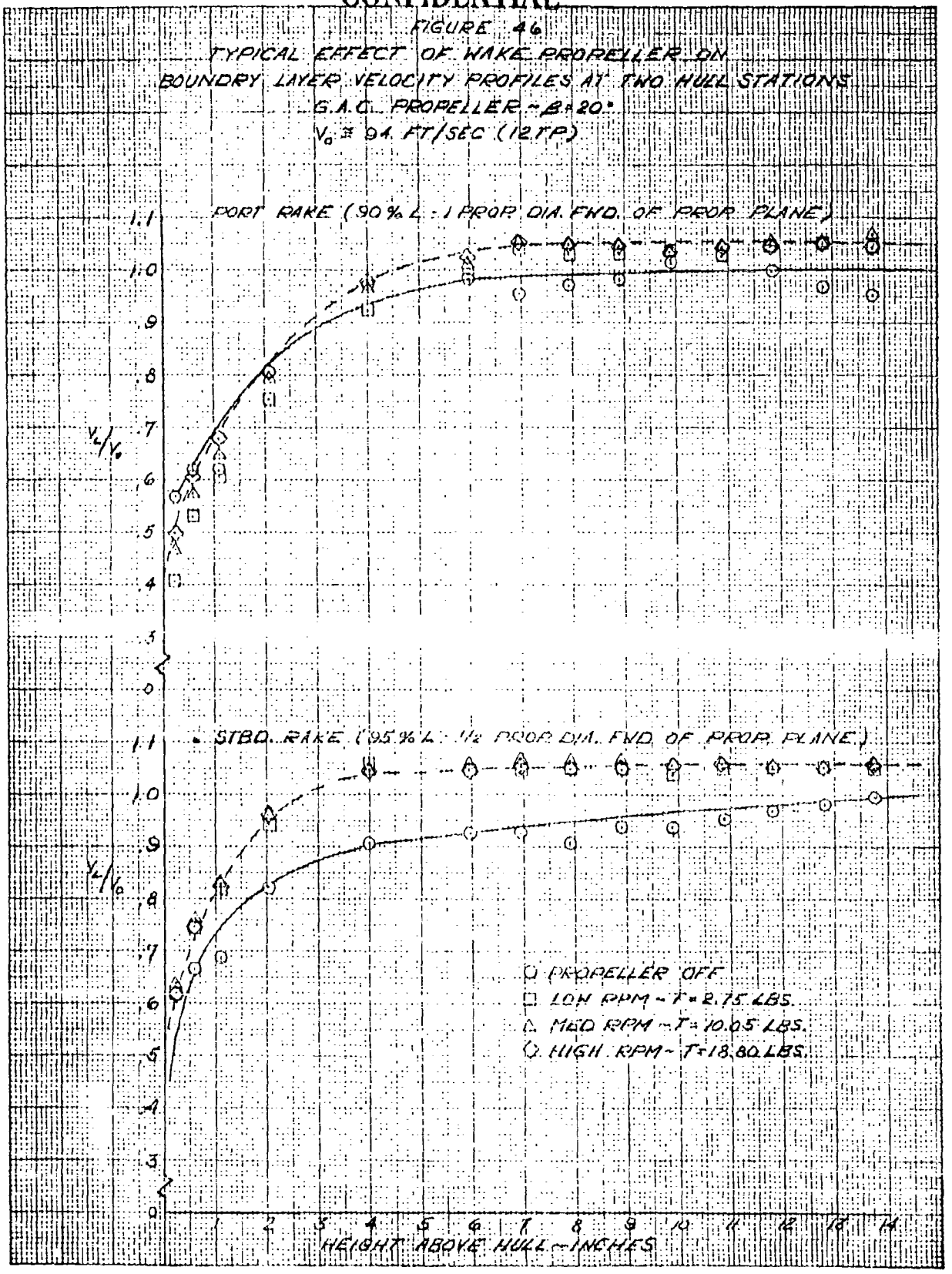

CONFIDENTIAL

PREPARED BY BPS
CHECKED BY K.A.Y.
DATE APRIL 15, 1961
REVISED

GOODYEAR
GOODYEAR AIRCRAFT CORPORATION
AKRON, OHIO

PAGE 86
MODEL 1/20-EPG-3W (MOD)
GER 10176
REF NO.

CONFIDENTIAL

FIGURE 47
TYPICAL EFFECT OF WAKE PROPELLER ON
BOUNDARY LAYER VELOCITY PROFILES AT TWO HULL STATIONS
G.A.C. PROPELLER - β=20°
V_o = 140 FT/SEC (21 TP)

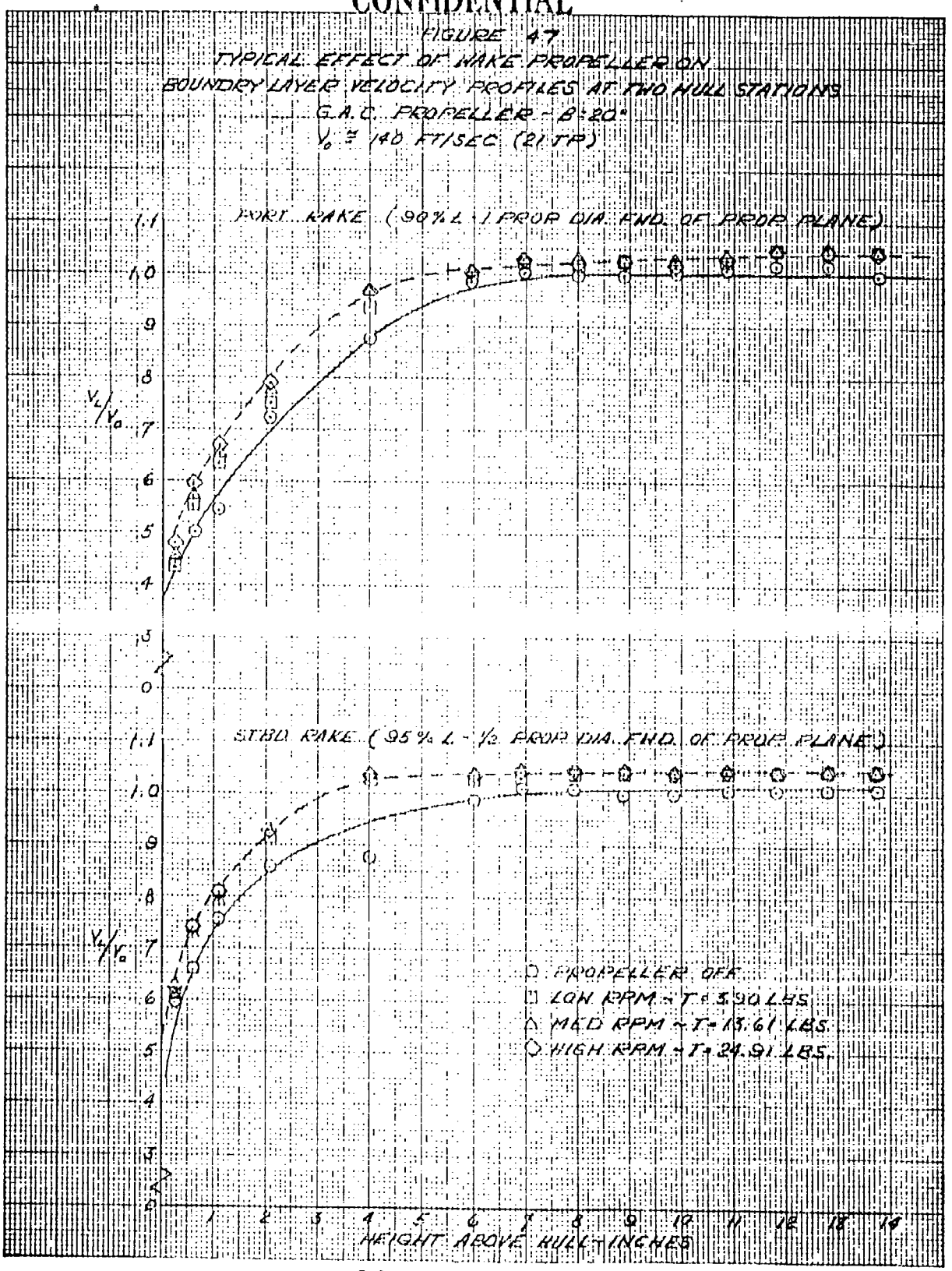

CONFIDENTIAL

JR 220 (12-60)

CONFIDENTIAL

FIGURE 48
VARIATION OF LOCAL STATIC PRESSURE IN THE WAKE BEHIND THE AIRSHIP MODEL FOR TWO TUNNEL VELOCITIES

PROPELLER OFF - GAC TAIL CONE ON
RAKE LOCATED ONE FOOT BEHIND GAC PROPELLER PLANE

□ p_L FOR V_0 = 112 FT/SEC (66 MPH)
▽ p_L/p_0 FOR q_0 = 14.90 LBS/FT²
○ p_L FOR V_0 = 156.5 FT/SEC (92 MPH)
△ p_L/p_0 FOR q_0 = 29.80 LBS/FT²

LOCAL STATIC PRESSURE - p_L - LBS/FT²

RATIO LOCAL STATIC PRESSURE TO FREE STREAM STATIC PRESSURE - p_L/p_0

DISTANCE FROM ℄ AIRSHIP - z - INCHES

CONFIDENTIAL

AR 230 (10-60)

PREPARED BY RPS
CHECKED BY K.A.Y.
DATE APRIL 15, 1961
REVISED

GOODYEAR
GOODYEAR AIRCRAFT CORPORATION
AKRON, OHIO

PAGE 88
MODEL 1/20-2PG-3W (M00)
GER- 10176
REF NO.

CONFIDENTIAL

FIGURE 49
COMPARISON OF LOCAL STATIC PRESSURE RATIO IN THE WAKE WITH AND WITHOUT WAKE PROPELLER OPERATION

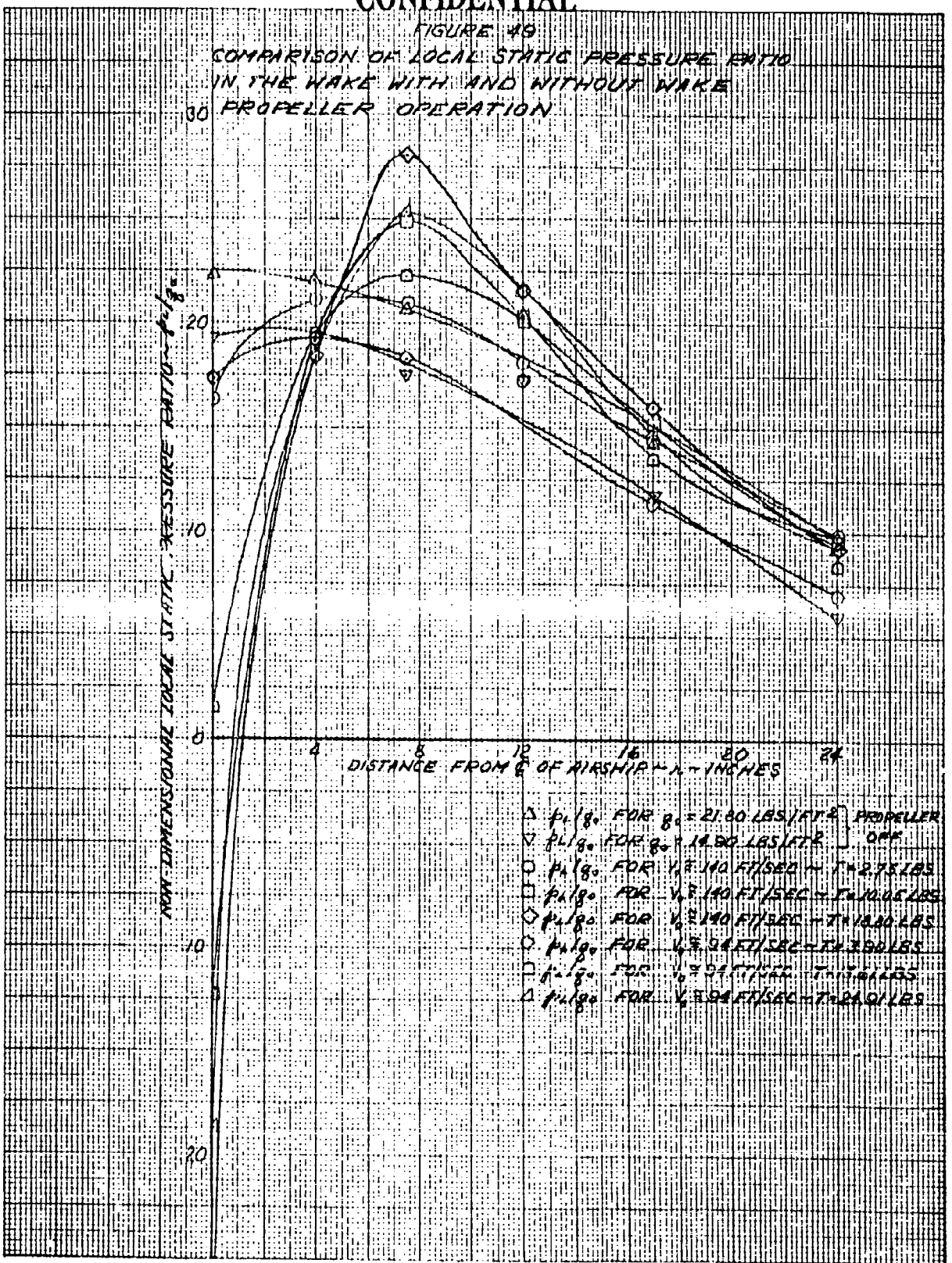

CONFIDENTIAL

JB 220 (12-60)

PREPARED BY B R S
CHECKED BY K.A.K.
DATE APRIL 15, 1
REVISED

FIGURE 50
COMPARISON OF WAKE VELOCITY DISTRIBUTION
BARE HULL DATA

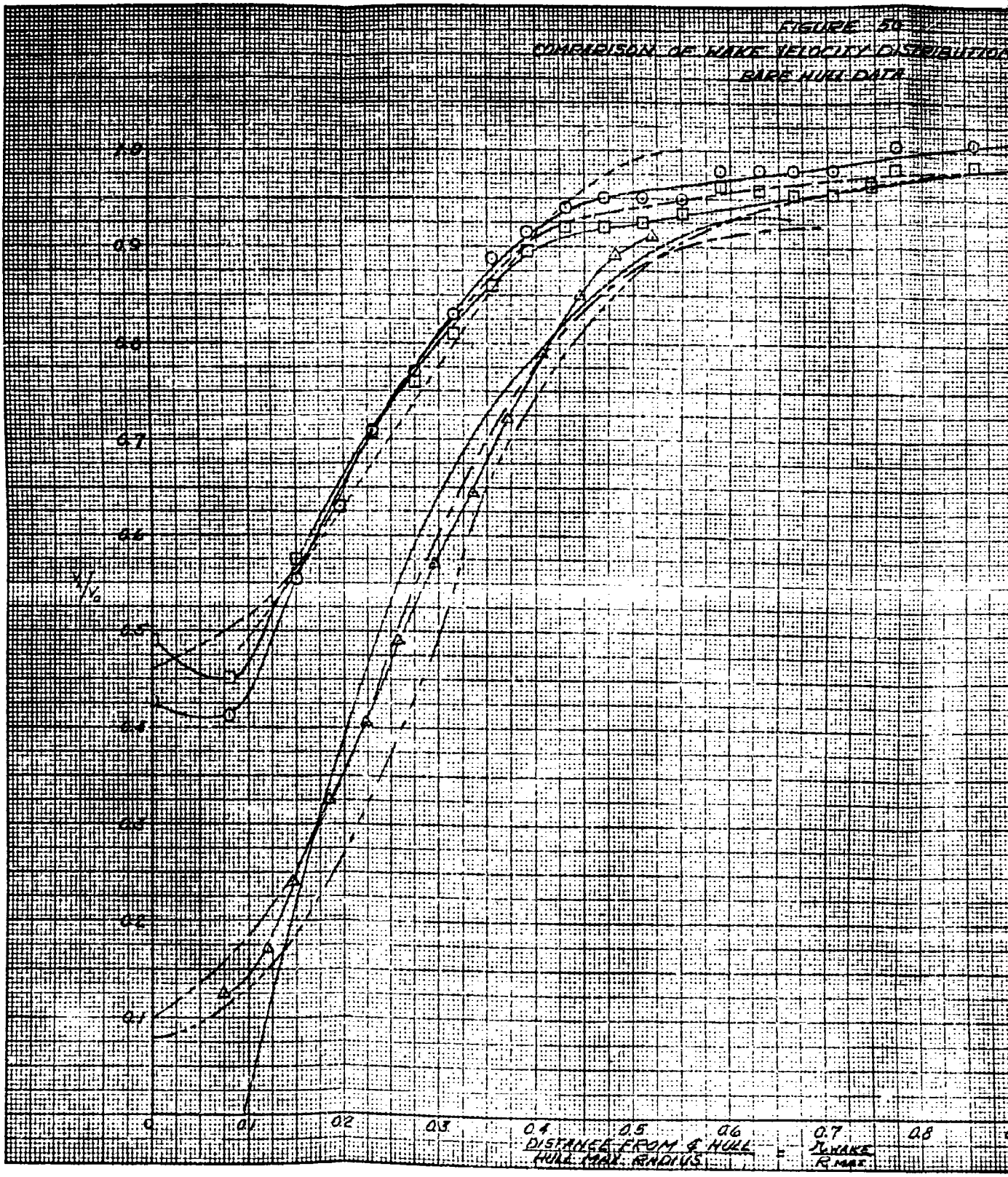

1

PREPARED BY R.R.S
CHECKED BY K.A.Y.
DATE APRIL 15, 1961
REVISED

GOODYEAR
GOODYEAR AIRCRAFT CORPORATION
AKRON, OHIO

PAGE 89
MODEL 1/20 ZPG-3W (MOD)
SER 10176
REF NO.

CONFIDENTIAL

FIGURE 59
WAKE VELOCITY DISTRIBUTIONS FOR VARIOUS AIRSHIPS
BARE HULL DATA

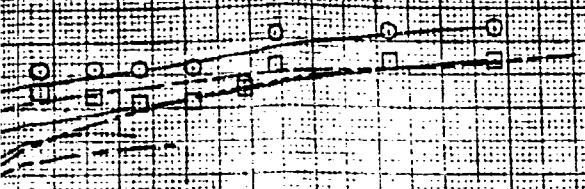

SYMBOL	AIRSHIP OR MODEL	V_0 FT/SEC.	RAKE LOCATION AFT OF NOSE
○	1/20-SCALE ZPG-3W MODEL	112.0	5.4%L
□	1/20-SCALE ZPG-3W MODEL	135.3	5.4%L
△	1/15-SCALE XZPG-2 MODEL	135.0	0.5%L
——·——	K-10 AIRSHIP FLT. TEST (REFERENCE 2)	73.0	0.5%L
——·——	AKRON (MOD.)-DGAI TESTS L = 49.75" D = 12.07" (REFERENCE 4)	117.2	5.0%L
——·——	AKRON (MOD.)-DGAI TESTS (REFERENCE 4)	146.7	0.5%L
———	1/20-SCALE ZPG-3W MODEL V_0 DETERMINED FROM V_1 MEASUREMENTS DURING PREVIOUS TESTS	139.0	THEO. FAIR AFT
———	1/20 SCALE ZPG-3W MODEL V_0 MEASURED BY SURVEY ON DUMMY TAIL CONE	139.0	PROP. PLANE FWD OF AFT END OF TAIL CONE

R_{MAX} = MAX. RADIUS OF AIRSHIP HULL

0.6 0.7 0.8 0.9 1.0
R/R HULL
R/R MAX

2

CONFIDENTIAL

PREPARED BY
CHECKED BY
DATE APR
REVISED

FIGURE 51
EFFECT OF WAKE PROPELLER OPERATION
VELOCITY DISTRIBUTIONS FOR SEVERAL
G.A.C. WAKE PROPELLER

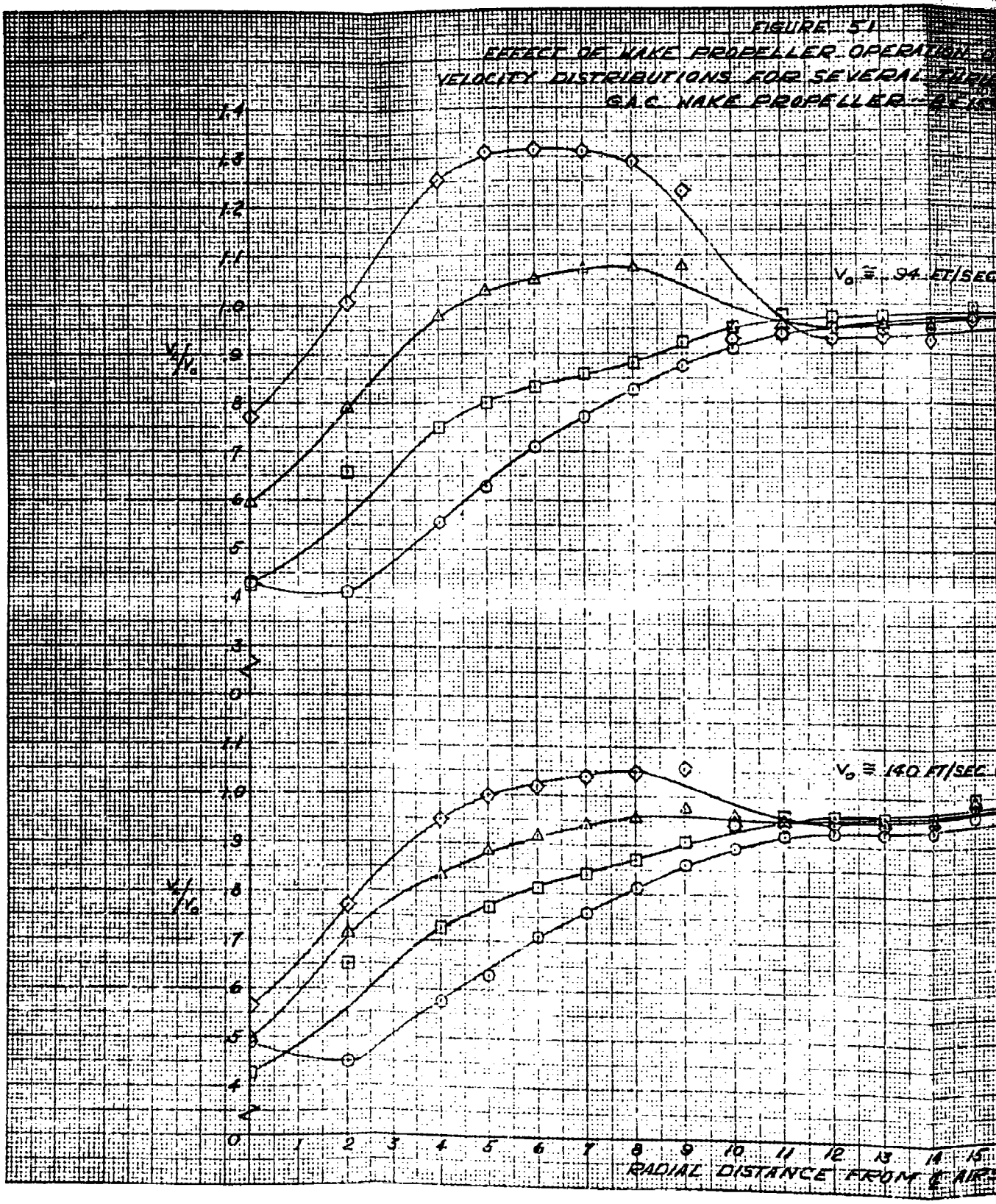

1

PREPARED BY RPS
CHECKED BY K.A.Y.
DATE APRIL 15, 1961
REVISED

GOODYEAR
GOODYEAR AIRCRAFT CORPORATION
AKRON, OHIO

PAGE 90
MODEL 1/20 - ZPG-3W (Mod)
GER- 10176
REP NO.

CONFIDENTIAL

FIGURE 51
EFFECT OF PROPELLER OPERATION ON WAKE
ONS FOR SEVERAL THRUST CONDITIONS
AKE PROPELLER - $\beta = 15°$

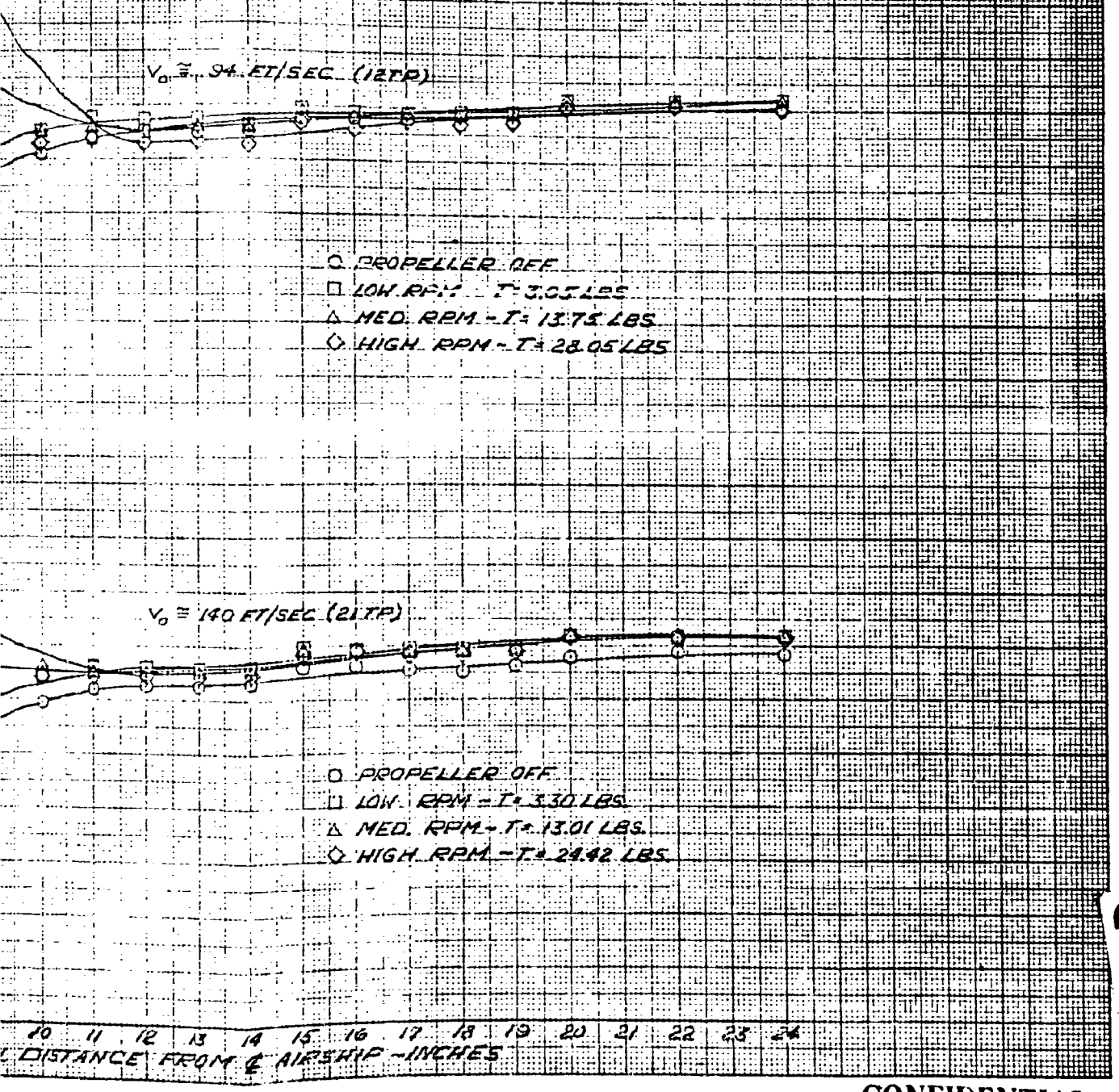

2

CONFIDENTIAL

PREPARED BY RFS
CHECKED BY K.A.V.
DATE APRIL 18, 1961
REVISED

FIGURE 52
EFFECT OF WAKE PROPELLER OPERATION ON WAKE
VELOCITY DISTRIBUTIONS FOR SEVERAL THRUST CO
G.A.C. WAKE PROPELLER - B = 20

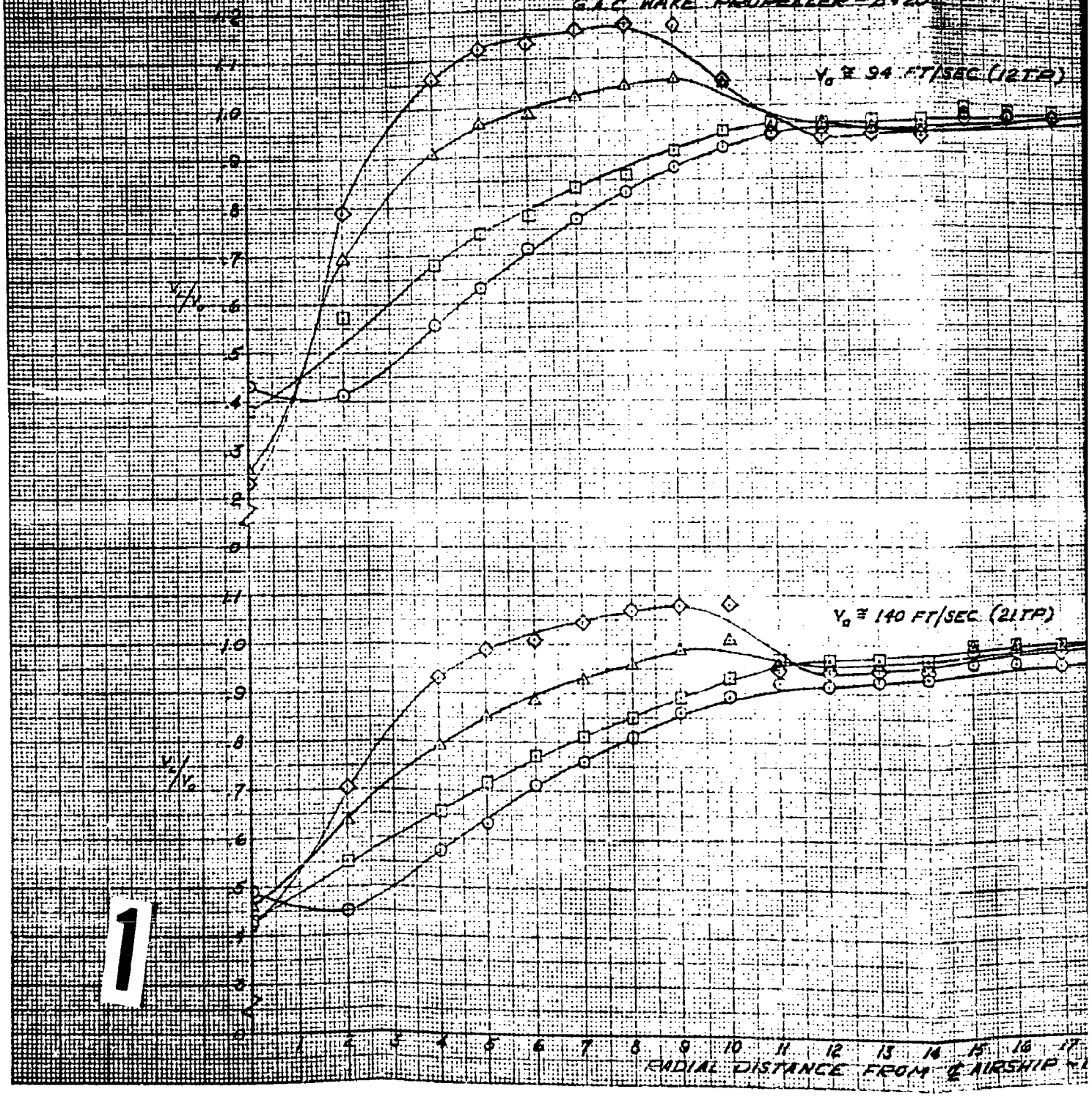

1

FIGURE 52
PROPELLER OPERATION ON WAKE
SITIONS FOR SEVERAL THRUST CONDITIONS
KE PROPELLER - $\beta = 20°$

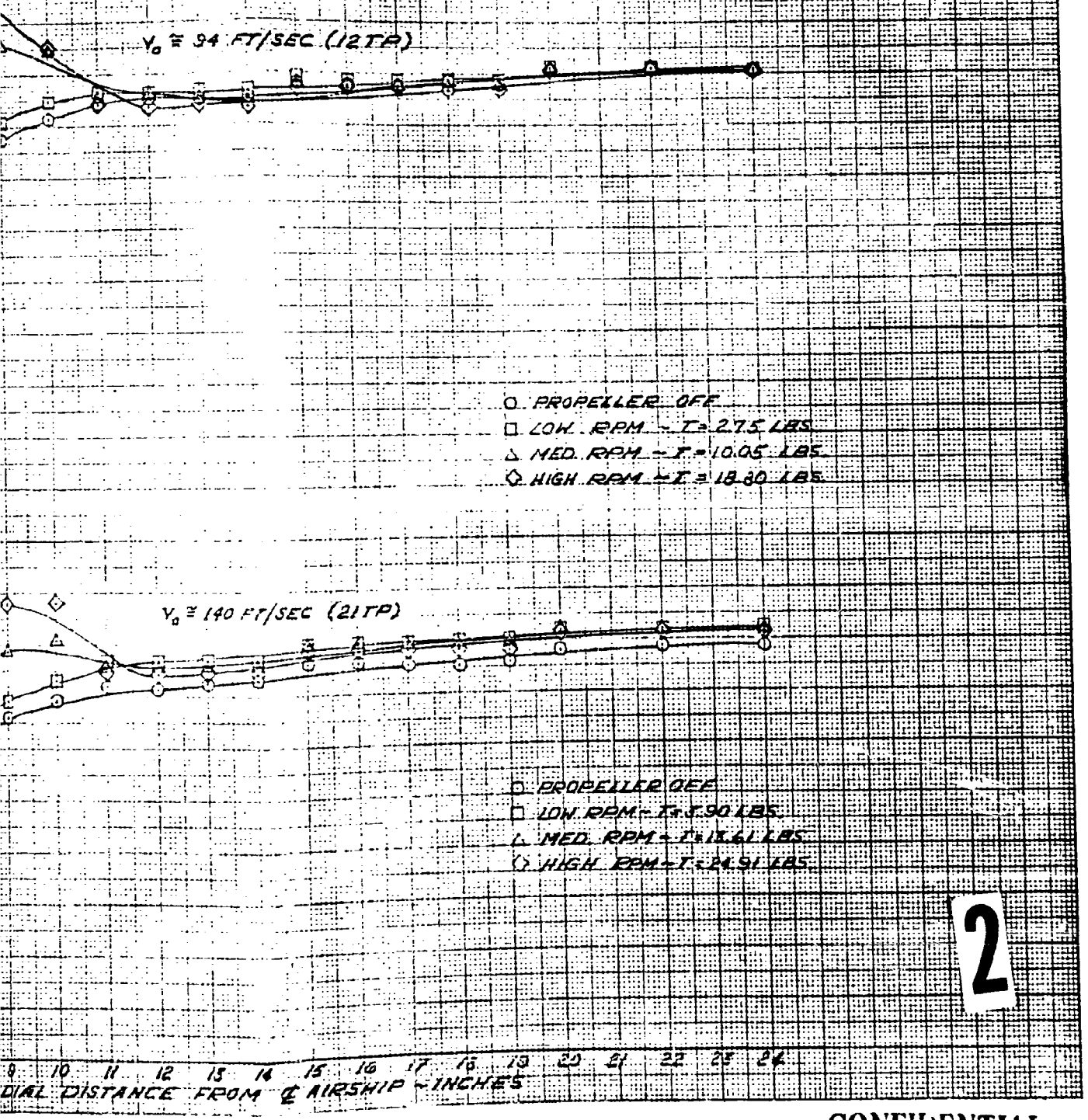

2

PREPARED BY BRS
CHECKED BY K.A.Y.
DATE APRIL 15, 1
REVISED

FIGURE 5.8
EFFECT OF WAKE PROPELLER OPERATION ON
VELOCITY DISTRIBUTIONS FOR SEVERAL THRUST
G.A.C. WAKE PROPELLER - β = 25°

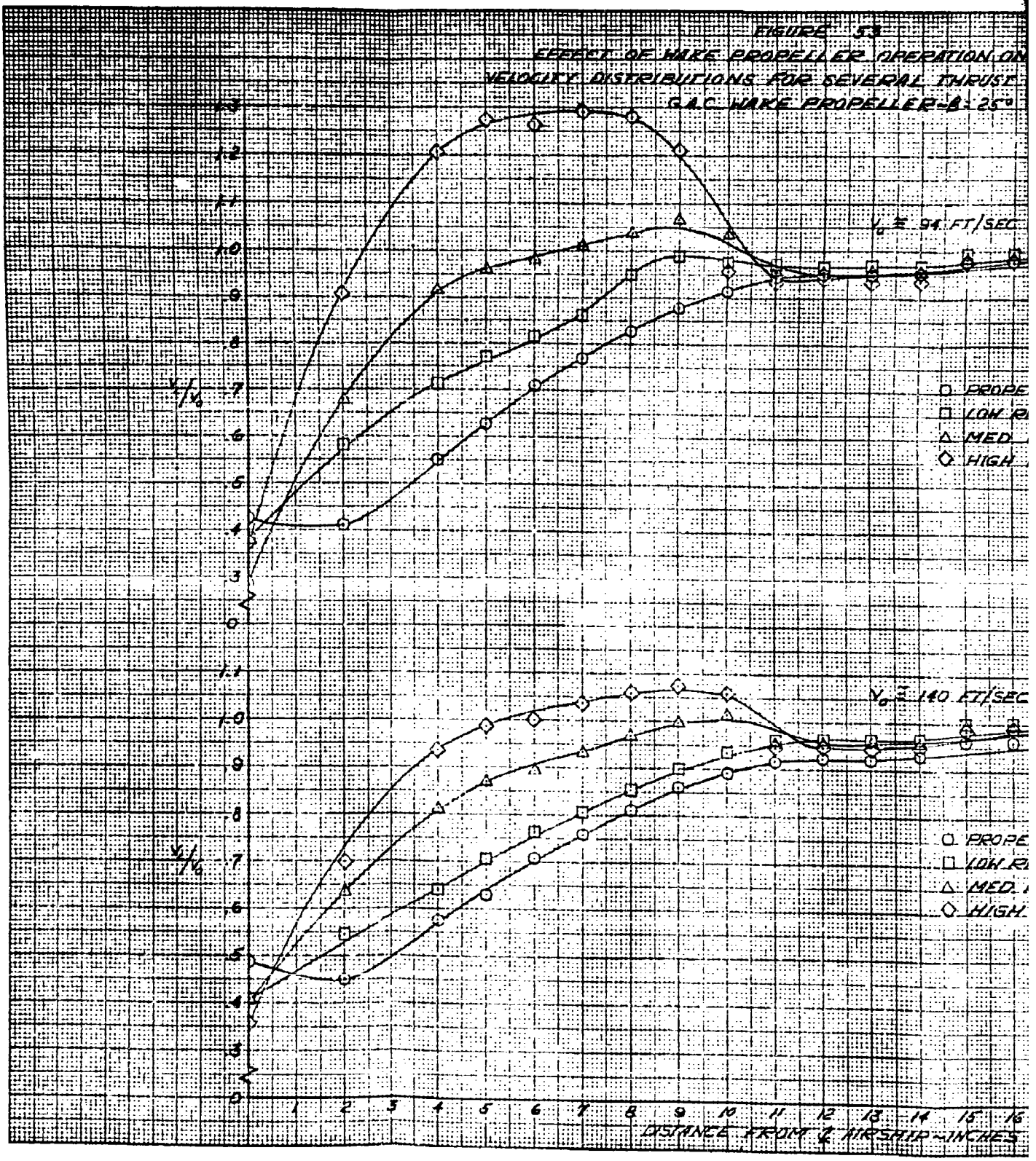

CONFIDENTIAL

FIGURE 53
WAKE PROPELLER OPERATION ON WAKE
DITIONS FOR SEVERAL THRUST CONDITIONS
G.A.C. WAKE PROPELLER-B = 25°

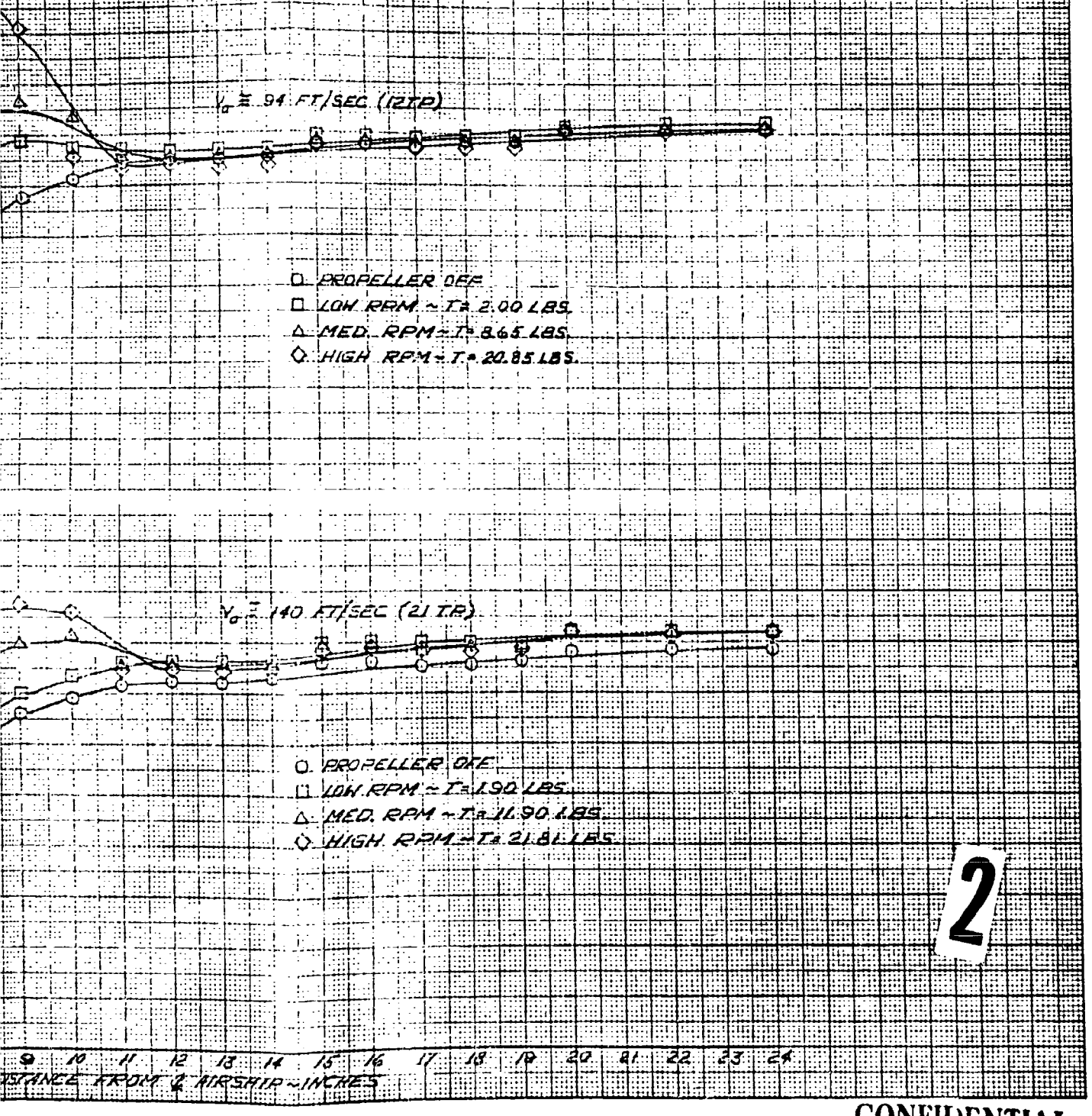

2

CONFIDENTIAL

PREPARED BY BPS
CHECKED BY K.A.Y.
DATE APRIL 15, 1961
REVISED

FIGURE 54
EFFECT OF WAKE PROPELLER OPERATION O
VELOCITY DISTRIBUTIONS FOR SEVERAL THRUS
TRANSCENDENTAL PROPELLER - 2

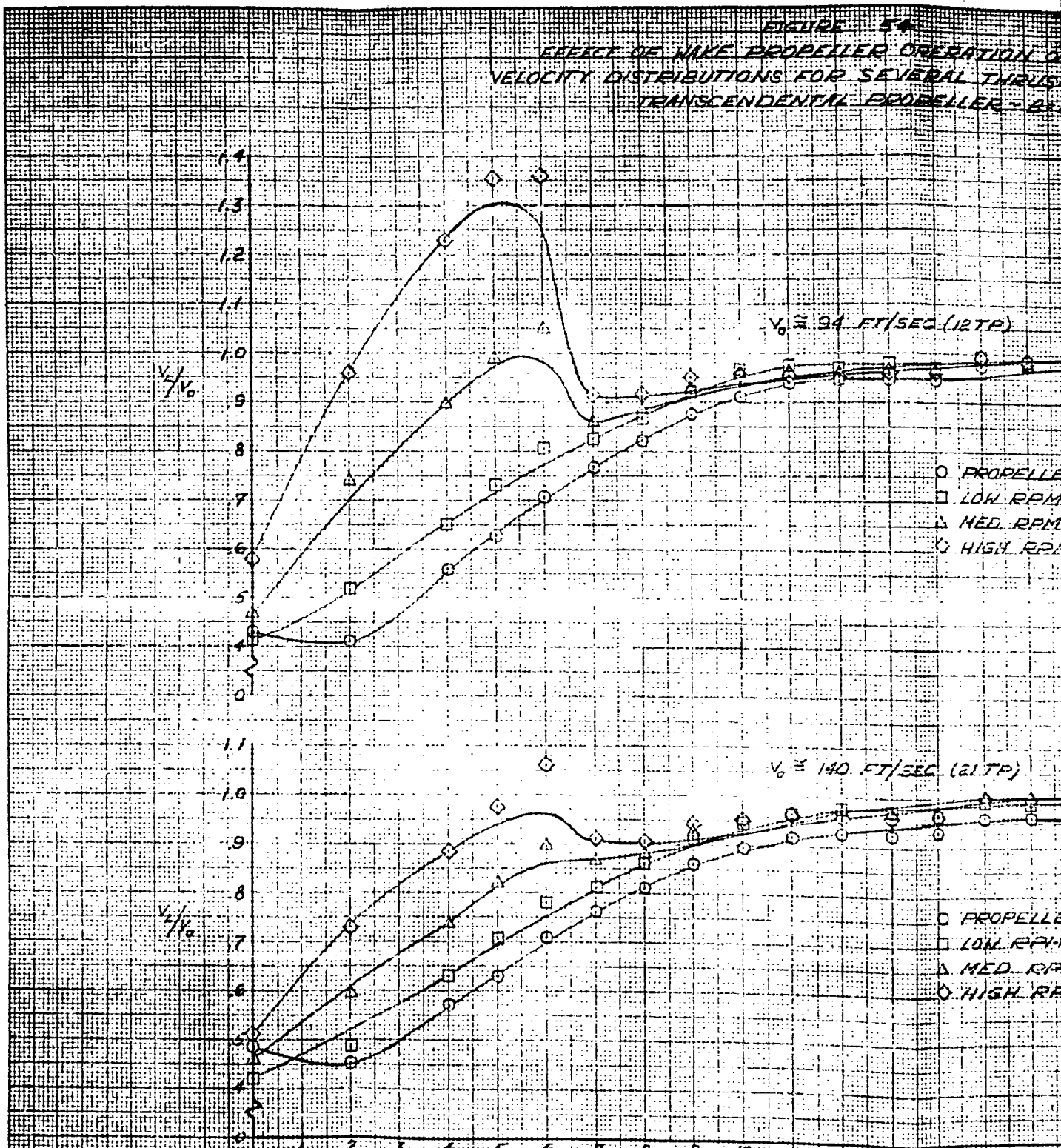

1

CONFIDENTIAL

FIGURE 54
WAKE PROPELLER OPERATION ON WAKE
IBUTIONS FOR SEVERAL THRUST CONDITIONS
NISCENDENTAL PROPELLER - $\beta = 20°$

$V_o \cong 94$ FT/SEC (12 TP)

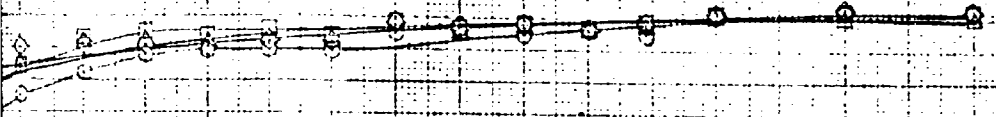

- ○ PROPELLER OFF
- □ LOW RPM ~ T = 1.00 LB.
- △ MED. RPM ~ T = 6.10 LBS.
- ◇ HIGH RPM ~ T = 13.65 LBS.

$V_o \cong 140$ FT/SEC (21 TP)

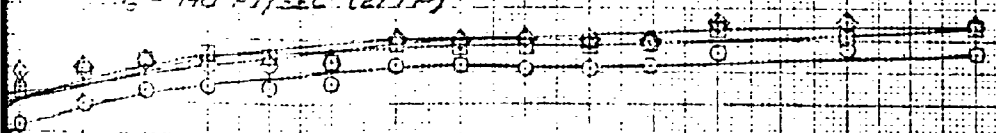

- ○ PROPELLER OFF
- □ LOW RPM ~ T = 1.70 LB.
- △ MED. RPM ~ T = 4.65 LBS.
- ◇ HIGH RPM ~ T = 11.35 LBS.

2

9 10 11 12 13 14 15 16 17 18 19 20 21 22 23 24
DISTANCE FROM ℄ AIRSHIP ~ INCHES

CONFIDENTIAL

CONFIDENTIAL

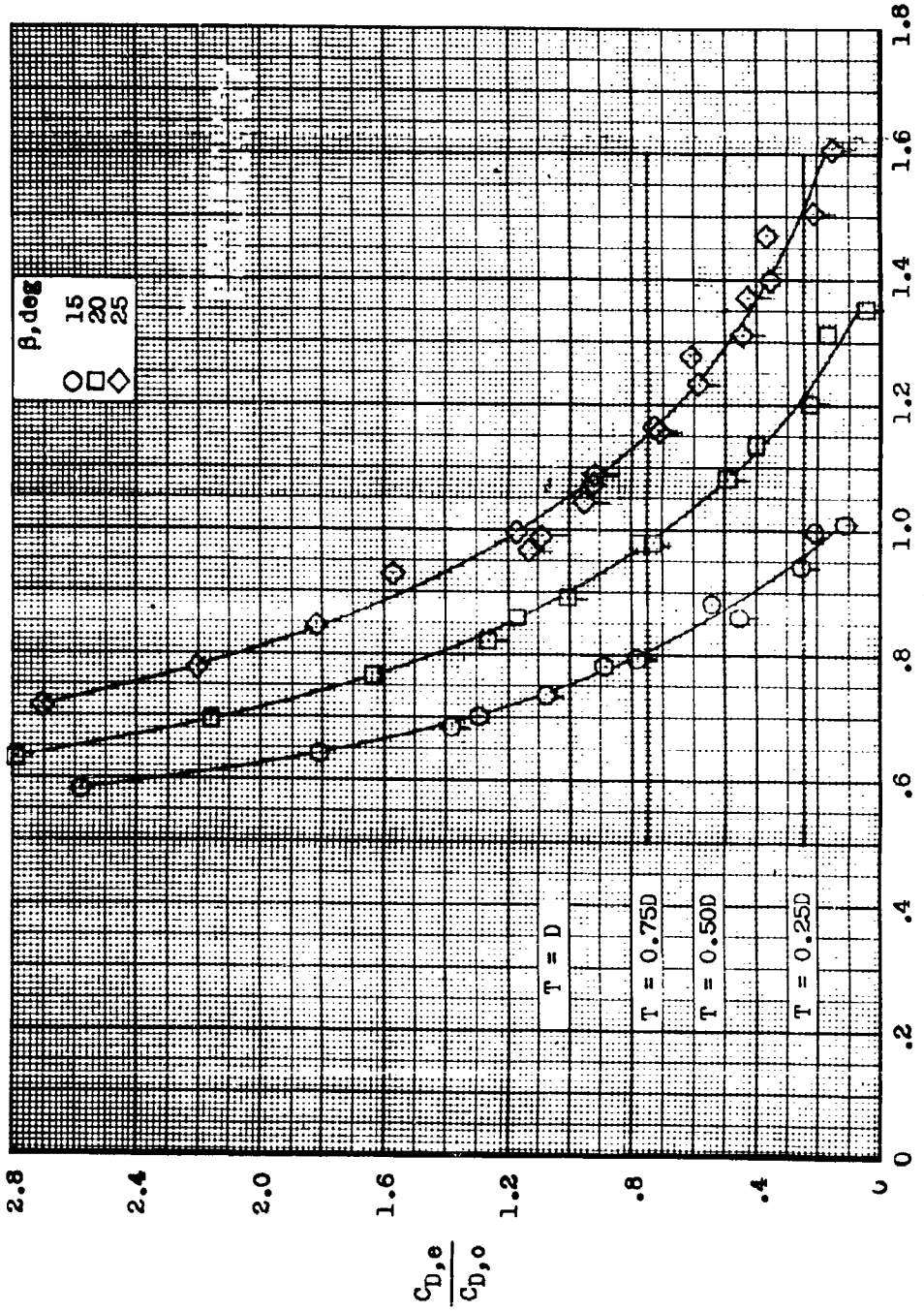

Figure 55 - Ratio of Effective Drag Coefficient to Basic Drag Coefficient for Various Advance Ratios and Blade Angles - GAC Wake Propeller

CONFIDENTIAL

CONFIDENTIAL

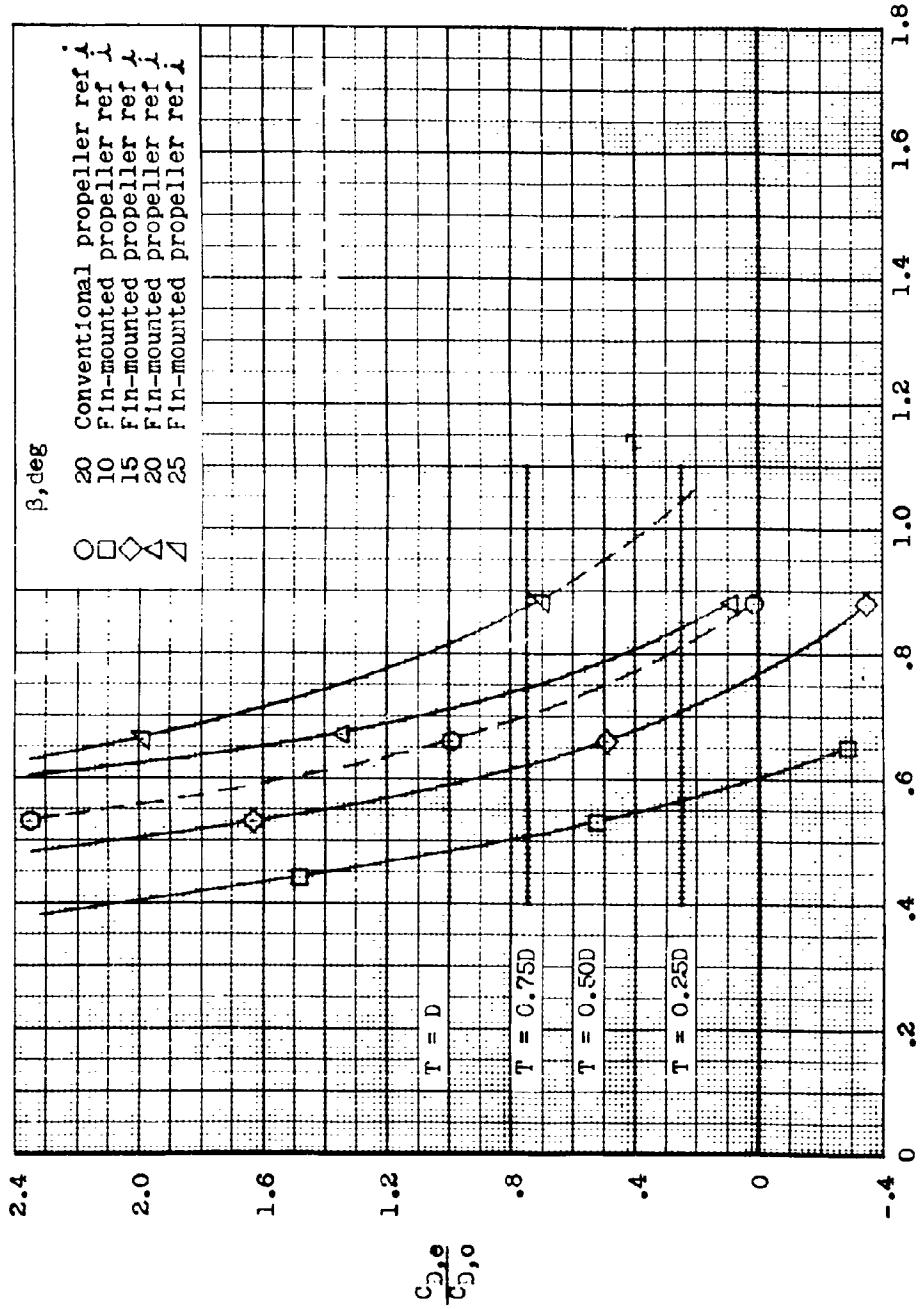

Figure 56 - Ratio of Effective Drag Coefficient to Basic Drag Coefficient for Various Advance Ratios and Blade Angles - Conventional and Fin-Mounted Propellers

CONFIDENTIAL

CONFIDENTIAL

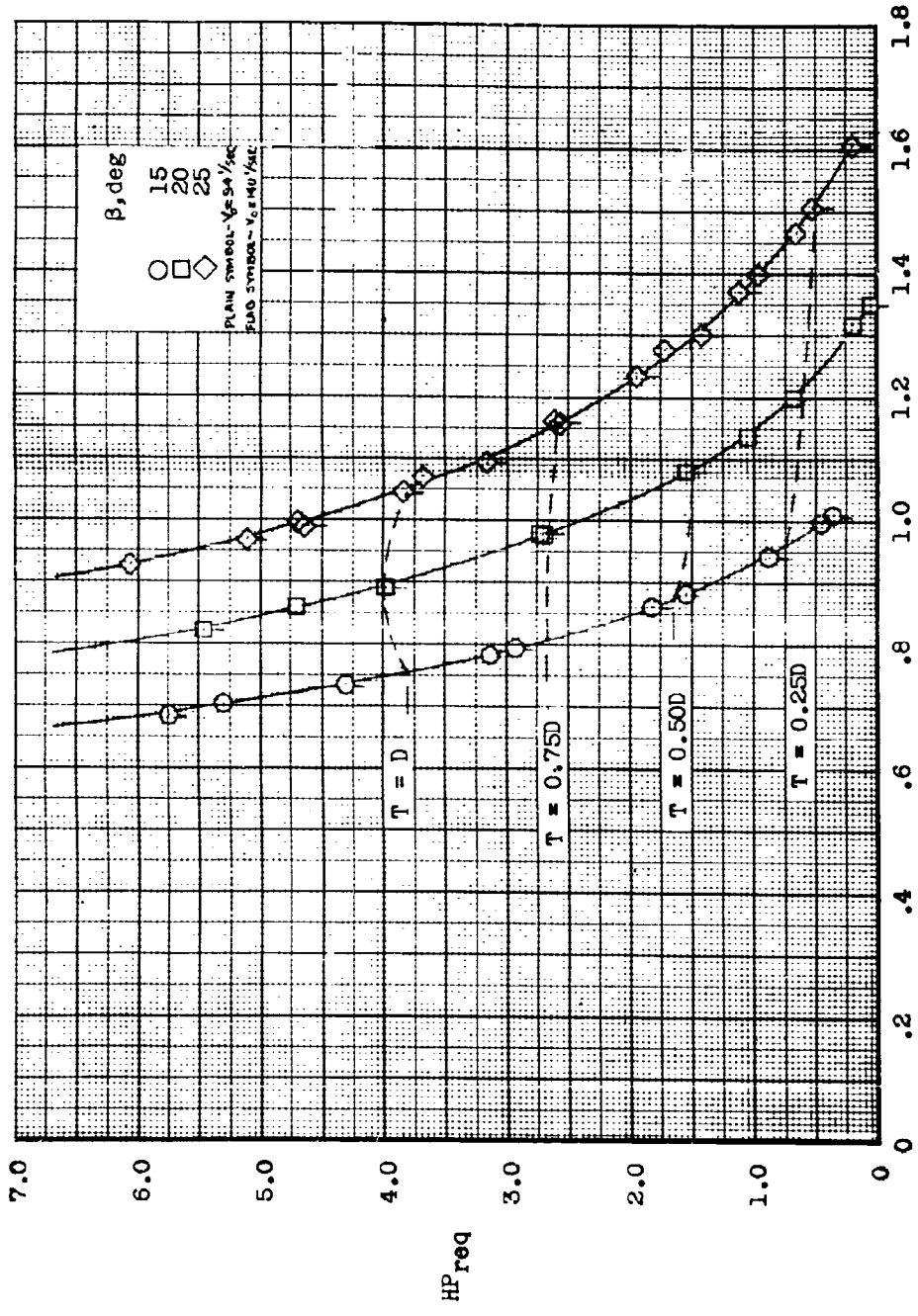

Figure 57 - Horsepower Required for Varied Flight Conditions - GAC Wake Propeller

CONFIDENTIAL

CONFIDENTIAL

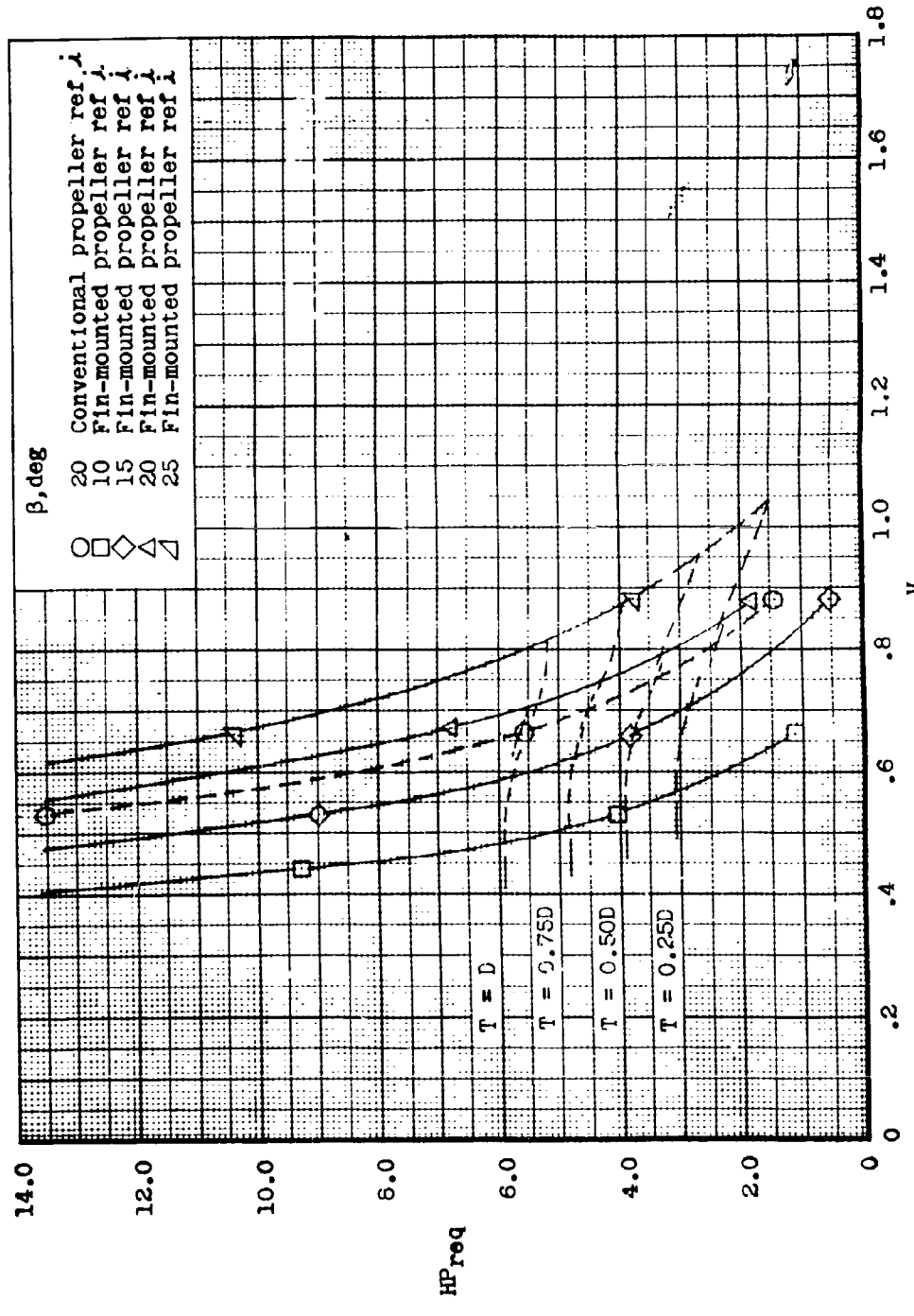

Figure 58 - Horsepower Required for Varied Flight Conditions - Conventional and Fin-Mounted Propellers

CONFIDENTIAL

CONFIDENTIAL

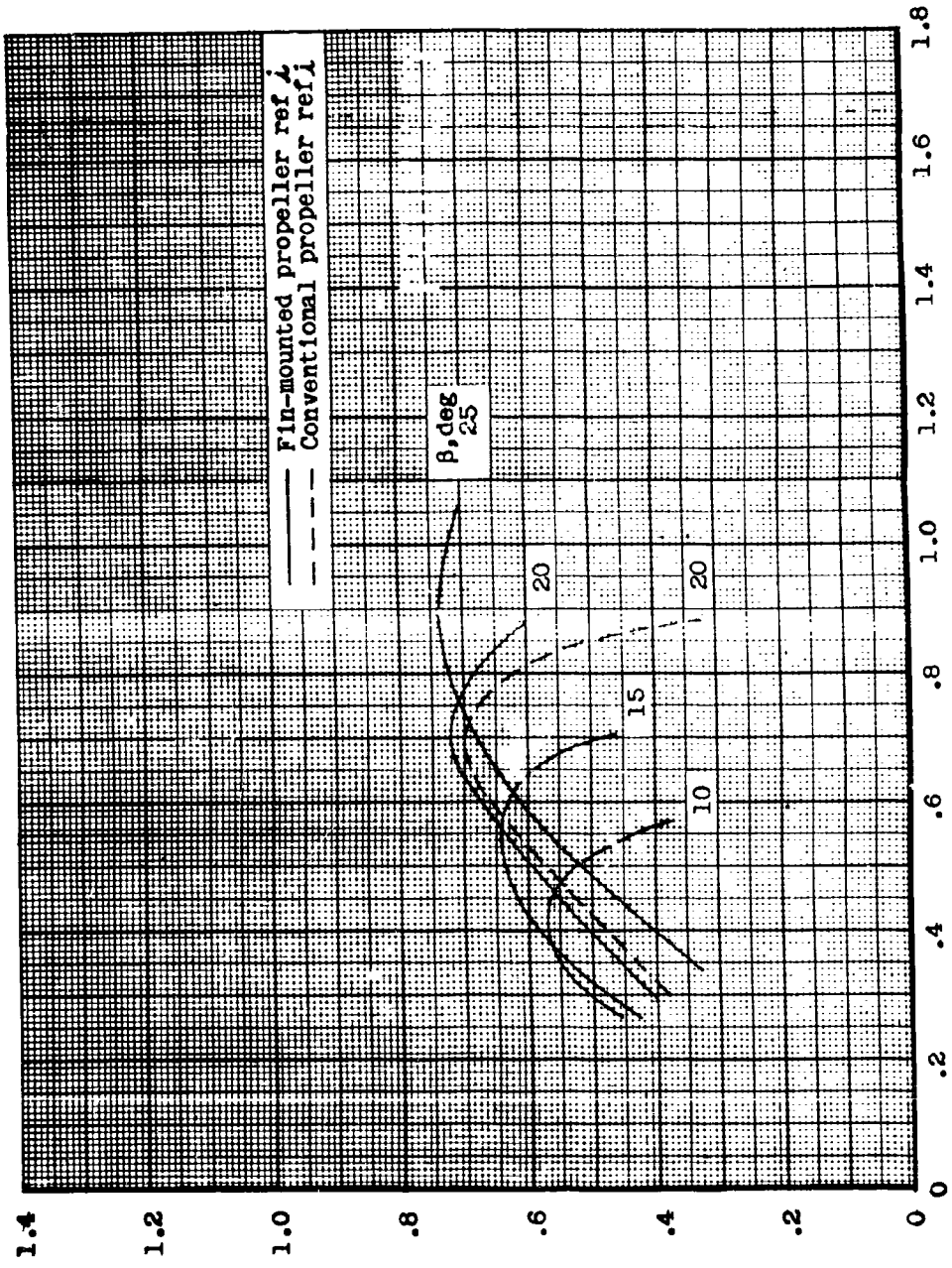

Figure 59 - Variation of Propeller Efficiency with Advance Ratio and Blade Angle - Conventional and Fin-Mounted Propellers

CONFIDENTIAL

CONFIDENTIAL

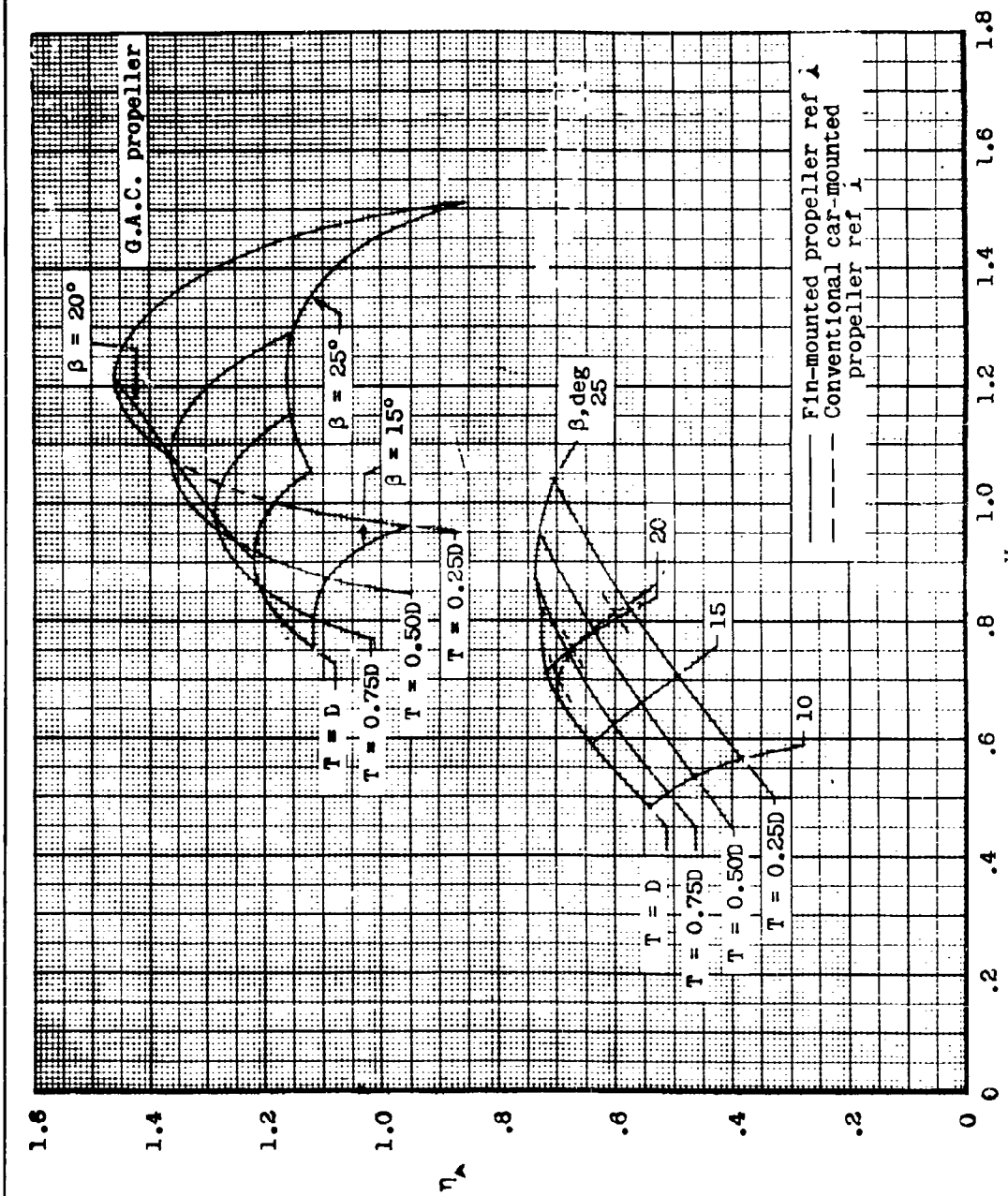

Figure 60 - Comparison of Apparent Propeller Efficiencies for Varied Flight Conditions

CONFIDENTIAL

CONFIDENTIAL

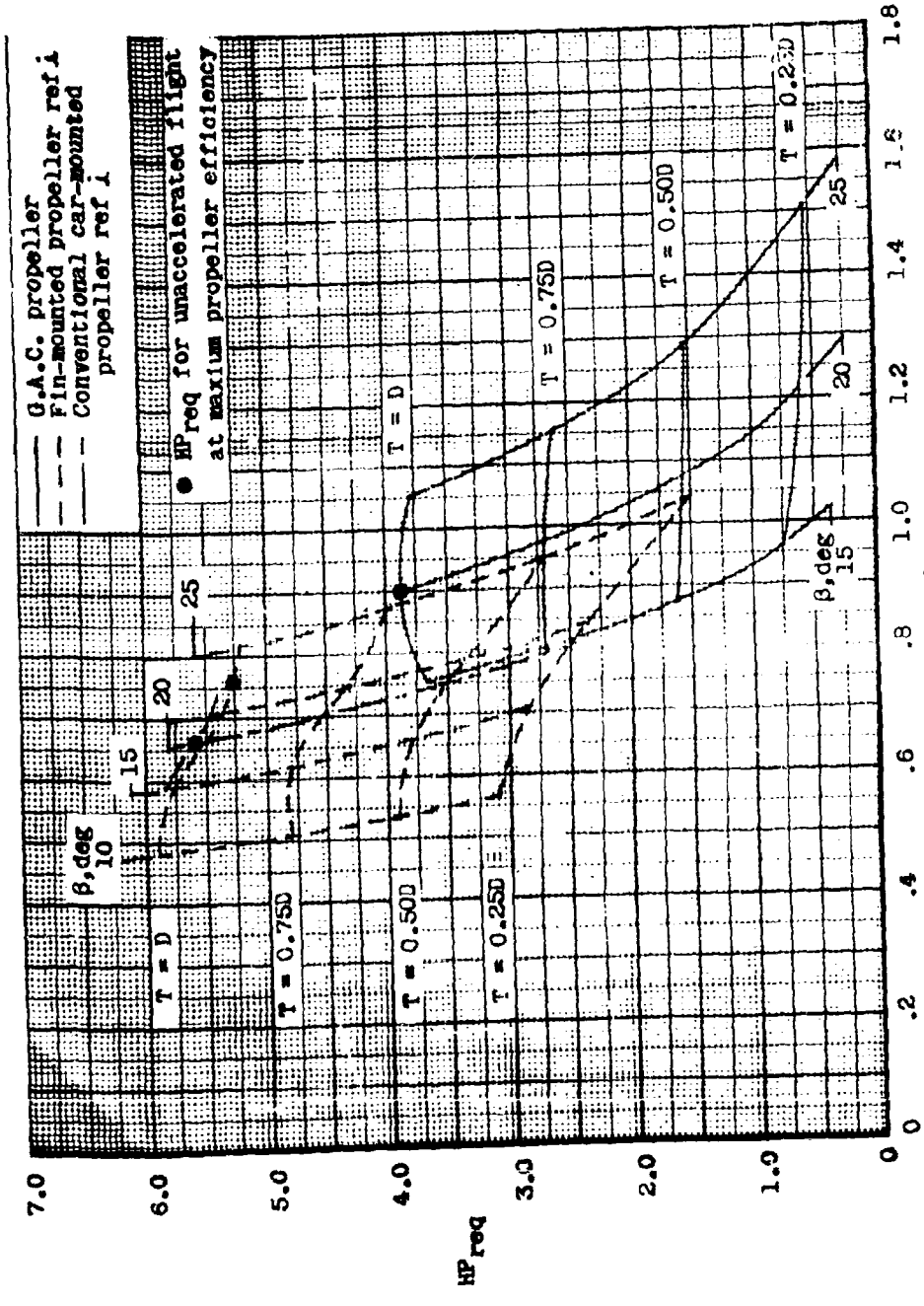

Figure 61 - Comparison of Horsepower Require.. for Varied Flight Conditions

CONFIDENTIAL